POLYMER NANOLITHOGRAPHY

by

JENNIFER M. VANCE

A dissertation submitted to the Graduate Faculty in Chemistry in partial fulfillment of the requirements for the degree of Doctor of Philosophy, The City University of New York

2010

This manuscript has been read and accepted for the
Graduate Faculty in Chemistry in satisfaction of the
dissertation requirement for the degree of Doctor of Philosophy.

Dr. Charles Michael Drain

_____ _____

Date Chair of Examining Committee

Dr. Mahesh K. Lakshman

_____ _____

Date Executive Officer

Dr. James D. Batteas

_____

Dr. Hiroshi Matsui

_____

Dr. Nan-loh Yang

_____

Supervisory Committee

THE CITY UNIVERSITY OF NEW YORK

Abstract

POLYMER NANOLITHOGRAPHY

by

Jennifer M. Vance

Adviser: Professor Charles Michael Drain

Nanolithography involves making patterns of materials with at least one dimension less than 100 nanometers. Surprisingly, writable CDs can provide polymer nanostructures for pennies a piece. Building on work previously done in the Drain lab, with an inherited home-built oven press, this research will explore the relationships between polymer chemical reactivity, polymer printing, and material surface energies. In addition, a relatively inexpensive entry point into high school and undergraduate education in nanolithography is presented. The ability to pattern cheaply at the nanoscale and microscale is necessary and attractive for many technologies towards biosensors, organic light emitting diodes, identification tags, layered devices, and transistors.

Acknowledgements

I have many people to thank. I have learned so much from this experience. Many thanks to my mentor, Dr. Charles Michael Drain, who provided such a creative project, which entwines science and art, two areas I value greatly. I thank Dr. James Helt for pioneering this project and building much of the equipment used. I also thank Dr. Giorgio Bazzan and Dr. Roberto de la Rica for sharing their expertise in nanolithography with me. I am deeply grateful to my committee members: Drs. James D. Batteas, Hiroshi Matsui, and Nan-loh Yang for their support, guidance, and expertise. I also thank Dr. Kevin Song and Dr. Illona Krectzmar for SEM images of polyaniline lines. I thank Dr.Yalin Wang for XPS measurements. I am also grateful to Adi Sahar for her creative work on the J.Chem. Ed. project, and her friendship and encouragement. The Graduate Center library was a tremendous resource, and I was able to write for hours in such a pleasant place, for which I am thankful. I thank my friends Lourine Clark, Glen and Carole Kleinknecht, Sharon Tanaka, Olimpio Wen, Laura Gauthier, and Loretta Chan for their prayers, encouragement, support and friendship. I'm grateful for my community at Redeemer Presbyterian Church. I thank my parents, Ed and Marilyn Vance. I thank my dad for sharing his enjoyment of science and my mom for sharing her enjoyment of art with me.

"What saves a man is to take a step. Then another step." C. S. Lewis

Table of Contents

List of Tables

List of Figures

List of Abbreviations

AFM……..…..Atomic Force Microscope

CD-R…….…...……..Writable compact disc

DCM…….……..Dichloromethane

DPN…….Dip-pen lithography

DVD…….Digital video disc

IR…….Infrared Spectroscopy

ITO……..Indium tin oxide

LDPE……Low density polyethylene

LED……...…Light emitting diode

NIL……..Nanoimprint lithography

NMP……...N-Methylpyrrolidone

OFET…….….Organic field effect transistor

PANI……..Polyaniline

PC……...…….Polycarbonate

PDMS…….…….Polydimethylsiloxane

PET……..Polyethylene terephthalate

PMMA……..……..polymethylmethacrylate

PS……...……Polystyrene

SAM……...Self-assembled monolayers

SEM……Scanning electron microscopy

TCPP……5, 10, 15, 20-tetrakis-(4-carboxyphenyl)-porphyrin

Tg……..Glass transition temperature

μCP…….Microcontact printing

UV-vis…….Ultraviolet-visible spectroscopy

XPS……..X-ray photoelectron spectroscopy

Chapter 1

Introduction to Polymer Nanolithography

1.1 Introduction

Polymer nanolithography involves making patterns of polymers with at least one dimension less than 100 nm.[1] Organic polymers frequently provide access to facilitated device fabrication via solution and thin film processing and lower costs.[2] Compatibility with patterning cells and proteins in life science applications is attractive as well.[3] A few of the many applications of nanolithography include plastic light emitting diodes (LEDs), photonic bandgap crystals, radio frequency tags, microfluidic channels, cell and protein arrays, organic field effect transistors (OFETs), and biochips.[2,4-8] In order to fabricate polymer patterns, the tension between monetary cost and desired nanostructure-resolution usually presents a substantial challenge. Even so, depending on the desired application, several typical nanolithography tools are available. Most commonly utilized for polymer nanolithography are photolithography, nanoimprint lithography (NIL), microcontact printing (μCP), dip-pen nanolithography (DPN), and ink-jet printing.[2] In addition, the Drain lab has developed a relatively inexpensive type of nanolithography called thermal contact nanotransfer.

1.2 Photolithography

Photolithography involves patterning a photoresist-coated substrate by shining light through a patterned rigid mask onto the surface (Fig. 1.1). During development, a solvent dissolves the exposed polymer resist (positive) or the unexposed polymer resist

(negative).[9] Sub-100 nm features are possible with this technique.[2] Increasingly complicated optics and shorter light wavelengths (extreme ultraviolet) are needed for smaller resolutions.[1] The cost for instrumentation and photomasks utilized for this technique can be a limiting factor.[10] Photomasks, which provide the desired pattern are frequently prepared by highly specialized equipment such as scanning beam lithography. Photolithography is currently used for patterning silicon wafers on a large scale.[10] Alignment for multilayered devices works well and large surface areas can be patterned with this technique.[2] However, only flat surfaces can be patterned, and polymers can undergo photo-oxidation when oxygen is present during device fabrication.[10]

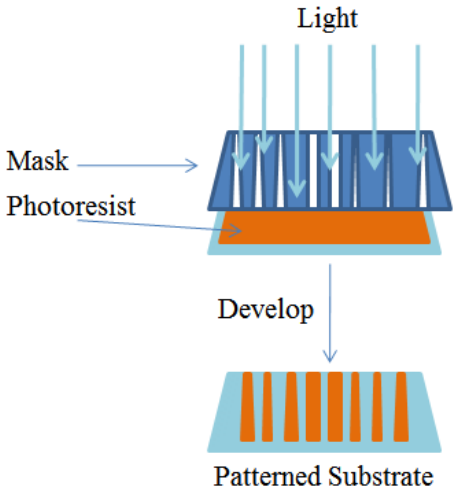

Figure 1.1 Photolithography involves shining light through a patterned mask onto a photoresist, which coats the desired substrate. Light often initiates the crosslinking of the photoresist polymer. The development step either washes away the light exposed regions (positive photoresist) or the unexposed regions (negative photoresist) to reveal a polymer pattern.

1.3 Nanoimprint Lithography

Nanoimprint Lithography (NIL) is not limited by the wavelength of light, as opposed to photolithography (Fig. 1.2). This technique is reported to be high throughput and capable of producing features as small as 5 nm.[2] With NIL, a mold or stamp is prepared by scanning beam lithography. In general, two forms of NIL are commonly utilized: thermal NIL and UV-NIL.[5] Thermal NIL coats the substrate with a thermoplastic such as polycarbonate (PC), polymethylmethacrylate (PMMA) or polystyrene (PS). The polymer resist is heated above the Tg and pressed into the mold. After cooling, the mold is removed. The recessed parts of the pattern are etched away with reactive ion etching or oxygen plasma. Conversely, UV-NIL spin casts a viscous UV sensitive polymer onto the substrate. A transparent mold is pressed into the polymer, and UV light photo-crosslinks the resist. Reactive ion etching follows mold removal. Lower pressures and shorter processing times are possible for UV-NIL, but evaporation of the resist solvent can pose a processing problem.[2] With UV-NIL, radical polymerization reactions can be inhibited by the presence of oxygen and the material can undergo defect inducing shrinkage.[11] The mold itself requires costly and specialized equipment for production, as well.[2]

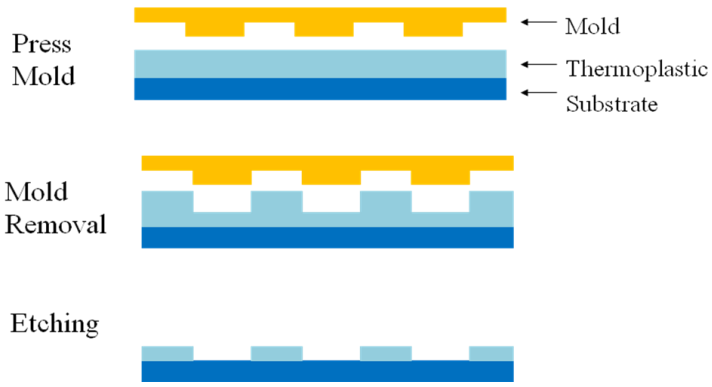

Figure 1.2 For thermal NIL, a thermoplastic is coated over a substrate. The polymer is heated above the Tg, and a mold is pressed into the plastic. After mold removal, reactive ion etching or oxygen plasma are used to remove the recessed areas of the film. Alternatively for UV-NIL, the thermoplastic is replaced with a viscous UV sensitive polymer, which undergoes crosslinking after light is shined through a transparent mold. pressed into the viscous polymer solution. After mold removal, the reactive ion etching or oxygen plasma step reveals the final polymer pattern.

1.4 Microcontact Printing

Alternatively, μCP is a type of soft lithography, which frequently involves a polydimethylsiloxane (PDMS) stamp (Fig. 1.3).[10] This technique tends to produce the most optimal features at the sub-micron range. Sub-100 nm structures have been reported, but are more difficult and less common.[2] The PDMS stamp is coated or "inked" with the polymer or organic material of choice and is then pressed against the substrate.[12] In order to facilitate adhesion of the ink to the surface, some methods of passivating the stamp have been reported, such as polyfluorinated thiols.[2] Problems with the PDMS stamp at smaller feature sizes include swelling, pairing, sagging, buckling, and nanostructure collapse. The PDMS stamp is also obtained from a master that is usually produced by costly scanning beam lithography.[10,12]

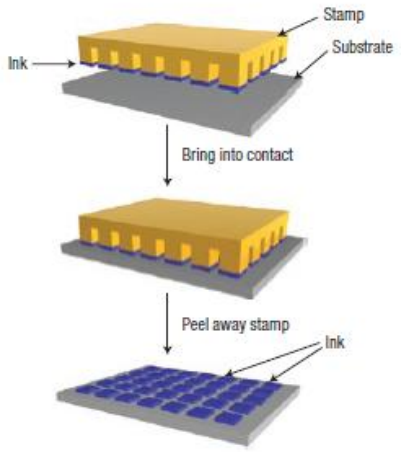

Figure 1.3 For µCP printing, a PDMS stamp is inked with the desired polymer or organic material, and pressed onto a substrate. The stamp is removed to reveal the pattern. (Illustration used with permission from Nature Publishing Group © 2008)[2]

1.5 Di-pen Lithography

Rather than obtaining a pattern from a stamp, dip-pen lithography (DPN) is direct-write, and uses an atomic force microscope (AFM) tip as the pen for writing. The AFM tip is inked with the polymer or organic material.[13] A water meniscus forms between the surface and the tip. Nanostructure sizes are dictated by the AFM tip size and the water meniscus. Scanning speed, humidity, temperature, and surface chemistry also contribute. Matching a negatively charged polymer to a positively charged surface can result in better printing, as well.[2] DPN is much slower than the other parallel techniques, and is difficult to do over mm scale. However, there are 2 dimensional AFM tip arrays, with multiple AFM tips able to write simultaneously.[13]

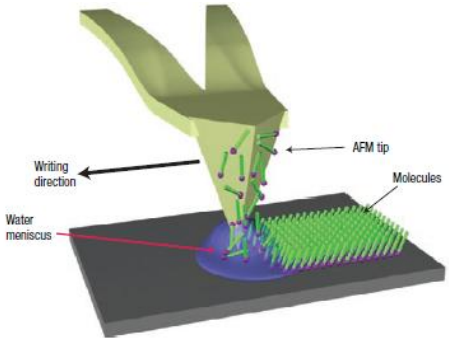

Figure 1.4 Dip-pen lithography employs the small size of an AFM tip as a writing tool. The AFM is inked, and forms a water meniscus with the surface. The polymer or organic material is deposited on the surface in a direct-write process. (Illustration used with permission from Nature Publishing Group © 2008)[2]

1.6 Ink-jet Printing

Ink-jet printing, a direct-write method for nanolithography does not have the resolution of DPN, but is high throughput. Printed features have been reported as small as 10 µm, and are limited by the ink-jet droplet size. When droplets of printed polymer dry, the drying mixture of solvents can produce varied structures and defects, due to Marangoni convection, which is a result of different solvent surface tensions.[2,14] Layered devices also require carefully chosen solvents for multiple layer deposition, as earlier layers can dissolve underneath.[2]

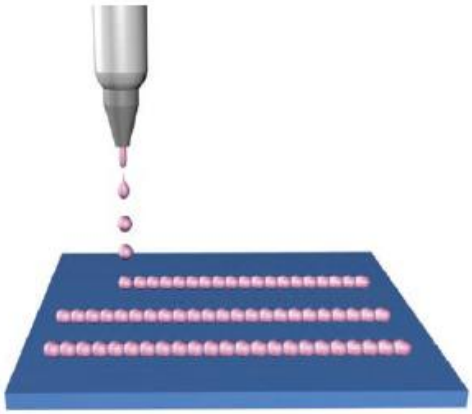

Figure 1.5 Ink-jet printing is high throughput and involves dispensing solutions of polymers and organic materials onto a substrate. (Illustration used with permission from Nature Publishing Group © 2008)[2]

1.7 Thermal Contact Nanotransfer

Developed in the Drain lab, thermal contact nanotransfer employs printing inexpensive writable compact discs (CD-Rs), which function as stamps, in order to produce polycarbonate nanostructures with heat and pressure. Printing temperatures are below the polymer Tg and required pressures are 10^3 times less than thermal NIL. Reported in the literature, the three layer model for thin film polymer physics explains observed printing (Figures 6-9).[15,16] More details for this method are presented in the subsequent chapters to this work.

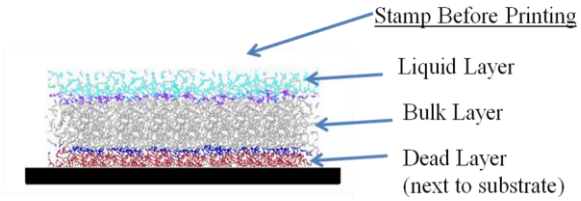

Figure 1.6 Thermal contact nanotransfer involves a plastic CD-R stamp, which before printing has three layers. The liquid layer is at the air interface and next to the bulk layer. The dead layer is next to the substrate and the bulk polymer. Between each of these layers is a boundary layer. Each layer has a different Tg and a different mobility.

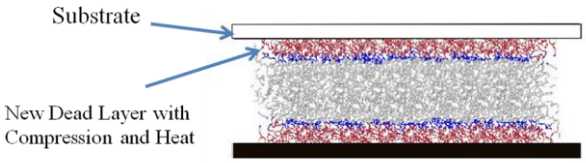

Figure 1.7 When the substrate is placed against the stamp with heat and pressure, a new dead layer is formed.

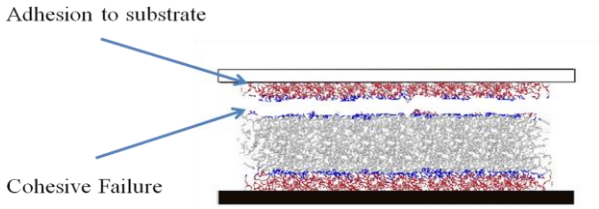

Figure 1.8 After cooling, the substrate is removed from the stamp. Cohesive failure results at the boundary between the dead and bulk layers, as the dead layer adheres to the substrate and is pealed away.

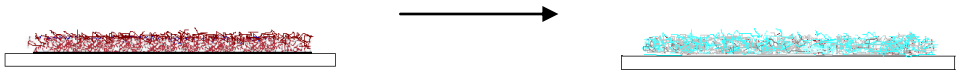

Figure 1.9 The dead layer adhered to the substrate is exposed to air is a liquid layer.

1.8 Summary

Access to polymer nanolithography techniques that are inexpensive and with good coverage is important for research institutions as well as commercial production. Photolithography, nanoimprint lithography, microcontact printing, dip-pen lithography, and ink-jet printing are all excellent examples. However, highly specialized and expensive equipment for scanning beam lithography is often required to provide the template for nanostructures, or as in the case of DPN, serial nanolithography can be very slow and require several experiments, despite the advantages of a direct-write method. Thermal contact nanotransfer nanolithography is another possible method for generating nanostructures from inexpensive CD-Rs.

1.1 References Chapter 1

(1) Xia, Y.; Rogers, J. A.; Paul, K. E.; Whitesides, G. M. *Chem. Rev.* 1999, *99*, 1823-1848.

(2) Nie, Z.; Kumacheva, E. *Nature Materials* 2008, *7*, 277-290.

(3) Schmidt, R. C.; Healy, K. E. *Journal of Biomedical Materials Research Part A* 2009, 1252-1261.

(4) Geissler, M.; Xia, Y. *Advanced Materials* 2004, *16*, 1249-1269.

(5) Balla, T.; Spearing, S. M.; Monk, A. *J. Phys. D: Appl. Phys.* 2008, *41*.

(6) Singh, T. B.; Sariciftci, N. S. *Annu. Rev. Mater. Res.* 2006, *36*, 199-230.

(7) Yablonovitch, E.; Gmitter, T. J.; Meade, R. D.; Rappe, A. M.; Brommer, K. D.; Joannopoulos, J. D. *Physicall Review Letters* 1991, *67*, 3380-3383.

(8) Siegel, A. C.; Tang, S. Y.; Nijhuis, C. A.; Hashimoto, M.; Phillips, S. T.; Dickey, M. D.; Whitesides, G. M. *Accounts of Chemical Research* 2010.

(9) Gates, B. D.; Xu, Q.; Stewart, M.; Ryan, D.; Wilson, C. G.; Whitesides, G. M. *Chem. Rev.* 2005, *105*, 1171-1196.

(10) Xia, Y.; Whitesides, G. M. *Annu. Rev. Mater. Sci.* 1998, *28*, 153-183.

(11) Cui, B.; Cortot, Y.; Veres, T. *Microelectronic Engineering* 2006, *83*, 906-909.

(12) Quist, A. P.; Pavlovic, E.; Oscarsson, S. *Anal. Bioanal. Chem.* 2005, *381*, 591-600.

(13) Huo, F.; Zheng, Z.; Zheng, G.; Giam, L. R.; Zhang, H.; Mirkin, C. A. *Science* 2008, *321*, 1658-1660.

(14) Reis, N.; Ainsley, C.; Derby, B. *Journal of Applied Physics* 2005, *97*, 1-6.

(15) Fukao, K.; Miyamoto, Y. *Physical Review E.* 2000, *61*, 1743-1754.

(16) Forrest, J. A.; Dalnoki-Veressb, K. *Advances in Colloid and Interface Science* 2001, *94*, 167-196.

Chapter 2

Polymer Nanolithography by Thermal Contact Nanotransfer

Giorgio Bazzan, Jennifer Vance, Charles Michael Drain

2.1 Introduction:

A number of different methods can be used to fabricate nanoscale patterns, such as photolithography and soft lithography. Among these technologies nanoimprinting lithography (NIL), also known as embossing lithography, has attracted increasing attention in recent years as an inexpensive alternative for nanopatterns fabrication. MIT's Technology Review has put NIL as one of 10 emerging technologies that are likely to change the world.[1]

NIL was first introduced by Chou *et al* in 1997,[2] and typically a rigid patterned mold is pressed into a thin thermoplastic polymer film coating a substrate. After heating the polymer above its glass transition temperature (T_g) it becomes fluid, flowing into the recessed features of the stamp under the applied pressure. Polymer and mold are then cooled to a temperature below T_g of the polymer, and the mold is separated from the polymer. A thickness contrast is created in the polymer on the surface and the thinner parts of the relief are anisotropically removed by oxygen plasma etching, producing the isolated features on the surface (Fig. 2.1).[3] This leaves a pattern of the polymer and the exposed surface. This lithography has many advantages, for example simple processing and low cost, because it does not require expensive instrumentation and clean room. NIL

affords products with very small lateral resolution,[4] less than 10 nm, with high replication, fidelity, and throughput.[5]

NIL relies on viscous polymer flow during the polymer film deformation to create the thickness contrast, hence high temperature (50-100 °C) and pressure (up to 10 MPa) are required to obtain reliable pattern transfer.[6,7] Typically, mold surface treatment or modification is necessary for clean release of the mold from the patterned polymer substrate.[8] Several modifications to NIL have been introduced to overcome or minimize these problems and to further develop the technique, including: (a) low-pressure nanoimprinting[9] that uses a special fluoropolymer film mold; (b) reversal imprinting[10] wherein the polymer is spin coated on the hard mold and then transferred to the substrate; (c) room-temperature imprinting[11] in which the polymeric film coating the substrate is treated with solvent vapor; and (d) step-and-flash imprint lithography[12] (SFIL) that uses a low-viscosity pre-polymer material that is then photocured using UV light transmitted through the transparent mold.

NIL can be applied to a wide range of materials, both inert polymers and functional materials can be used,[13] which allows the formation of a variety of organic-based optoelectronic devices. In organic optoelectronics, the embossed film consists of materials that either play an active role in a device (e.g. electroluminescent layer) or serve as structures onto which active materials are deposited. A variety of devices have been fabricated using NIL, including nonlinear optical (NLO) polymer nanostructures,[14] high resolution organic polymer light-emitting (OLED) pixels,[15] and organic thin-film transistor (TFT).[16]

Herein we describe a new polymer nanolithography technique, based on thermal contact nanotransfer, that results in nano- to micro- scaled patterns of ca. 10 nm thick polymer on ceramic surfaces. The present method evolved from our previous work on the nanofabrication of polymer insulated gold nanowire patterns by self-organization of polymer films on ceramic surfaces,[17] and from our method to fabricated patterns of gold nanowires on polymer surfaces.[18] These three patterning methods exploit the unique physical properties of ultrathin polymer film dynamics at interfaces.[19,20] Multiple stamping processes on a single substrate afford more complex multilayered patterns, and the polymers can be doped with fluorescent dyes and other functional materials to afford photonic patterns. A significant advantage of the thermal contact nanotransfer method is that inexpensive CDs and DVDs can be used as the stamps and that the method can be affected by inexpensive, laboratory-built, stamping apparatus. Secondly, this process results in patterns of films similar to the NIL method, albeit with smaller heights, but obviates the need for the etching step.

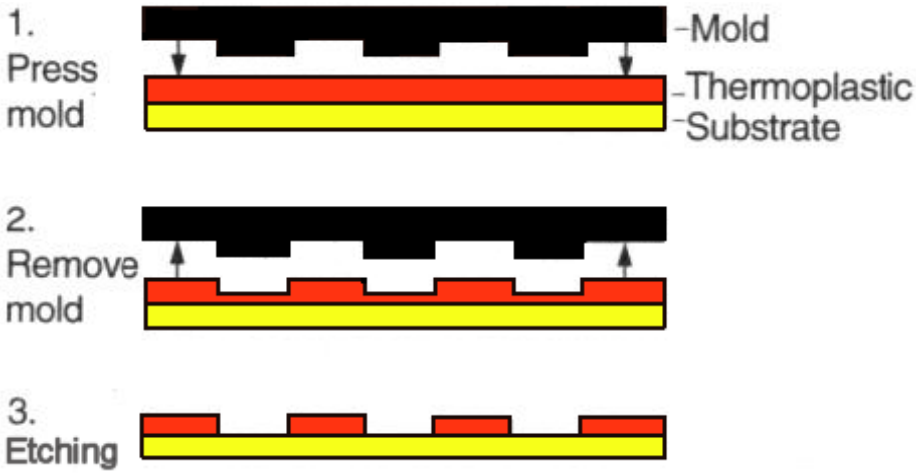

Figure 2.1 Schematic of NIL process. Compression molding is used to create a thickness contrast on the polymer film deposited on the substrate. Anisotropic etching is used to expose the substrate material.

There are numerous potential applications of nanopatterns of polymers on surfaces, which range from the masking of the ceramic substrate for chemical modification, deposition of materials on the unmasked substrate, and the utility of creating nanostructures for more complex devices.

2.2 Experimental Procedure

The stamping process has been carried out using a home built stamping apparatus (built by Dr. James Helt, Appendix 5.1). The polymeric nanostructures are formed by the compression of a thermoplastic polymer stamp against a ceramic substrate, the system is then briefly heated, and the stamp is subsequently separated from the substrate after cooling. We used glass and indium-tin oxide (ITO) as substrates. The resulting structures were then characterized with atomic force microscopy (AFM), scanning electron microscopy (SEM), and confocal microscopy.

Atomic force microscope (AFM) measurements were conducted with an Asylum Research MFP-3D AFM (Santa Barbara, CA). Images were acquired in air using commercial silicon tips (MikroMasch USA, Portland, OR) in AC mode (tapping mode) (NSC15/AlBS) with a typical tip radius of curvature of less than 10 nm (NSC15, force constant = 40N/m, resonance frequency = 325 kHz). The z scale was calibrated using commercial calibration grids (MikroMasch USA, Portland, OR). Some of the AFM data was analyzed with the WSxM 4.0 Develop 11.6 Image Browser.[21] Scanning electron microscopy (SEM) images were obtained with a Carl Zeiss DSM 940. To minimize charging, the typical SEM imaging conditions used an electron beam current at the sample of ~110 mA with an acceleration voltage of 3.1 kV. A Varian Cary Bio-3

spectrophotometer was used for UV-visible spectroscopy, in double-beam mode. Steady-state fluorescence spectra were taken on a Fluorolog-3, with excitation at the maximum UV-visible absorbance (Soret band). Confocal images were recorded with a Leica TCS SP2 using the 514 nm laser excitation of the porphyrin Q-band.

Polymer Stamp Preparation

Recordable compact discs (CD-R) were used as polymer stamps. CD-R generally consist of four material layers: (1) a grooved polycarbonate substrate ~1.2 mm thick, (2) a thin layer of organic dye, (3) a thin metallic layer, (4) a protective coating of lacquer (Fig. 2.2). The metal used as reflecting layer can be silver, silver alloy, aluminum, or gold. An aluminum coated CD-R was used for preparing grooved polycarbonate stamps directly. Alternatively, a gold coated CD-R was passivated and utilized as a replication master for the preparation of stamps from other polymeric materials, such as low density polyethylene (LDPE). Specifically, Imation (5067 149RE 19948), and Delkin Archival Gold (6298 2131 5612) were used. The aluminum coated CD-R were cut in 22x22 mm pieces and the gold-coated CD-R were cut into larger pieces, in order to cover a 22x22 mm pieces of LDPE. For both types of CD-R, the samples were immersed in concentrated HNO_3 for 3 minutes, then were rinsed copiously with water, and dried under a stream of N_2 gas.

HNO_3 treatment of the Imation CD-R, which have a metallic layer of aluminum,[*] results in the delamination of the protective lacquer layer and dissolution of the Al layer,[22] leaving a grating structure of polycarbonate with lines ~120 nm deep, ~900 nm

[*]Imation technical information see www.imation.com

wide and a pitch of 1.6 μm (Fig. 5.3). UV-visible analysis of the CD-R after the delaminating process indicates the recording layer containing the dye (usually a phthalocyanine) is removed as well. The samples prepared in this way were then directly used for stamping without further processing.

As an aside, rinsing the Imation CD-Rs with water, drying with a stream of nitrogen, and applying Scotch® tape was found to be a nitric acid free method for delamination. The dye was easily removed with a brief absolute ethanol rinse, and 5 minutes of tap water, nanopurified water rinse, followed by drying with a stream of nitrogen. Non-nitric acid treated CD-Rs were found to stamp ITO and glass, but the overall sample coverage of the lines was found to be less than the nitric acid treated CD-R stamped lines. All of the stamped polycarbonate lines in this paper were from nitric acid treated CD-Rs. Comparative contact angle experiments with CD-Rs exposed to increasing amounts of time in nitric acid, revealed a slight decrease in contact angle (see supporting information). Hydrolysis and nitration of polycarbonate surfaces has been reported in the literature with a mixture of concentrated nitric acid and concentrated sulfuric acid. These modified surfaces were used for nickel deposition onto Lexan® (polycarbonate), for commercial use.[23] Since our conditions are not as harsh, the concentrated nitric acid is only modifying the surface slightly (as seen by IR, UV-vis, and X-ray spectroscopy), which provides comparatively better adhesion with the ITO surface (see Appendix 2.7).

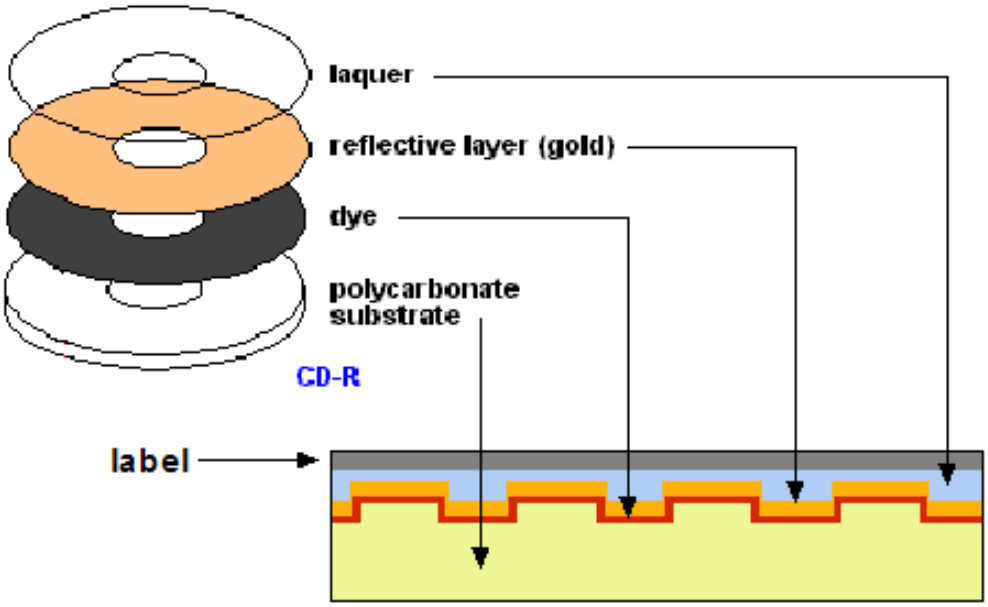

Figure 2.2 Schematic of a recordable compact disc (CD-R) composition. CD-R generally consist of four layers of material: (1) a grooved polycarbonate substrate ~1.2 mm thick, (2) a thin layer of photosensitive organic dye, (3) a nanometer thick metal layer, (4) a protecting coating of lacquer. (Reproduced with permission from Computer Desktop Encyclopedia © 1981-2010 The Computer Language Co. Inc., (www.computerlanguage.com)

When the Delkin Archival Gold CD-R, with a reflective layer of >92% gold, was treated with HNO_3 only the protective polymer film is removed.[24] The gold coated CD-R have similar feature sizes to the Imation CD-R, with a layer of gold of ~ 50 nm, as estimated by AFM after etching the Au layer with Transene gold etchant type TFA (Danvers, MA) (Fig.2.4). Self-assembled monolayers (SAMs) of 1-octanethiol were prepared by immersing freshly prepared gold substrates into a dilute solution (1.0 mM) of 1-octanethiol in absolute ethanol for 18-24 h.

The gold substrates modified with SAMs were rinsed sequentially with absolute ethanol and water, and then dried with N_2 gas. The completeness of the film coverage was

assayed by the observed differences in the water contact angles on the untreated and treated surfaces. Greater contact angles for deionized water on the gold substrate modified with SAMs are expected due to the hydrophobicity of the hydrocarbon chains compared to the bare gold surface. This quick assay confirms the coverage of the gold

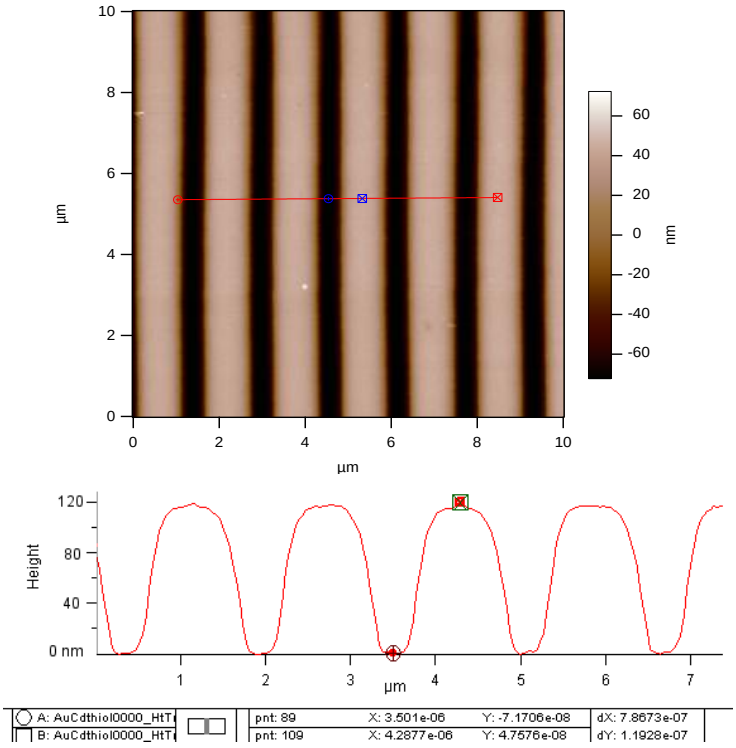

Figure 2.3 AFM images of a Imation CD-R after treatment with conc. HNO_3. Surface topography of the bare polycarbonate grating structure with lines ~120 nm deep,~900 nm wide and a pitch of 1.6 µm.

surface by the alkanethiols SAM. AFM analysis of the modified gold substrate shows that the passivation with the SAM does not modify the morphology of the gold surface.

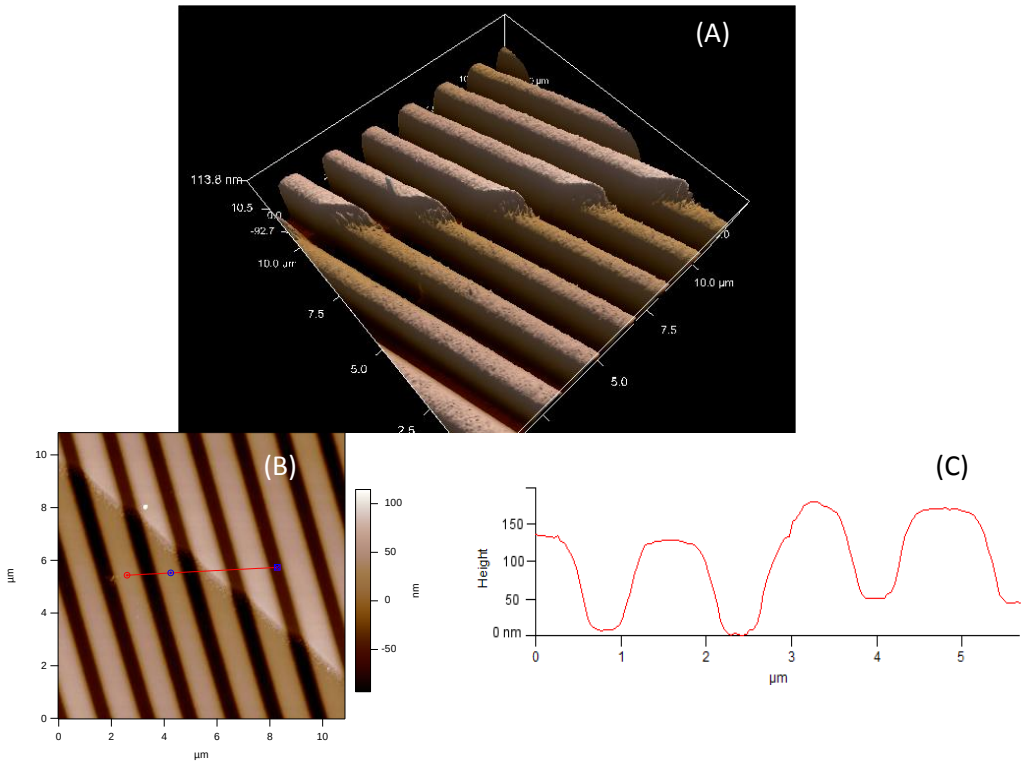

Figure 2.4 AFM images of a Delkin Archival Gold CD-R, after treatment with conc. HNO_3 and etching of part of the layer of gold with Transene gold etchant type TFA (Danvers, MA). The gold thickness is ~50 nm. The CD-R has similar features sizes to the Imation CD-R. (A) - (B) Height images. (C) Line trace.

Doped Polymer Stamps

The stamps can be doped with a fluorescent dye such as porphyrins. We chose tetra(4-carboxyphenyl)porphyrin (TCPP) as a doping agent because porphyrins have ~ $2x10^5$ O.D. in the Soret band near 420 nm and ~10% fluorescence quantum yield, and they are cheap to synthesize and remarkably stable, which make this a good starting point to develop the doping method, doped stamps, and product characterization. The surface doping is accomplished by dipping the polymer stamp into a 1:100 CH_2Cl_2:CH_3CH_2OH solution containing ~0.1 mM of TCPP for 10 seconds, immediately rinsing with copious amounts of water and drying under nitrogen. The doped polycarbonate has been characterized by UV-vis and fluorescence spectroscopy.

2.3 Results and Discussion

Fabrication of polymer patterns

The stamping process is very simple and enables the fabrication of nanoscaled polymeric patterns on ceramic substrates in a one step method. Using a pneumatic press, fitted with a heating-cooling system and a programmable temperature controller, the treated CD-R was compressed against a glass or ITO substrate. After heating the stamp-substrate sandwich to less than the glass transition temperature (T_g) of the polymer and cooling it back to room temperature, the substrate was either pried from the stamp using a pair of tweezers, or separated by sonication in water (Fig. 2.5).

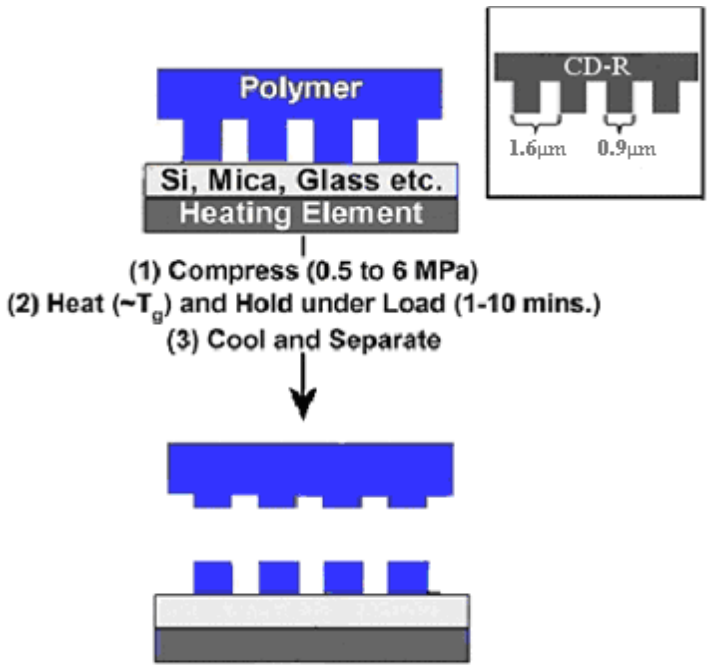

Figure 2.5 (A) Schematic of the stamping process. The polymeric nanostructures are formed by the compression of a thermoplastic polymer stamp against the substrate (glass or ITO), the system is then briefly heated, and subsequently the stamp is separated from the substrate after cooling. **(B)** Depicts the repeat grating structure of commercial CD stamps, which possess a recess depth ~ 150nm.

The stamping process, usually carried out with a 22x22 mm section of a CD-R on an ozone cleaned ITO substrate, uses a 2-step temperature program (heating/cooling) while the stamp is compressed against the substrate. A typical profile of the temperature program is shown in the appendix (Figure A2.1). Stamp and substrate are held under a compressive load (contact pressure) of ca. 20 kPa at 45 °C for 5 minutes, to let the system reach a thermal equilibrium. The heating ramp represents the maximum heating capacity of the apparatus ~45 °C/min (it takes approximately 2 minutes to reach the dwell temperature). During the heating ramp, the pressure was increased incrementally to 70 kPa. The best patterns were obtained from dwell temperature ranges from 110-115 °C and the minimum dwell time to obtain structures with high fidelity is 1-2 minutes, and longer dwell times do not increase the quality of the transfer. The system is then allowed to cool (under load) at a rate of ~15 °C/min to room temperature. The applied load is then slowly removed and the stamp is separated from the substrate.

The fabrication of the polymeric features is a consequence of the cohesive failure inside the polymeric material due to formation of a polymer-polymer "interface" and the explanation for this behavior can be found in the studies of the properties of confined polymer films. There is a fairly large literature on the physical properties of ultra-thin polymer films[19,20,25-29] since understanding these properties are important in many applications, including protective and lubricating coatings,[30] adhesives, composite materials, and microelectronics.[13,31] A generally accepted model to explain the behavior of thin polymer films at interfaces is the *three-layer model*, which describes polymer films as possessing three layers with different mobilities and glass transition temperatures. Near the substrate there is a *dead layer* in which the polymer chain mobility, and

therefore the T_g, is strongly influenced by interactions with the substrate. Strong dead layer – substrate interactions reduce the mobility and raise the T_g. At the polymer-air interface there is a *liquid-like* layer with a greater mobility and therefore a lower T_g. Between these two layers there is a *bulk-like* layer which has the same mobility as that of the bulk samples.[32] Thus there are polymer-polymer interfaces that dictate the location of cohesive failure and enable the present stamping method (Fig. 2.6).

This model is attractive because it can address the inhomogeneities that experimental results and theoretical calculations show exist in such supported thin films of polymers. "It is plausible that there are boundary layers between the bulk-like layer and the liquid-like layer and between the bulk-like layer and the dead layer"[33] and this can account for the anisotropic adhesive interactions between the layers. In fact, it has been suggested, from recent modeling of unentangled polycarbonate on a nickel surface, that interfacial polymer segregation could compromise cohesion between the adsorbed ("dead") and adjacent bulk-like macromolecules.[34]

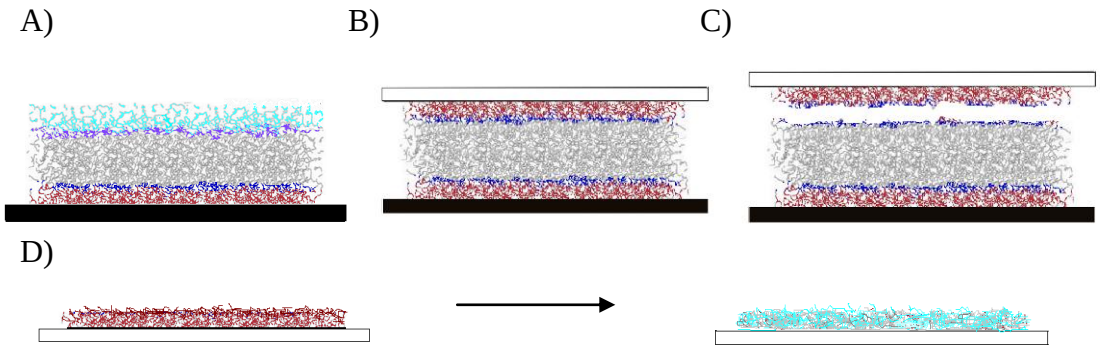

Figure 2.6 Schematic representations of the *three-layer model* used to describe the behavior of thin polymer films at interfaces. A) Substrate supported thin film representing the CD stamp before compression against the ceramic substrate in the C-clamp. B) Film confined between the glass substrate and CD during the stamping process. Red: *dead layer* where the polymer chain mobility is strongly diminished by interactions with the substrate. Gray: *bulk-like* layer where the polymer chains have mobilities described by the bulk properties. Light blue: *liquid-like* layer, at the polymer-air interface, has polymer chains with higher mobility. Dark blue: interfaces between these layers where the polymer separates in the stamping process. C) Ceramic substrate is removed from stamp, along with the polymer dead layer. D) The printed dead layer becomes a liquid layer, upon exposure to air.

AFM topography images (Fig. 2.7) show that uniform patterns can be transferred from a CD stamp using a dwell temperature of 110°C and a dwell time of two minutes. The polymeric features on the substrate are well defined with a typical height of 12-15 nm. This is comparable to the *dead layer* persistence lengths (4-13 nm) extracted from recent thin film polycarbonate studies.[35] Consistent with our previous work,[17] the present findings indicate that the intrapolymer interface between the dead and bulk layers forms a shear plane that allows the patterning of surfaces. The comingled roles of temperature and pressure in the stamp processing increase the polymer interactions with the ceramic substrate to form a well defined dead layer and allow the polymer strands to reorganize to further delineate the boundary with the bulk layer to create a shear plane.

The glass transition temperature of polycarbonate is ~150 °C,[36] but T_g depends on molecular weight distribution and on presence of additives (e.g. CD-R contain glass fillers), for the optical recording media it was determined to be 145 °C by differential scanning calorimetry.[17] Thus this polymer nanolithographic technique enables fabrication of structures at temperature well below a polymer's bulk T_g. For the CDs used in this study, the optimal temperature for the stamping process is ~ 110 °C. Patterns have been fabricated with temperature as high as 135 °C, while for temperature closer to T_g there is a decrease in the structural fidelity. The serrated structure of the top of the polymer in the stamped pattern is thought to arise from the dead-layer bulk-layer fracture during the stamp-substrate separation. Humidity, the amount of water using in rinsing, stamp drying time, and the speed of releasing the pressure, are all variables that have been observed to influence the serrated structure and height of the lines. A better separation technique than prying the stamp from the substrate is needed, preliminary results show that sonication in water may be a promising alternative.

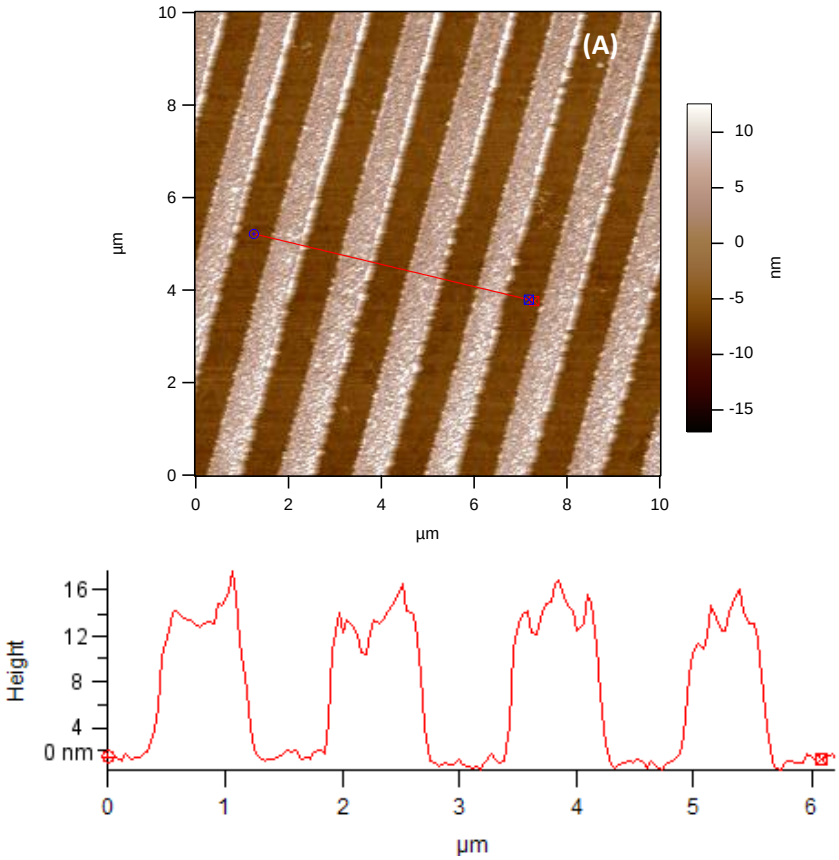

Figure 2.7 ITO patterned with a CD-R stamp using a dwell temperature of 130°C and a dwell time of two minutes. AFM images acquired in tapping mode. the polymeric features on the substrate are well defined with a typical height of 12-15 nm.

To verify that the polymer is not spreading over the entire substrate surface during the stamping process (i.e. there is no polymer in the grooves of the product), part of the polymer lines have been nanoshaved using a silicon AFM tip during contact mode imaging (Fig. 5.8). Since the minimum height in the cross section analysis of the nanoshaved part does not change compared to the part of the sample with the stamped pattern, we can conclude that the polymer film does not spread over the surface during the heating/compression process. The section analysis in fact has the typical surface roughness profile of the bare ITO surface used in these studies.

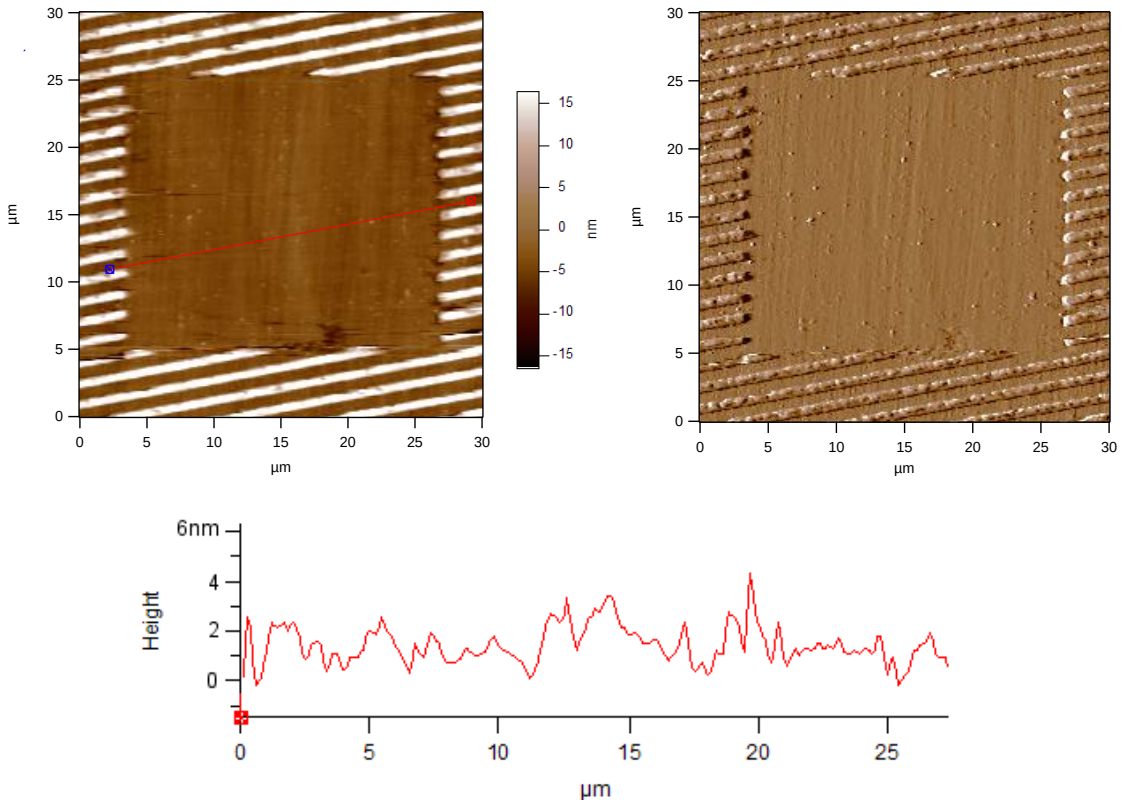

Figure 2.8 AFM images acquired in contact mode after nanoshaving some of the polymer structure. Left: height image. Right: friction image. The section analysis does not show the presence of polymer film and has the typical roughness profile of a bare ITO surface, which confirms that the polymer does not spread over the part of the substrate not in contact with the polymer during the stamping process.

Mechanical and chemical stability of the polymer patterns

The stability of the stamped structures has been evaluated. The polymer features on the ITO and substrates adhere well using a qualitative, but widely used "Scotch® tape peel test,"[37] wherein a piece of Scotch® tape is pressed against the patterned substrate and peeled off. No apparent damage was observed by optical microscopy after removing the Scotch® tape.

Secondly, sonication of the patterned ITO in water leaves the polymer lines intact without any observable damage to the structures. Notably, sonication in polycarbonate solvents such as toluene or dichloromethane does not completely destroy or remove the patterned polymer, but this treatment does have some effect on the polycarbonate features. This effect is clearly illustrated in the AFM images after sonicating in organic solvents. Figure 2.9A shows a polycarbonate pattern on ITO obtained with two minute dwell time at 135 °C but separated from the stamp at 45°C; the section profile shows the typical ~ 900 nm wide lines with edge features or protrusions that are 15-20 nm. Prominent edge features are in general observed when the system is not allowed to cool to room temperature before separation. Sonication of this stamped product on ITO in CH_2Cl_2 for two minutes removes some polycarbonate, and results in smoothing the prominent edges to leave 5-6 nm thick lines (Fig 2.9B). After two more minutes of sonication in the same solvent the lines are ca. 4 nm high and much smoother (Fig. 2.9C). Treatment of the sample for four more minutes further reduced the height by ca. 1 nm (Fig. 2.9D) to leave ca. 3 nm high features. Thus, the polycarbonate patterns show a remarkable stability against solvent delamination. Moreover, brief sonication in organic solvents can actually be used as part of the processing to further modulate (reduce) the thickness of the polymer patterns and to smooth the topology on top of the polymer lines. This secondary step allows formation of patterns with a more uniform height that are only few nanometers thick. This stability can also be exploited to chemical modify or dope the patterned products.

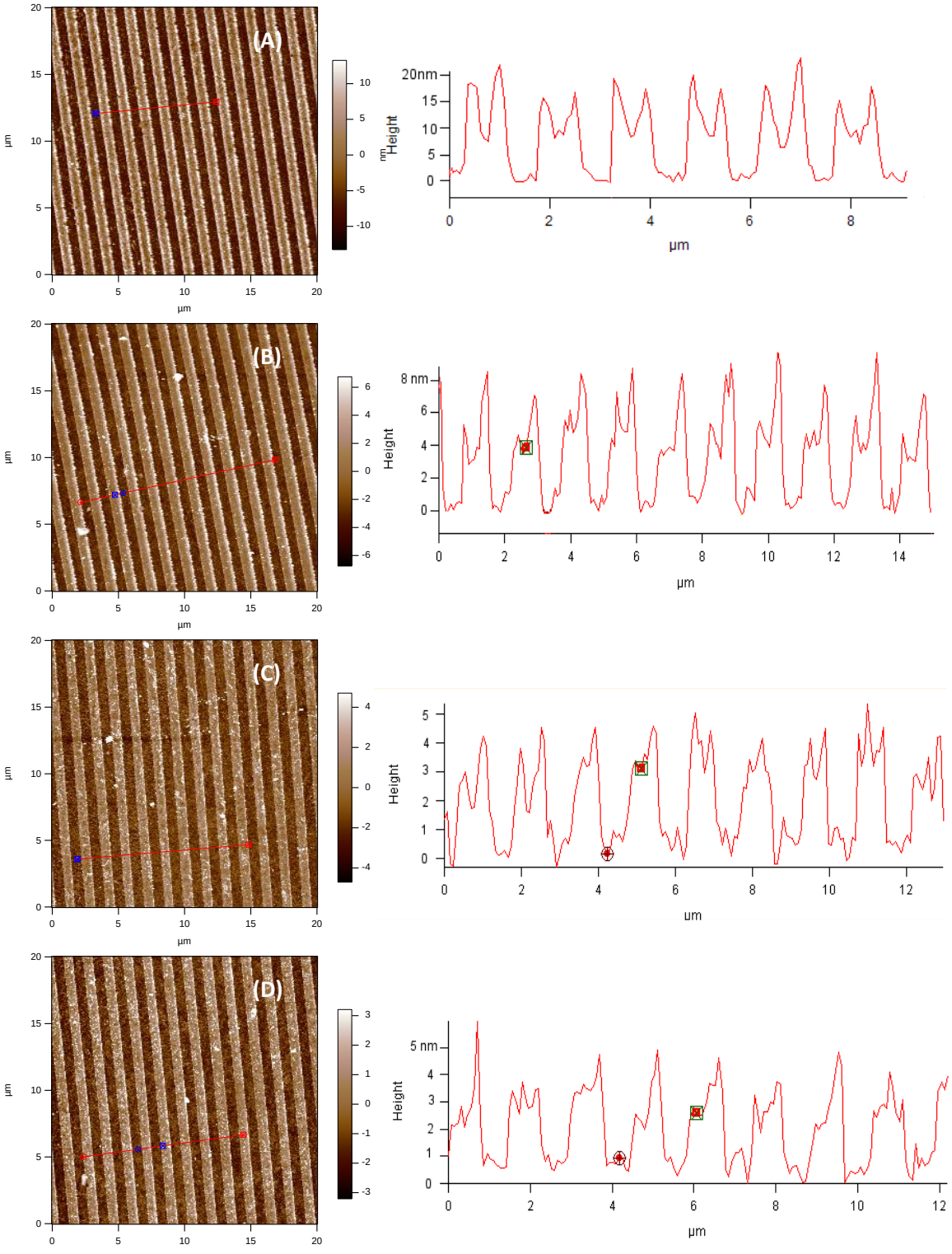

Figure 2.9 Effect of sonication in CH_2Cl_2 of the patterned ITO. **(A)** Pattern on ITO before solvent treatment. **(B)** After two min. sonication in CH_2Cl_2. **(C)** After two more min. (four min. total). **(D)** After four additional min. (eight min. total). The polycarbonate patterns show a remarkable stability against solvent treatment, and this method can actually be used to reduce and smooth the features thickness.

Fabrication of crosshatched lines

Changing the pattern of the polycarbonate stamp will afford different patterns on the ceramic surfaces. It is also possible to fabricate more complicated, 3-dimensional structures on substrates using polymer nanolithography, as demonstrated by the preparation of crosshatched patterns of polycarbonate on ITO. These structures are very easily obtained by successively stamping an ITO substrate with two different CD-R stamps. The processing conditions for the first stamping step are the same as describe before, while the best transfer for the second stamping step is achieved using slightly higher dwell temperature (115°C) and contact pressure (90 kPa) then those used for the first. AFM images of a characteristic crosshatched pattern obtained in this way are shown in Figure 5.10. The section analysis (Fig. 2.11) shows the usual thickness of ~10 nm for the first lines stamped with typical prominences arising from the separation of the stamp from the substrate. The second set of polycarbonate lines on the bare ITO surface are 25-30 nm thick and have similar roughness, thus the second stamping process deposits lines that are about 2-3 times as thick as the first on the bare ITO substrate. At the intersection where one line is on top of the other, the second set of lines is ca. 20 nm high measured from the top of the first lines. The overall feature height for the entire crosshatched pattern is about 30 nm and this likely represents the dead-bulk shear plane in the polycarbonate at the elevated temperatures and pressures used for the second stamping procedure. The serrated structure of the polymer pattern is thought to arise from the fracture during the stamp-substrate separation. Figure 2.9 reveals much larger protrusions at the intersection of the polymer lines, and we hypothesize that at this point the polymer

stretches more during separation as a consequence of the different interactions with the material underneath, ITO and polycarbonate.

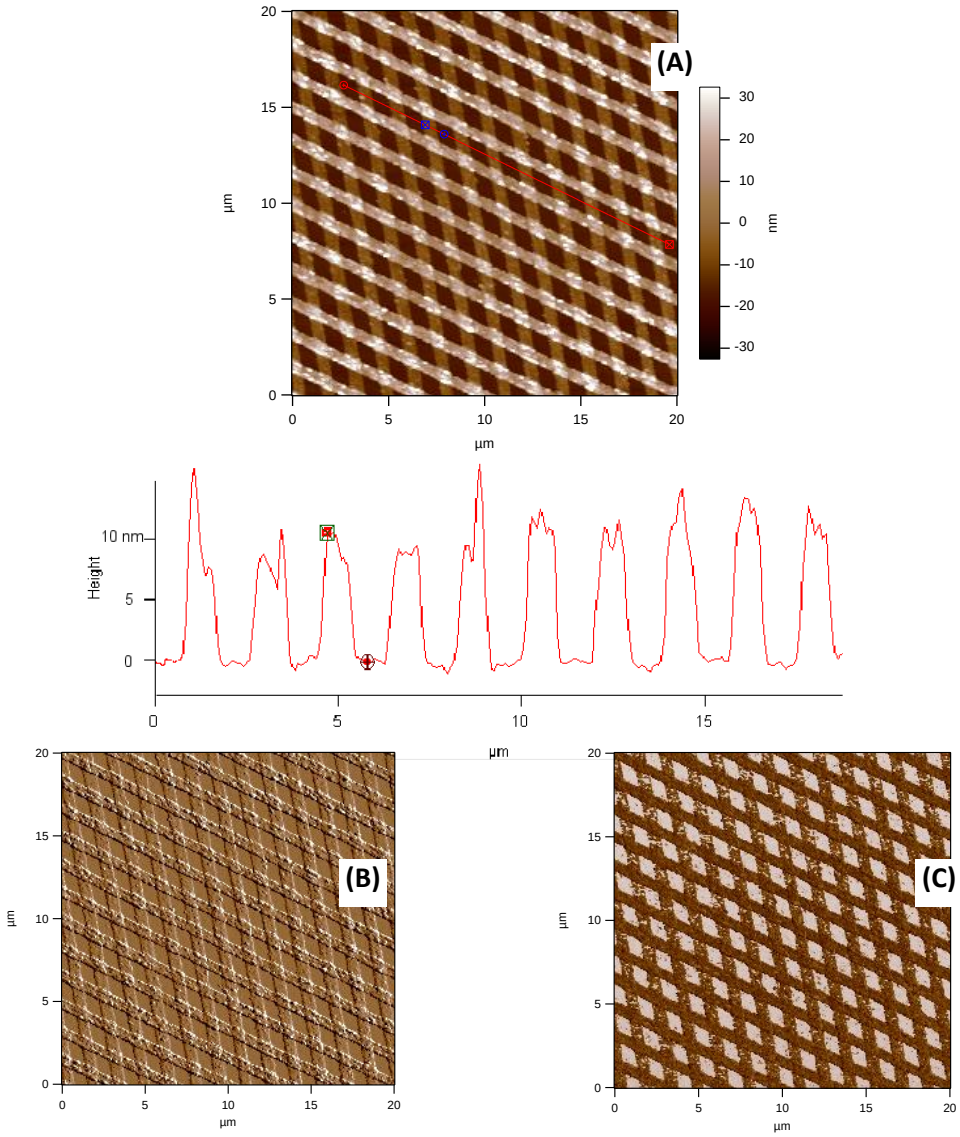

Figure 2.10 ITO patterned with crosshatched lines. AFM images acquired in tapping mode, (A) height image, (B) amplitude image, (C) phase image. The polymeric features on the substrate are well defined.

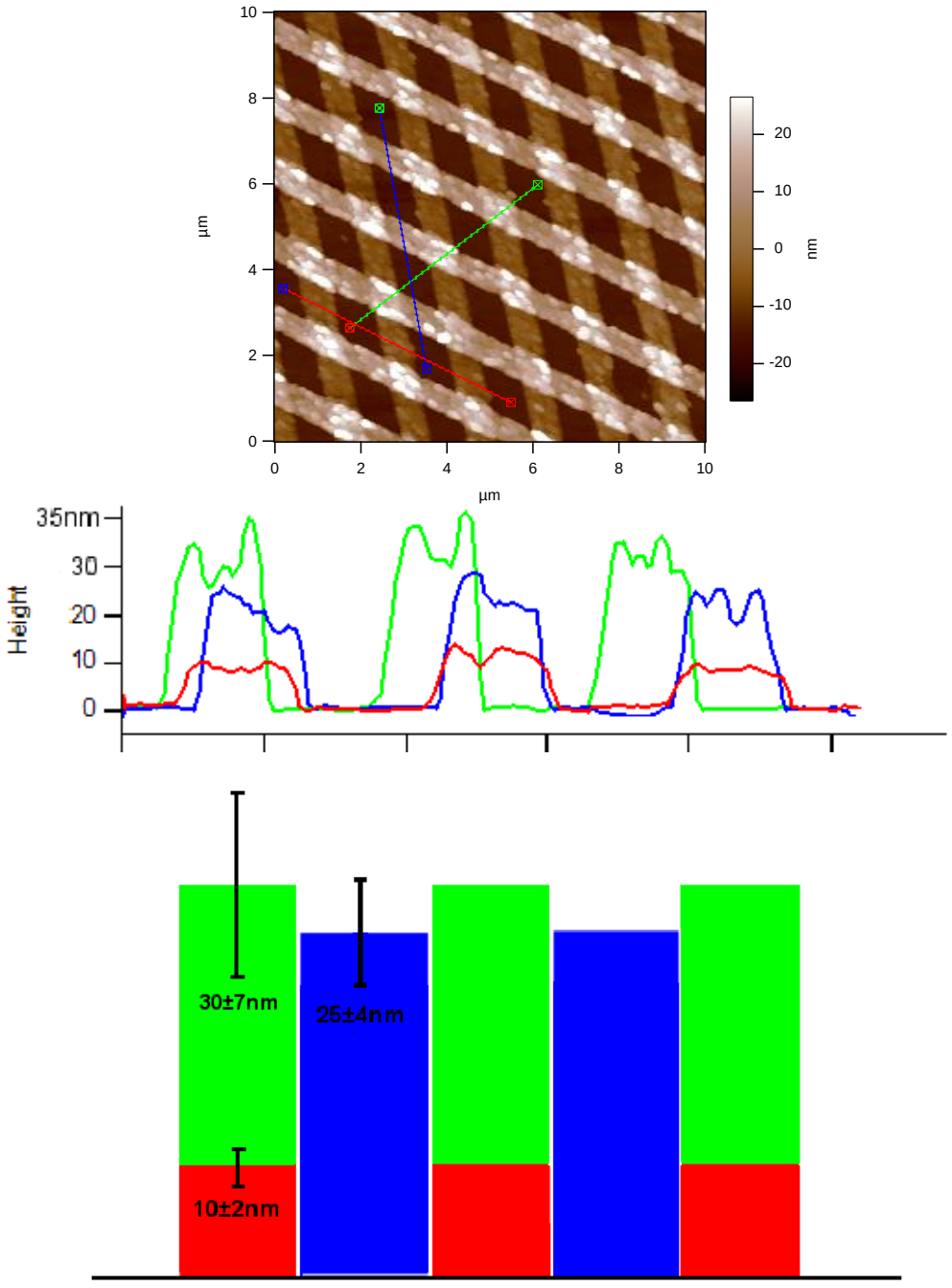

Figure 2.11 Detailed analysis of the crosshatched patterns indicate that under the elevated temperature and pressure of the second stamping step results in features with greater heights to yield a patterns of about 25-30 nm (see text). Bottom: schematic representation of the pattern profile. The colors correspond to the ones in the section analysis: initial stamp product (red), second stamp product on the substrate (blue), and second stamp product on top of the first (green).

The stamping process produces reproducible structures with high fidelity over large areas as shown by AFM images of a 50 µm x 50 µm area (maximum scan size of the instrument, Fig. 2.12A). Scanning electron microscope images also display the quality of the crosshatch pattern over 50 µm x 50 µm area and 300 µm x 300 µm area (Fig 2.12B-C). Optical microscopy indicates good quality structure over much of the substrate with domains of many mm^2. The SEM images were obtained without any previous preparation of the sample, since the polymeric features are only a few nm thick, it is not necessary to coat the sample with a layer of conductive material. The shadows present on Figure 2.12C are due to the previous SEM scans that left the polycarbonate partially charged.

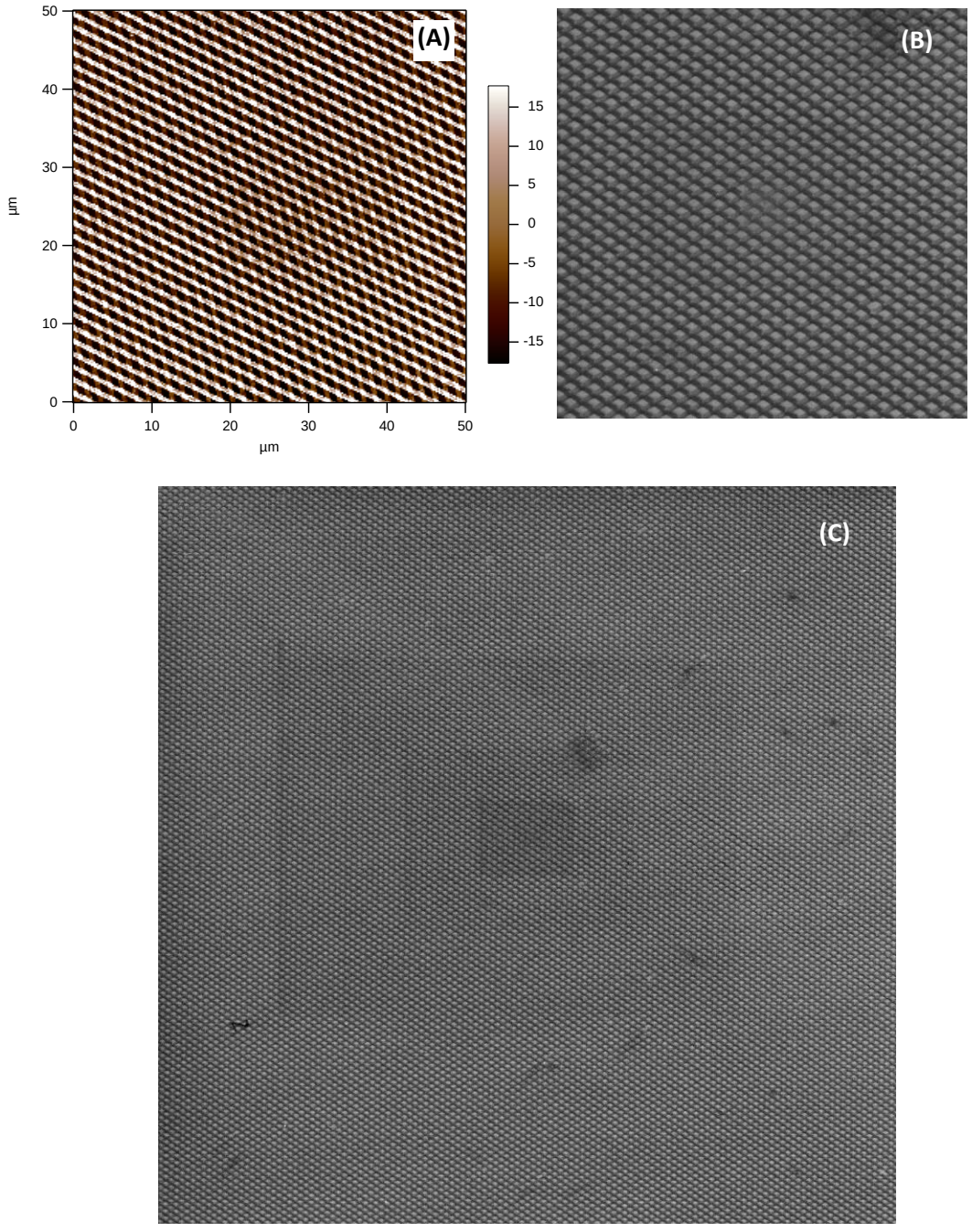

Figure 2.12 Surface coverage and fidelity of the crosshatch pattern. (A) AFM image over a 50 µm x 50 µm area. Scanning electron microscope images of a (B) 50 µm x 50 µm area, and (C) 300 µm x 300 µm area.

Fabrication of fluorescent patterns

As outlined in the introduction, there are numerous needs for nanoscaled patterns of fluorescent materials such as for OLEDs, sensors, and for other photonics applications. It has been shown that the products of polymer nanolithography can be subsequently modified.[38] Alternatively, the integration of a fluorescent dye into the thermoplastic stamp allows polymer nanolithography of molecularly doped structures.

The stamps can be doped with a fluorescent dye such as TCPP. The doped stamps have the characteristic UV-vis and fluorescence spectra for this molecule, and indicate that TCPP resides in the first few nanometers of the polymer. AFM analysis of the doped stamp shows that the doping treatment does not produce significant changes in the surface morphology of the stamp. The patterns fabricated using these TCPP-doped CD stamps were made under the usual stamping conditions (dwell time = 2 min., dwell temperature = 130°C) on ITO and produced fluorescent lines on the substrate that can be characterized by AFM and confocal microscopy. An example of these patterned fluorescent lines is shown in Figure 2.13, in which an image obtained with the microscope in reflectance mode is compared to the fluorescent image. The images show a part of the ITO with imperfect fabrication to appreciate the details of the fluorescence analysis. The florescent image is obtained using a 514 nm excitation wavelength, therefore exciting the TCPP on the first Q-band. (The confocal microscope does not have a laser at the wavelength of the Soret band.) Therefore even using a dilute solution of the porphyrin, and doping the polycarbonate for only a few seconds, lines with good fluorescence intensity were fabricated.

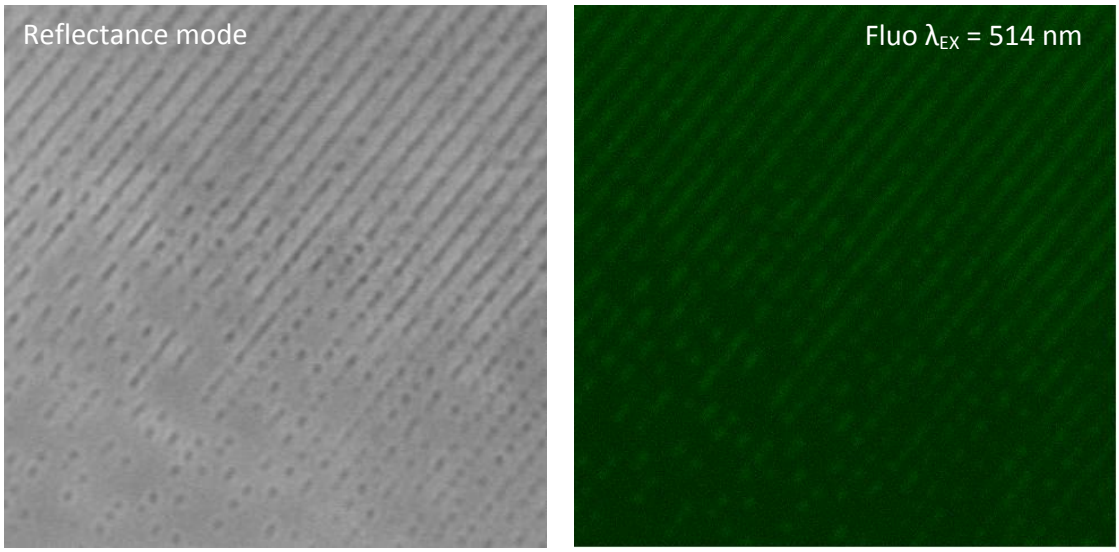

Figure 2.13 Pattern fabrication using a stamp doped with a fluorescent porphyrin produces fluorescent lines on ITO. Left: reflectance image of imperfect sample. Right: the corresponding fluorescent image, obtained using a 514 nm excitation wavelength. Images acquired with a Leica confocal microscope using a 63X objective. Images size: 40 μm x 40 μm.

Passivated Gold-Coated CD-R as template for stamp fabrication

To expand the use of the polymer nanolithography by thermal contact nanotransfer to polymers other than polycarbonate (CD-R) it is necessary to fabricate patterned polymer samples to use as a stamp. The simplest and most commonly used methods to replicate patterns, such as molding and embossing, utilize hard molds that are mostly made of Si or SiO_2, fabricated with traditional photolithography or related techniques. These masters can be quite expensive and difficult to find. Since we were interested in developing the methods rather than the exact topography of the stamp, we decided to use the gold-coated CD-R for this purpose. To avoid sticking of the molded polymeric material on the gold surface during the stamp preparation, a low surface

tension coating for the gold was prepared. Treatment with an alkanethiol forms a low surface energy SAMs on the gold limiting the strong tendency of adhesion of the polymer with the mold.

The covalently bonded SAMs are chemically and thermally stable, and this allowed the passivated gold-coated CD-R to be used multiple times for stamp preparation. The use of these gold-CD-R masters is limited by the thermal plastic properties of the polycarbonate (T_g = 145°C). Consequently, stamps can be prepared only using polymeric materials with a T_g below the polycarbonate T_g. We prepared a stamp of low density polyethylene (LDPE) by compression molding of 1.5 mm thick LDPE sheets, obtained from TAP Plastics (Figure A2.4). The T_g of LDPE is reported to be -20 °C. Variations in that value are reported to be from differences in crystallization. The sheet was cut into 22 mm x 22 mm pieces, rinsed with nanopure water, and dried with nitrogen gas. LDPE sheets were molded into stamps with the passivated gold CD-R (Figure 1). Before the sample was molded, the LDPE and passivated CD-R Gold were placed on the oven press for 5 min at 45 °C and 20 kPa to reach thermal equilibrium. The best conditions for stamp formation were found to be at 70 kPa and 80 °C for 12 minutes on the oven press. After the sample cooled to 22 °C, the pressure was slowly released. The LDPE stamp was easily removed from the CD-R Gold. By AFM, the passivated CD-R Gold was found to still have well intact, undamaged grooves, even after six molding procedures. This process yields a stamp that is a replica of the CD-R features with lines that are ~ 100 nm high.

Stamping lines of LDPE was more successful on ITO substrates than glass. ozone cleaned ITO was placed in an oven, at 120 °C, overnight. The hot ITO was immediately

placed on the oven press with the LDPE stamp above at 20 kPa and 45 °C for 2 minutes. The smaller equilibrium time was found to be important. The pressure was then increased to 90 kPa over 40 seconds, and the sample was held at 45 °C for another 3 minutes. The sample cooled to 22 °C on the oven press. AFM images showed lines of LDPE on areas of more than a square centimeter by optical microscope. These lines had a more jagged top than the polycarbonate lines by AFM (Figure A5.5) AFM images taken 2 days after fabrication, showed well formed lines that were 23 nm (± 7 nm) in height, with a pitch of 1.5 μm, and a width of 980 nm (± 50 nm). LDPE lines on different samples generally have three different morphologies: well formed lines, squished lines, and silhouette lines (see Appendix 2.6) Stored at room temperature, the lines tend to delaminate quickly from the ITO. After one month, line quality has diminished and patches of delamination are visible. Also, LDPE lines printed on plastic Lexan® (polycarbonate) sheets, result in a more stable pattern. These results will be presented in another work.

An annealing experiment was carried out by placing the LDPE printed ITO, in an oven overnight at 120 °C. AFM images of the resulting sample showed beads of polymer in place of the well formed lines (see Appendix 2.6). One could imagine that heating ITO printed samples could provide access to a mild removal method type mask for patterning. A simple wash with nanopure water was found to rinse a large amount of the LDPE on the ITO surface by optical microscopy.

2.4 Conclusions

A new polymer nanolithography technique has been presented. For certain applications, this fabrication process can be an alternative or complementary to other successful and widely used methods such as nanoimprint lithography. The numerous studies and many potential applications discussed in the introduction show the importance of fabrication of polymer nanopatterns and that each method has an array of advantages that are application and material dependent. The polymer thermal-contact nanotransfer demonstrated here can make nanofabrication accessible to many researchers without requiring special equipment, complex masters, or multistep processing, in contrast to many previously developed soft nanolithographic techniques. To make this method available to a broad cross section of the scientific community, it was designed such that readily available nanopatterned materials (e.g. CD and DVD) could be used as the stamp.

With this method, polymer patterns can be fabricate in a very fast manner (two minutes dwell time, ~15 minute total process time) using temperatures 20-30 °C below the polymers' T_g and at a relatively low pressure. This is in stark contrast to conventional NIL, which uses temperature 50-100 °C above the polymers' T_g. Moreover, the fabrication of multilevel patterns has been demonstrated to yield a simple means of fabricating three-dimensional polymer nanostructures. This latter aspect of the present method indicates that it can be used to stamp polymeric features on polymer substrate that possess higher T_g than the patterned polymer – thus allowing the fabrication of flexible samples.

We have focused on the formation of patterned lines on simple ceramic substrates created from commercial CD stamps to enable polymer nanolithography to be done routinely by almost any lab, but other patterns from polycarbonate are feasible, as are other substrates such as mica. More studies are necessary to evaluate the effect of the polymer molecular weight and the substrate on the thickness of the polymer patterns. The maximum thickness of the features is a limiting factor for this method as it is dictated by the thickness of the dead layer to ca. 5 – 20 nm for the polycarbonate used, but solvent treatment post fabrication allows the formation of structures that are just a few nanometers thick, and removed polymer can, in principle be recovered and recycled.

Future work will focus on the fabrication of patterned arrays of other polymers such as polystyrene, polyester, and conducting polymers. The use of dye-doped polymers or polymers containing other functional molecules can be used by this polymer thermal nanotransfer method. It remains to be seen if polymer blends, and block co-polymers can be used.

2.5 Chapter 2 References

(1) Special; Report *Technol. Rev.* **2003**, *106*, 36.

(2) Chou, S. Y.; Krauss, P. R.; Renstrom, P. J. *Science* **1996**, *272*, 85-87.

(3) Stephen Y. Chou, P. R. K. P. J. R. *Applied Physics Letters* **1995**, *67*, 3114-3116.

(4) Michael, D. A.; Haixiong, G.; Wei, W.; Mingtao, L.; Zhaoning, Y.; Wasserman, D.; Lyon, S. A.; Stephen, Y. C. *Applied Physics Letters* **2004**, *84*, 5299-5301.

(5) Dahl-Young, K.; Hong, H. L. *Applied Physics Letters* **1999**, *75*, 2599-2601.

(6) Heyderman, L. J.; Schift, H.; David, C.; Gobrecht, J.; Schweizer, T. *Microelectronic Engineering* **2000**, *54*, 229-245.

(7) Zankovych, S.; Hoffmann, T.; Seekamp, J.; Bruch, J. U.; Torres, C. M. S. *Nanotechnology* **2001**, *12*, 91-95.

(8) Jung, G. Y.; Li, Z.; Wu, W.; Chen, Y.; Olynick, D. L.; Wang, S. Y.; Tong, W. M.; Williams, R. S. *Langmuir* **2005**, *21*, 1158-1161.

(9) Khang, D. Y.; Kang, H.; Kim, T. I.; Lee, H. H. *Nano Lett.* **2004**, *4*, 633-637.

(10) Huang, X. D.; Bao, L. R.; Cheng, X.; Guo, L. J.; Pang, S. W.; Yee, A. F. *J. Vac. Sci. Technol. B* **2002**, *20*, 2872-2876.

(11) Dahl-Young, K.; Hong, H. L. *Applied Physics Letters* **2000**, *76*, 870-872.

(12) Baily, T.; Choi, B. J.; Colburn, M.; Meissl, M.; Shaya, S.; Ekerdt, J. G.;

Sreenavasan, S. V. *J. Vac. Sci. Technol. B* **2000**, *18*, 3572-3577.

(13) Menard, E.; Meitl, M. A.; Sun, Y.; Park, J. U.; Shir, D. J. L.; Nam, Y. S.; Jeon, S.; Rogers, J. A. *Chem. Rev.* **2007**, *107*, 1117-1160.

(14) Guo, L. J.; Cheng, X.; Chao, C. Y. *Journal of Modern Optics* **2002**, *49*, 663-673.

(15) Cheng, X.; Hong, Y. T.; Kanicki, J.; Guo, L. J. *J. Vac. Sci. Technol. B* **2002** *20*, 2877-2880.

(16) Austin, M. D.; Chou, S. Y. *Applied Physics Letters* **2002**, *81*, 4431-4433.

(17) Helt, J. M.; Drain, C. M.; Bazzan, G. *J. Am. Chem. Soc.* **2006**, *128*, 9371-9377.

(18) Helt, J. M.; Drain, C. M.; Batteas, J. D. *J. Am. Chem. Soc.* **2004**, *126*, 628-634.

(19) Forrest, J. A.; Dalnoki-Veress, K.; Dutcher, J. R. *Physical Review E* **1997**, *56*, 5705.

(20) Keddie, J. L.; Jones, R. A. L.; Cory, R. A. *Faraday Discussions* **1994**, 219-230.

(21) Horcas, I. *Rev. Sci. Instrum.* **2007**, *78*.

(22) Rice, R. W.; Sarode, D. V. *Ind. Eng. Chem. Res.* **2001**, *40*, 1872-1878.

(23) Zarnoch, K. P. *J. Adhesion Sc. Technol.* **1994**, *8*, 501-509.

(24) Yu, H. Z. *Anal. Chem.* **2001**, *73*, 4743-4747.

(25) *Eur. Phys. J. E* **2002**, *8*, 101-261.

(26) Fryer, D. S.; Nealey, P. F.; de Pablo, J. J. *Macromolecules* **2000**, *33*, 6439-6447.

(27) Ranjeet, S. T.; David, S. F.; Silvia, P.; Martha, F. M.; Juan, J. d. P.; Paul, F. N. *Journal of Chemical Physics* **2001**, *115*, 9982-9990.

(28) Yamamoto, S.; Tsujii, Y.; Fukuda, T. *Macromolecules* **2002**, *35*, 6077-6079.

(29) Fryer, D. S.; Peters, R. D.; Kim, E. J.; Tomaszewski, J. E.; de Pablo, J. J.; Nealey, P. F.; White, C. C.; Wu, W. l. *Macromolecules* **2001**, *34*, 5627-5634.

(30) *Springer Handbook of Nanotechnology*; 1 ed.; Bhushan, B., Ed.; Springer: Berlin, 2004.

(31) Durig, U.; Cross, G.; Despont, M.; Drechsler, U.; Haberle, W.; Lutwyche, M. I.; Rothuizen, H.; Stutz, R.; Widmer, R.; Vettiger, P.; Binnig, G. K.; King, W. P.; Goodson, K. E. *Tribology Letters* **2000**, *9*, 25-32.

(32) DeMaggio, G. B.; Frieze, W. E.; Gidley, D. W.; Zhu, M.; Hristov, H. A.; Yee, A. F. *Physical Review Letters* **1997**, *78*, 1524-1527.

(33) Fukao, K.; Miyamoto, Y. *Physical Review E* **2000**, *61*, 1743-1754.

(34) Abrams, C. F.; Site, L. D.; Kremer, K. *Physical Review E (Statistical, Nonlinear, and Soft Matter Physics)* **2003**, *67*, 021807.

(35) Soles, C. L.; Douglas, J. F.; Wu, W. l.; Peng, H.; Gidley, D. W. *Macromolecules* **2004**, *37*, 2890-2900.

(36) LeGrand, D. G.; Bendler, J. T. *Handbook of Polycarbonate Science and Technology*, 2000.

(37) Araki, K.; Wagner, M. J.; Wrighton, M. S. *Langmuir* **1996**, *12*, 5393-5398.

(38) Beinhoff, M.; Appapillai, A. T.; Underwood, L. D.; Frommer, J. E.; Carter, K. R. *Langmuir* **2006**, *22*, 2411-2414.

2.6 Appendix 2.1

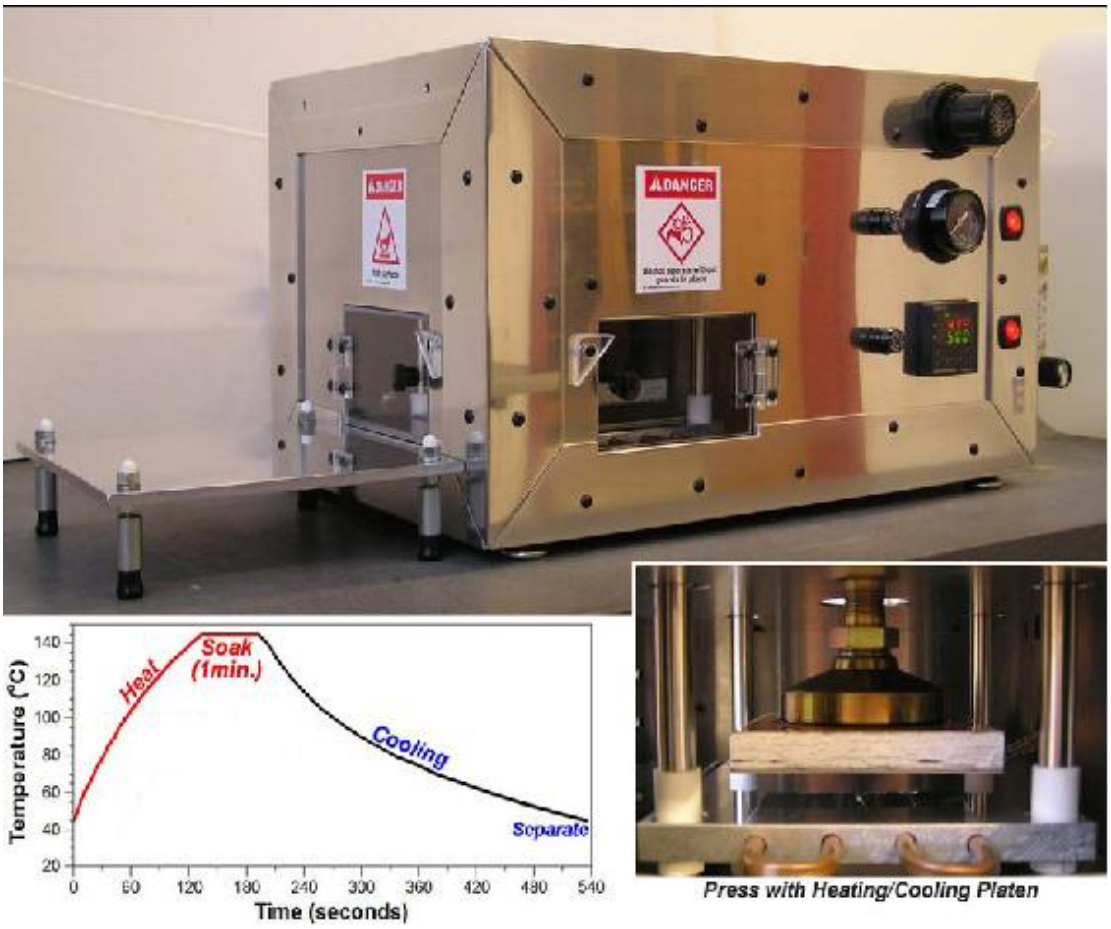

Figure A2.1 Top and right are photos of the home-built stamping apparatus. The right shows the pressure cell and heating platen. Bottom left: the graph of a typical temperature program used during thermal nanotransfer fabrication, showing 1 minute of dwell time. (Taken from Ref. 17)

Specifications for the custom pneumatic press used for the thermal synthesis and transfer of materials to and from polymers (T-STOMP) are provided in Table 2.1. A picture of the press is also provided in Figure A2.1.

Table A2.1 Specifications for Heated Pneumatic Press

Property	**Value**
Maximum compressive load	8,200 N
Wafer diameter capacity	100 mm
PID controlled programmable temperature segments	16
Heating Platen Power	1000 watts
Maximum operating temperature *(20 minutes)*	185°C
Maximum Heating Rate with Coolant flow >10 GPH	46°C/min
Dwell temperature overshoot during initial ramp	0.4 - 1.2°C
Critical cooling rate with coolant flow >10 GPH (21°C Water Coolant)	

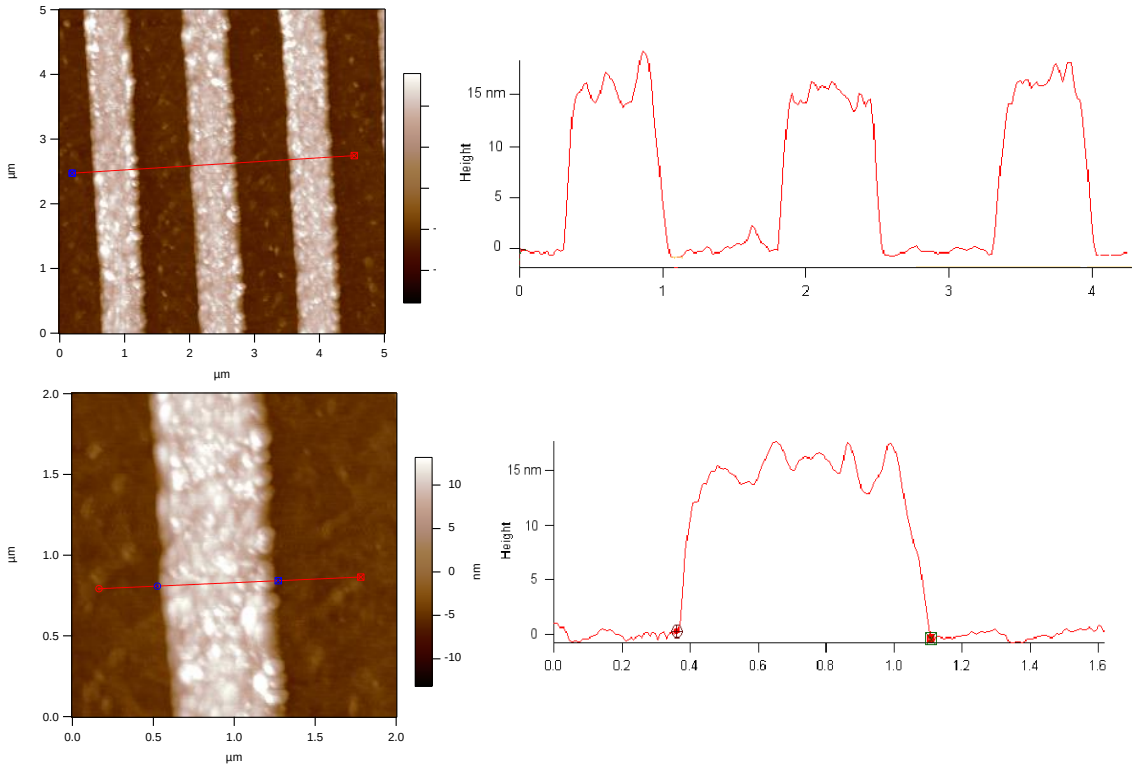

Figure A2.2 Details of the polymer lines fabricated on ITO using a CD-R stamp (dwell temperature of 130°C and a dwell time of 2 minutes). AFM images acquired in tapping mode, height image and section analysis. The polymeric features on the substrate are well defined with a typical height of 12-15 nm.

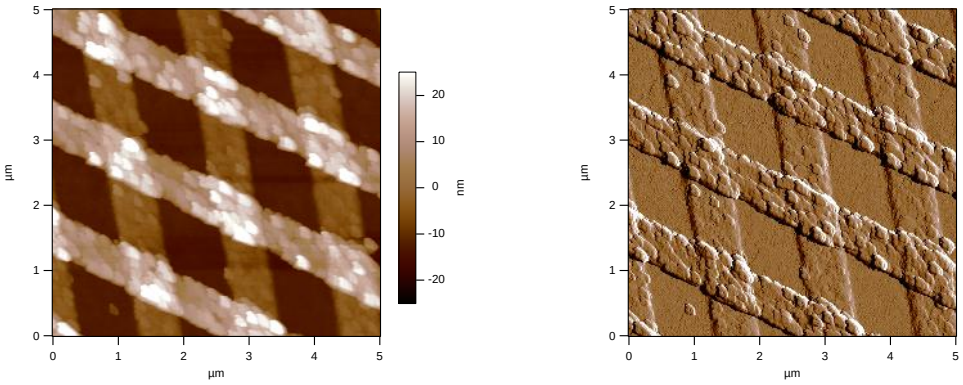

Figure A2.3 Details of the crosshatched polymer lines fabricated on ITO using a CD-R stamp (dwell temperature of 130°C and a dwell time of 2 minutes). AFM images acquired in tapping mode. Left: height image. Right: amplitude image.

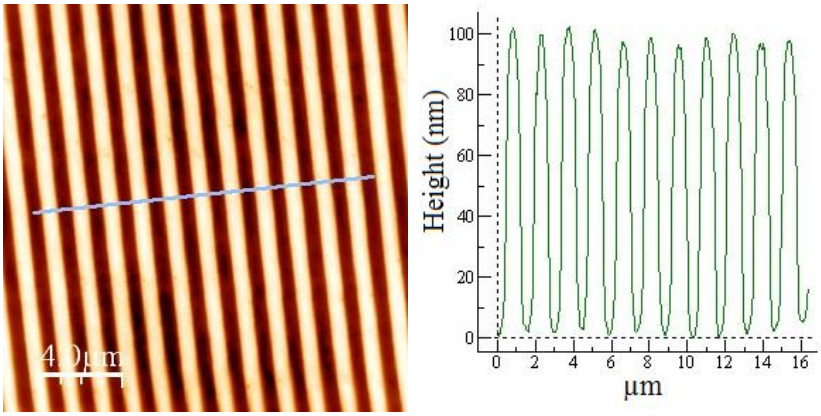

Figure A2.4 AFM images of low density polyethylene stamp prepared using passivated gold-coated CD-R as template formed by compression molding of LDPE sheets at 80°C for 12 minutes under an applied pressure of 70 kPa.

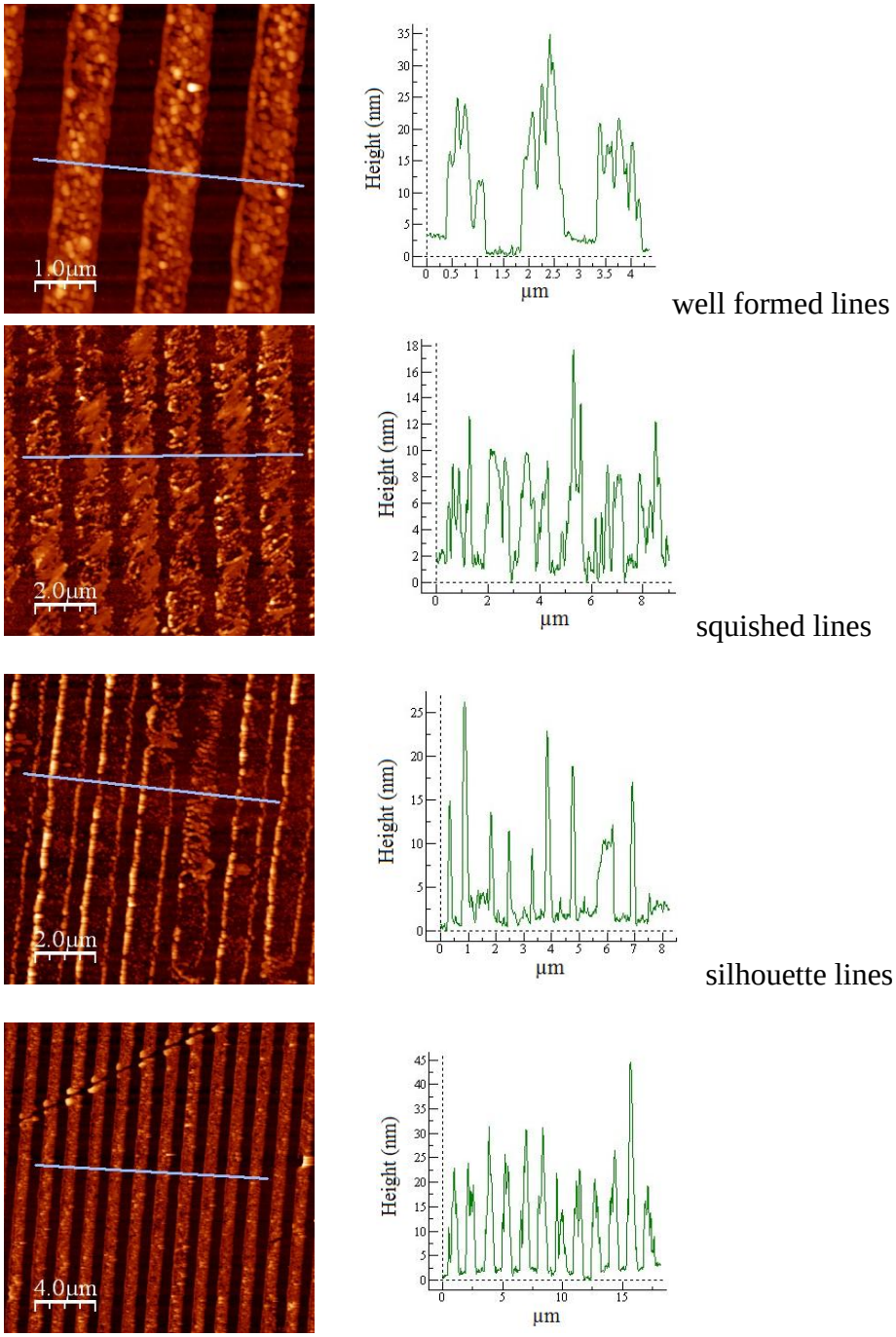

Figure A2.5 These AFM images are from the same sample. A polyethylene stamp was printed on ITO. There are 3 typical line structures, as seen above. The most well formed lines are more difficult to reproduce. A hot piece of ITO and a LDPE stamp were placed on the oven-press for 2 minutes at 45°C and 20 kPa. The pressure was increased to 90 kPa over 40 sec and maintained at 45°C for 220 seconds more. The sample was cooled to room temperature and gently pulled apart.

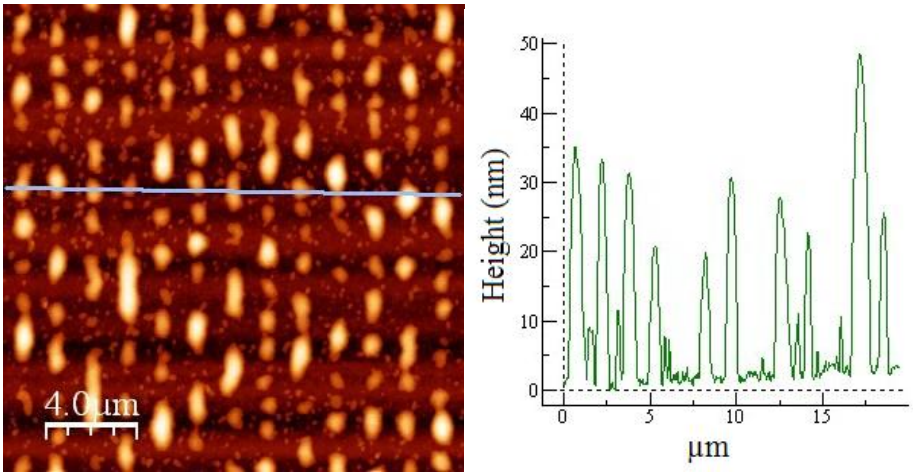

Figure A2.6 AFM image of the annealed low density polyethylene lines on ITO.

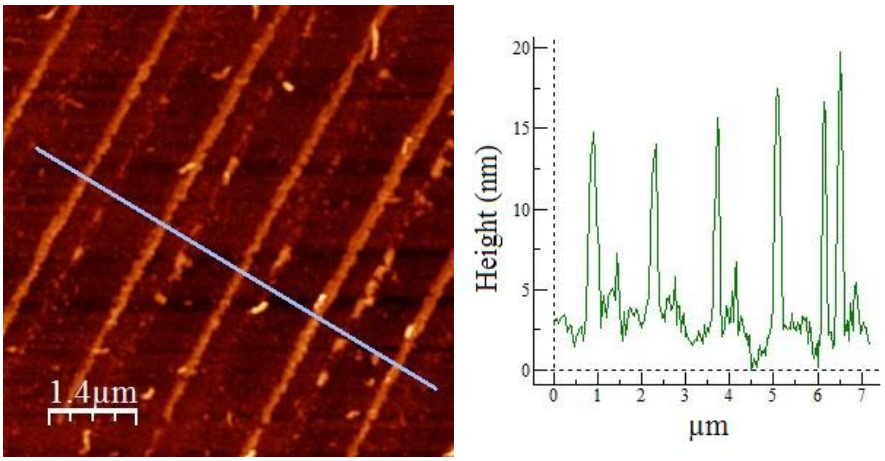

Figure A2.7 Scotch Tape Delaminated CDR printed on ITO

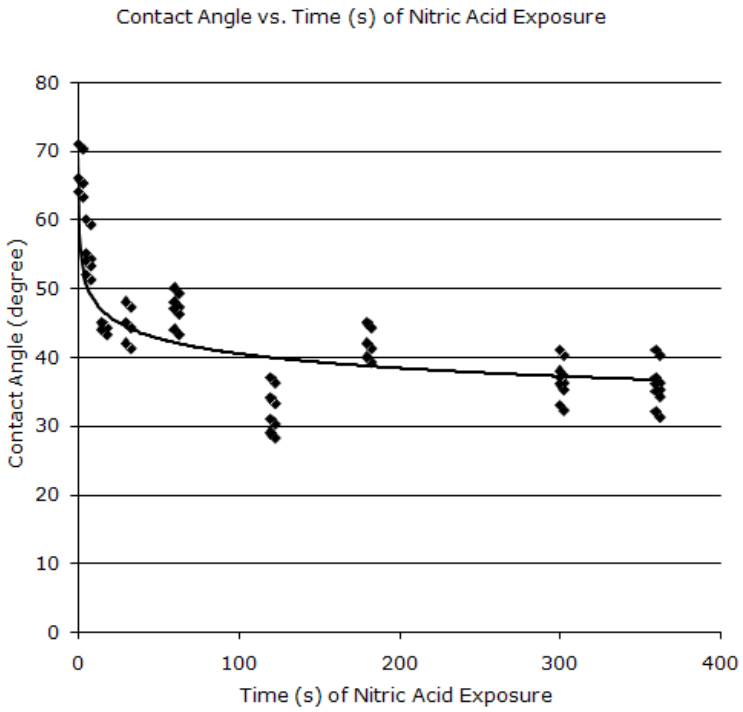

Figure A2.8 CD-Rs were exposed to increasing amounts of time in concentrated nitric acid. All pieces were rinsed with tap water for 5 minutes, followed by a brief rinse with nanopurified water. CD-R pieces were dried with argon. Qualitatively, with increasing time in nitric acid, the polycarbonate becomes more hydrophilic. Data is fit to a power curve.

2.7 Appendix 2.1

Chemical Analysis of Nitric Acid Treated CD-Rs

Introduction:

Building upon earlier results with nitric acid in the Drain lab, nitric acid treated CD-Rs have been observed to print at lower temperatures (a difference of 20 degrees) and with greater coverage (greater than 1 square centimeter) than CD-R's not treated with nitric acid. In order to have access to CD-R stamps without nitric acid, the top layers of lacquer and aluminum are removed with scotch tape. Even CD-Rs that have been treated with scotch tape, and then treated with nitric acid, print from edge to edge of the stamp. The presence of the aluminum layers during the acid delamination is not necessary for improved printing. With contact angle observations, the surface energy of the CD-Rs appears to be increasing with increasing nitric acid exposure.

CD-Rs are made of the polymer, polycarbonate, which consists of bisphenol A units linked with carbonate functional groups (Fig. A2.1). Questions were asked about how nitric acid was chemically modifying this polymer in order to lead to enhanced printing.

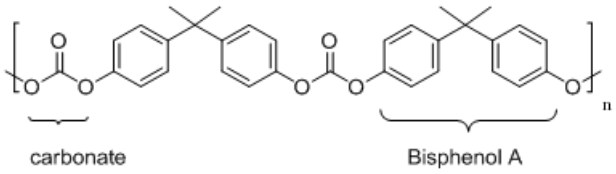

Figure A2.1: Structure of polycarbonate.

In the literature, concentrated nitric acid can chemically modify a polymer simply by donating protons to activate acid labile functional groups, oxidation, or nitration.[1] Bornmann and Wolf found that concentrated nitric acid was clearly nitrating an epoxy resin which contained aromatic amino groups, which are more electron donating and activating, than the phenols of polycarbonate[1]. Zarnoch reported that a 1:2 mixture of concentrated nitric and sulfuric acid (2-5 minutes at room temperature) was effective towards providing two nitro groups for every surface-exposed bisphenol A unit.[2] According to Zarnoch, the thin metal layer, that was anticipated to adhere to this nitrated polycarbonate surface, was unfortunately still easily removed. Nonetheless, this was overcome by treating the heavily nitrated polycarbonate surface with ammonium hydroxide and potassium hydroxide. The electron withdrawing quality of the nitro groups caused the polycarbonate to go through ammonolysis more easily in order to provide a surface covered in either phenol or nitrophenol functionality. Consequently, the increased hydrophilicity of the surface gave a contact angle of 0°C. In addition, when dried, the contact angle changed to greater than the original polycarbonate material, which suggested to the authors that the phenol polymer ends rearranged on the polymer surface, during this drying step. Consequently, these polycarbonate surfaces were not dried before the metallization step. The author also noted that nitrations of aromatic groups are most successfully completed with mixtures of nitric and sulfuric acids, as well as nitric acid and acetic anhydride.[2] Furthermore, concentrated nitric acid is normally not enough to fully nitrate a surface, without activation by strong electron donating groups, such as amino functional groups. Usually large scale nitration does not occur with only concentrated nitric acid.[1]

Zarnoch's method of utilizing 2:1 sulfuric and nitric acid was applied to CD-Rs. The CD-R's lost transparency and turned yellow. AFM data showed a highly pitted surface, and lines which were at least 100 nm shorter than before. Since the purpose for the CD-Rs, was for stamping, treating the CD-Rs with ammonium hydroxide made less sense, due to the inevitable drying step before printing. In addition, simple nitric acid treatment provides easily reproducible patterns and good coverage.

In addition, in 1969, a synthesis for nitrated polycarbonate by Sulzberg and Cotter consisted of nitrating bisphenol A before polymerizing.[3] From this paper, UV-visible and infrared data were obtained. Dinitrobisphenol A absorbs at 284 nm and 368 nm in chloroform. The second absorbance was particularly useful for searching for expected chemical traces of nitration. Furthermore, polymerized dinitrobisphenol A displays nitro group stretching at 1519 cm^{-1} and 1342 cm^{-1} in infrared spectra.[3]

Chemical Analysis of CD-Rs Treated with Nitric Acid

Experimental

Aluminum coated writable compact discs (CD-Rs) were cut into 2.5 cm x 2.5 cm pieces. One CD-R was completely submerged in concentrated nitric acid for 5 minutes, rinsed with tap water for 5 minutes, briefly rinsed with nanopurified water, and dried with a filtered nitrogen gas stream. The other CD-R was delaminated with scotch tape, rinsed with absolute ethanol, rinsed with tap water for 5 minutes, briefly rinsed with nanopurified water, and dried with a filtered nitrogen gas stream. Each CD-R was briefly rinsed (pattern side only) with dichloromethane (DCM) into a 50 mL beaker. Half of a Kim Wipe was folded and used to further wipe away the top patterned CD-R layer. The

Kim Wipe was placed in the beaker, covered in DCM and sonicated for 1 minute. The UV-visible spectrum was taken for each CD-R solution. In addition, a thin film of each solution provided an infrared spectrum. XPS experiments were conducted for CD-Rs prepared in the same way, but without the dichloromethane step.

Results and Discussion

The spectrum for the scotch tape delaminated (no nitric acid) CD-R was subtracted from the nitric acid treated CD-R spectrum (Fig. A2.2). A small peak was observed at 367 nm in dichloromethane, which corresponds to published data for nitrated bisphenol A at 368 nm in chloroform. A large amount of nitration would not be expected for this procedure. The concentration of nitration was calculated to be 1μM. The concentration of polycarbonate was calculated to be 0.2 mM, which provides that nitration is at trace levels of 0.5%, by this method (Fig. A2.2).[4] Also at longer wavelengths, peaks for a phthalocyanine dye were observed for the scotch tape (no nitric acid) CD-R, which shows that traces of this nitrogen containing dye were still present after this procedure. Any comparisons based on nitrogen content (such as XPS) are made difficult by this component of commercially prepared CD-Rs.

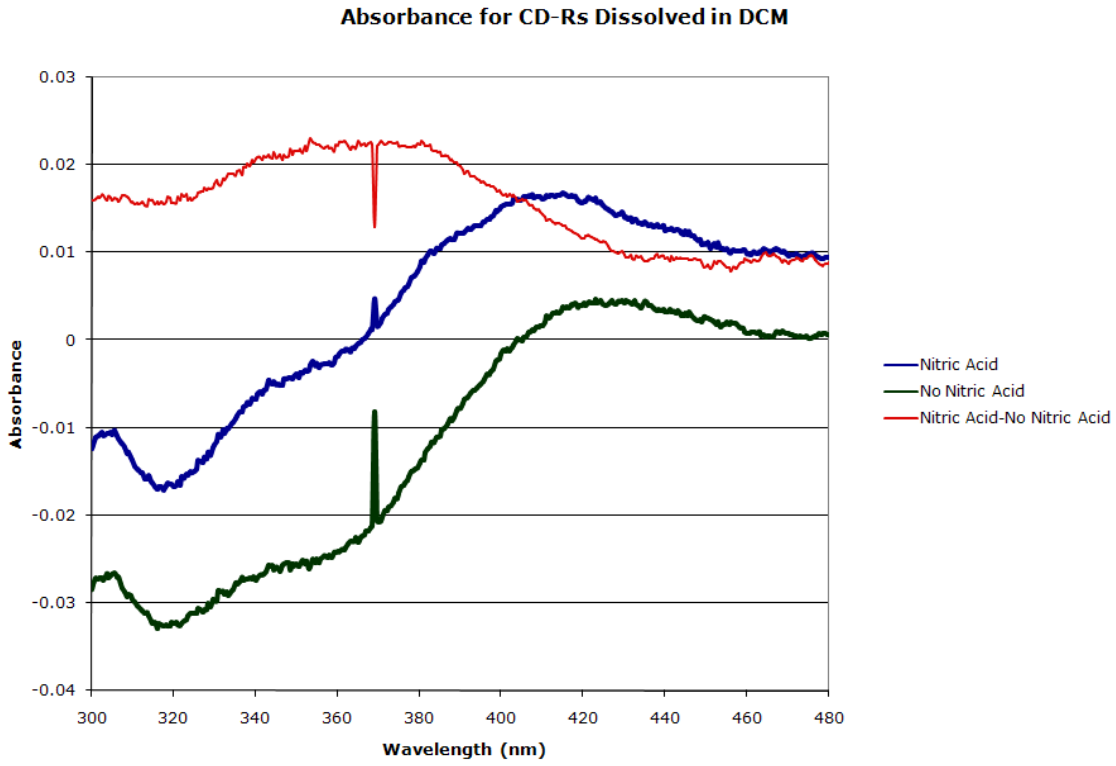

Figure A2.2: (red) Top trace is the result of subtracting the scotch tape (no nitric acid) treated CDR from the nitric acid treated CD-R spectrum. (blue) Second trace from the top is the nitric acid treated CD-R. (dark green) Bottom trace is the scotch tape (no nitric acid) treated CD-R. Absorbance at 367 nm is observed (red trace) for nitration.

Infrared spectra were taken for the nitric acid treated CD-R and the scotch tape (no nitric acid) treated CD-R (Fig. A2.3,4). Both spectrums matched the published (Aldrich FT-IR Collection) spectra for polycarbonate (Fig. A2.6). No obvious nitro stretches were observed at 1519 cm^{-1} and 1342 cm^{-1}, as seen in the literature for nitrated polycarbonate (Fig. A2.8).[3]

With the absence of obvious nitro group stretches, the spectra were scrutinized for other differences. First the spectra were subtracted from each other (nitric acid CD-R spectra – scotch tape CD-R spectra) (Fig. A2.5). No notable new peaks were observed, but the spectra were slightly shifted with nitric acid treatment. Secondly, the aromatic

C=C stretch peak's intensity at 1500 cm^{-1} was compared to the relative intensity of the carbonate C=O peak at 1780 cm^{-1} for both CD-Rs. If nitric acid is activating the hydrolysis of some the carbonate groups, increasing surface exposed phenols, a decreased ratio in the intensity of the C=O peak to C=C peak would be observed for the nitric acid treated polycarbonate. Since the C=C peak is dependent on the aromatic rings, this peak intensity was not expected to change with nitric acid treatment. Based on the peak intensities, there was 3% less carbonyl groups compared to aromatic groups in the nitric acid treated CD-R, which indirectly translates to a greater number of phenol groups. Third, the relative width to length of the peaks was examined. The nitric acid treated CD-R spectra peaks are broader. Perhaps this was due to minor oxidation of the polymer and / or collective effects of trace nitration. Other than these trace differences, the spectra are very similar and match the literature for polycarbonate. A comparison with the literature reported spectra of bisphenol A was also examined (Fig. A2.7). There are no peaks (except the O-H stretch) that are notably different between the spectra of polycarbonate and bisphenol A. All of the peaks seen in bisphenol A appear in polycarbonate, except with different intensities. Finding a direct peak for greater phenol content was not possible. There is obvious error in measuring IR peaks for comparison at such trace differences, but it appears that there is a small amount of hydrolysis of the polymer based on this method.

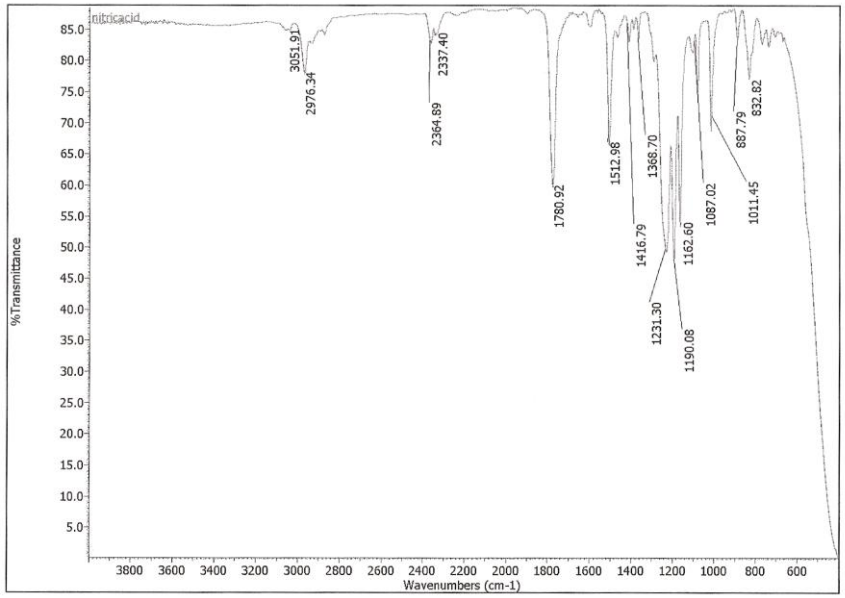

Figure A2.3: Infrared trace for a thin film from a nitric acid treated CD-R dissolved in dichloromethane.

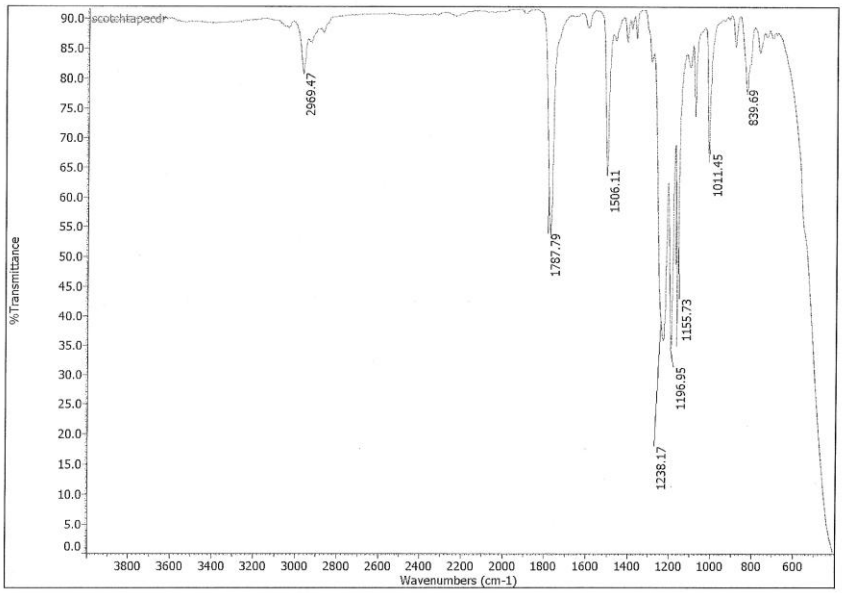

Figure A2.4: Infrared trace for a thin film from a scotch tape (no nitric acid) treated CD-R dissolved in dichloromethane.

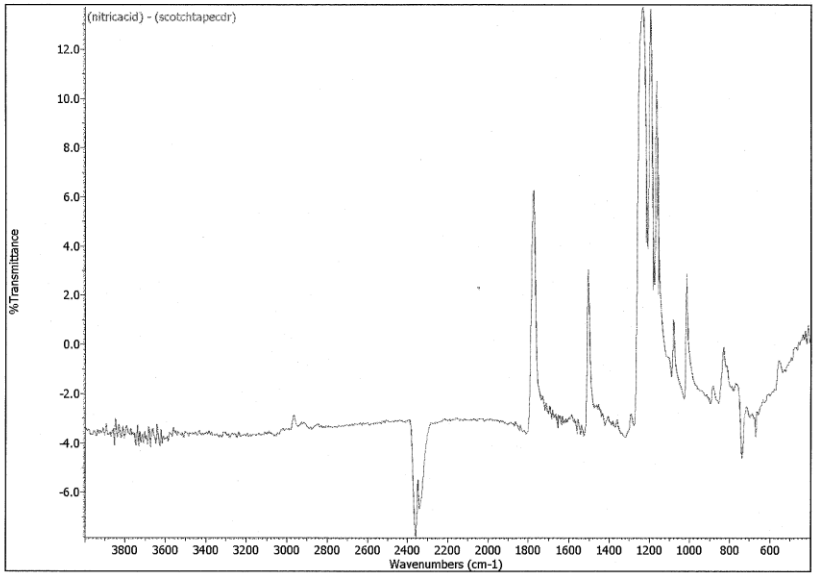

Figure A2.5: Infrared trace for the subtraction of the scotch tape (no nitric acid) trace from the nitric acid treated CD-R trace.

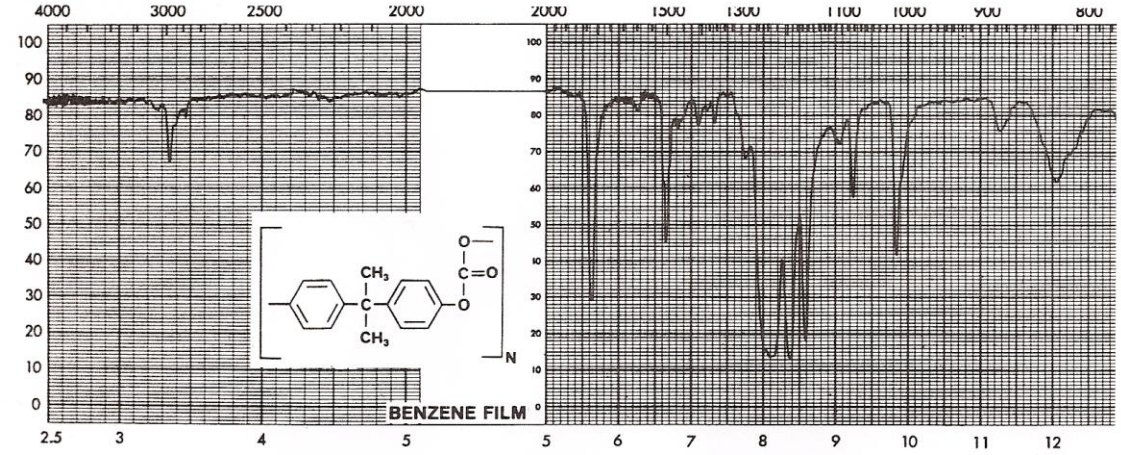

Figure A2.6: Infrared trace of low molecular weight polycarbonate. (Aldrich FT-IR Collection)

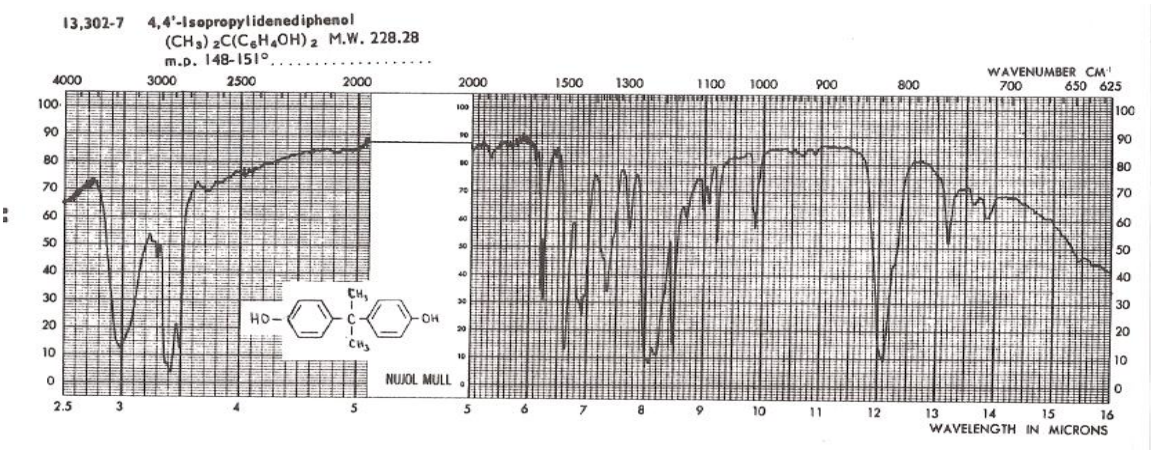

Figure A2.7: Infrared trace of bisphenol A. (Aldrich FT-IR Collection)

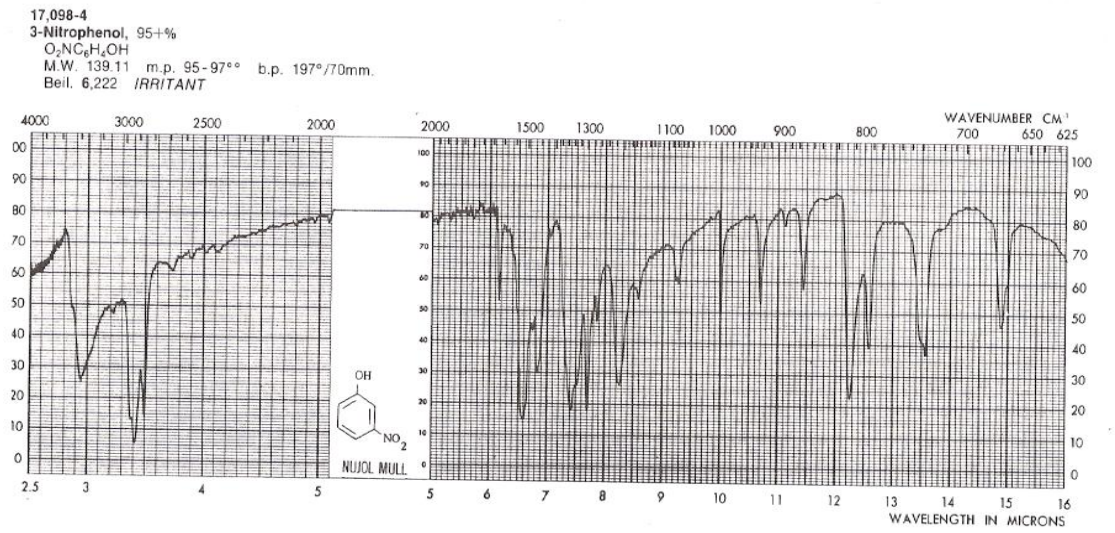

Figure A2.8: Infrared trace of 3-nitrophenol. (Aldrich FT-IR Collection)

X-ray photoelectron spectroscopy (XPS) was also conducted for a nitric acid treated CD-R and a scotch tape (no nitric acid) treated CD-R (Fig. A2.9, 10). Both spectra also displayed peaks for carbon at 285 eV and oxygen at 533 eV.[5] In addition, both spectra also contained nitrogen at 400 eV.[5] Nitrogen in the scotch tape (no nitric acid) treated CD-R could be explained by residual phthalocyanine dye present in the

scotch tape treated CD-R, which is added to writable CD-Rs and contains nitrogen. By UV-visible, the trace of this compound is observed. By UV-visible, no phthalocyanine dye is observed for the nitric acid treated CD-R. Presumably any new nitrogen would be from nitro functional groups.

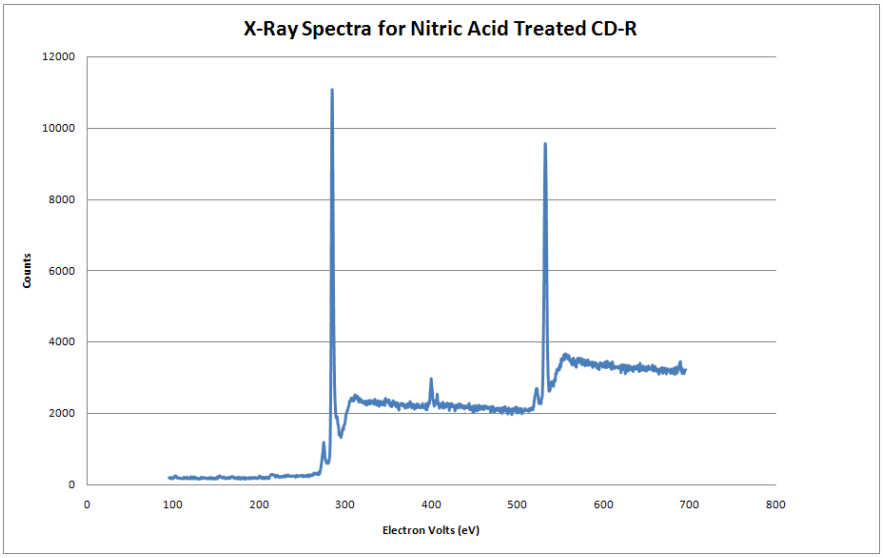

Figure A2.9: X-ray photoelectron spectra for a nitric acid treated CD-R.

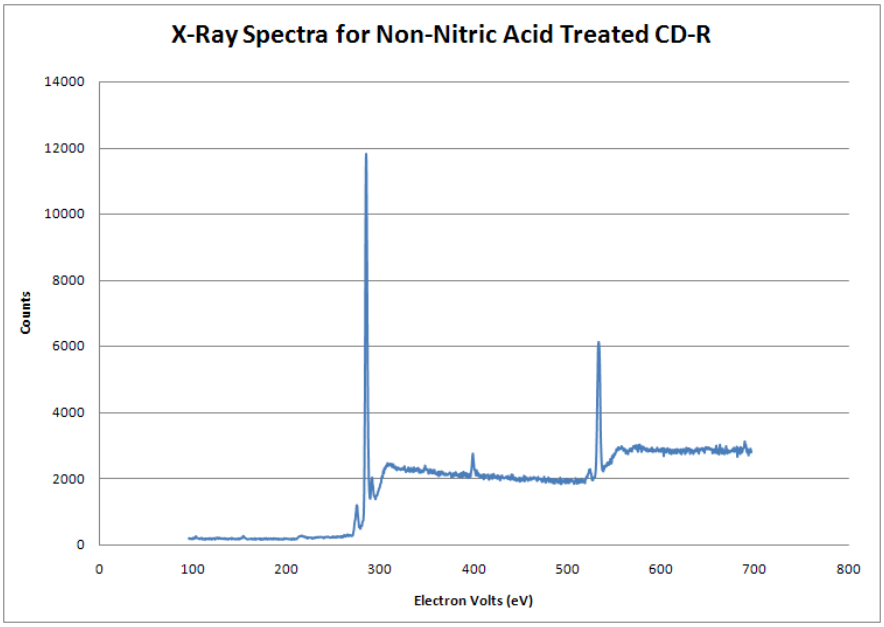

Figure A2.10: X-ray photoelectron spectra for a scotch tape (no nitric acid) treated CD-R.

Summary

Based on UV-visible spectroscopy, 0.5% of the nitric acid treated polycarbonate is nitrated. Based on IR spectroscopy, no nitro peaks are observable, but a 3% decrease in the ratio of carbonyls to aromatic groups indirectly points to greater phenol content, due to hydrolysis from nitric acid. Lastly, XPS does indicate the presence of nitrogen in nitric acid treated CD-Rs, which would not exclude the minor presence of nitro groups on the surface. Such seemingly small chemical changes translate to enhanced printing of CD-Rs.

A2.1 Appendix 2.7 References

(1) Bornmann, J. A.; Wolf, C. J. *Journal of Polymer Science: Polymer Chemistry Edition* **1984**, *22*, 851-856.

(2) Zarnoch, K. P. *J. Adhesion Sc. Technol.* **1994**, *8*, 501-509.

(3) Sulzberg, T.; Cotter, R. J. *Polymer Letters* **1969**, *7*, 185-191.

(4) Sivalingham, G.; Madras, G. *Applied Catalysis A : General* **2004**, *269*, 81-90.

(5) Wikipedia *Wikipedia The Free Encyclopedia* **2010**.

Chapter 3

Further Developments for CD-R Derived Polymer Nanolithography

3.1 Abstract

The ability to manipulate polymers at the nanoscale, in order to make patterns has been pursued by many different types of nanofabrication technologies, such as laser ablation, nanoimprint lithography, photolithography, microcontact printing, and micromolding in capillaries.[1-6] Polymers can provide device insulation,[7] segregation of dyes,[6] scaffolds for nanoparticles,[8] band gap separation between conductive materials, and bring inherent conductivity in themselves.[5] This work explores fabricating nanostructured replicas of simple and inexpensive writable compact discs (CD-Rs). The polymer, polyaniline (PANI) emeraldine base was patterned and through small changes in stamp preparation, a method towards modulating polymer line widths from 900 nm, to lines of 175 nm was also developed.

3.2 Introduction

Nanolithography implies the printing of structures with at least one dimension less than 100 nm. In our laboratory, Dr. James Helt developed a process of printing gold nanowires insulated by polycarbonate from gold sputter-coated polycarbonate compact discs.[9,10] Following this, further investigations were directed towards the printing of the original compact disc polycarbonate lines (Fig. 3.1). In addition, a method for molding polymers, other than polycarbonate, was explored by passivating commercially available

gold-coated CD-Rs with 1-octanethiol (Fig. 3.2). The resulting polymer stamps of other plastics have been printed on glass, indium tin oxide (ITO), and Lexan®.

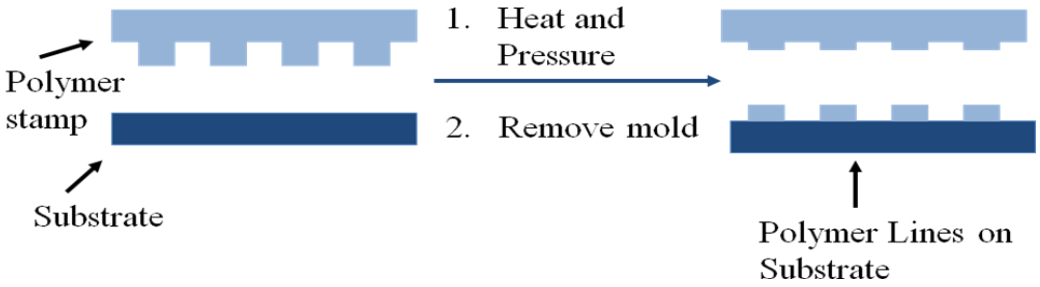

Figure 3.1 Schematic representation for CD-R derived polymer printing.

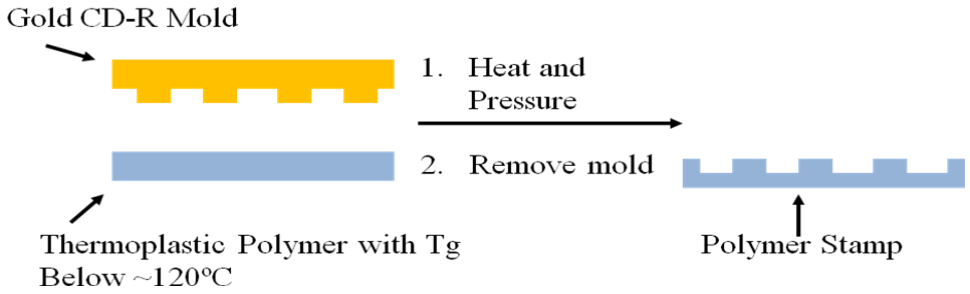

Figure 3.2 Passivated commercially available gold CD-Rs function as a mold for polymers of a lower Tg than polycarbonate. (Tg for PC is ~150 °C.)

In previous work, aluminum coated CD-R pieces were submerged in nitric acid. The CD-R's layers of lacquer, aluminum, and phthalocyanine were removed to reveal the bare polycarbonate lines. Concentrated nitric acid is known to nitrate aromatic functional groups. In general, polycarbonate is synthesized by reacting bisphenol A with phosgene (Fig. 3.3).[11] Polycarbonate has activated aromatic rings and carbonate groups, which could participate in nitration.[12] In addition, polymer breakdown might result, due to acid activation of the carbonate group and a loss of carbon dioxide. Contact angle experiments

conducted for increasing exposure time to nitric acid, have shown that the polycarbonate CD-R surface becomes more hydrophilic. CD-R masters prepared in this manner leave replica lines of 900 nm wide by 15 nm high and 600 nm apart with greater than 1cm^2 coverage.

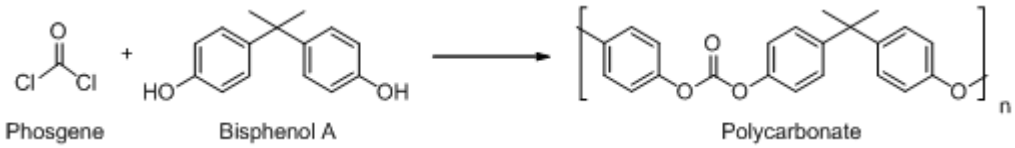

Figure 3.3 Typical synthesis of polycarbonate and structure.

A new method, which uses the same inexpensive aluminum coated CD-R material, has been developed to obtain lines from 200-500 nm in width, depending on printing conditions. If the aluminum and lacquer layer are removed by applying scotch tape, the polycarbonate lines are left with jagged edges. The CD-R is then submersed in nitric acid for 2 minutes, rinsed and dried to give a stamp. The CD-R edges are then printed with heat and pressure to give large area coverage and reproducibility on ITO and hydrophilic silicon wafers (Fig. 3.4).

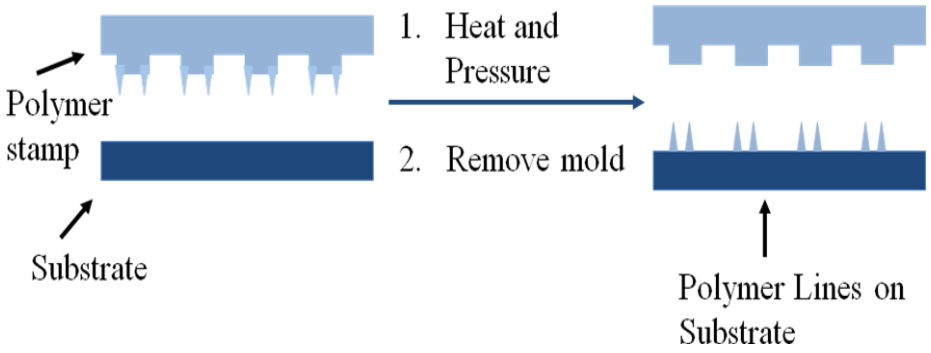

Figure 3.4 Schematic representation for CD-R derived polymer printing, enabled by removing the lacquer-aluminum layer prior to nitric acid treatment of stamp.

With the ease of preparing 1-octanethiol passivated gold CD-Rs as molds, effort was given to exploring the fabrication of polyaniline stamps, which could then be printed on different materials.[13] Polyaniline is usually described as having three different oxidation states (Fig. 3.5).[14] The fully reduced leucoemeraldine base, the blue-hued half-oxidized emeraldine base, and the brown fully oxidized pernigraniline forms are all insulating.

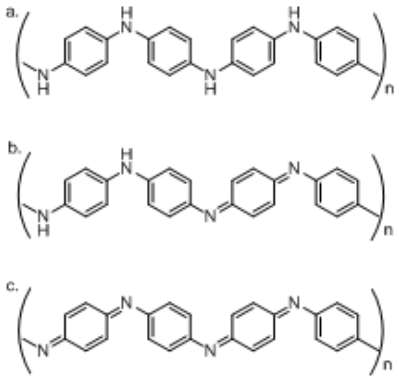

Figure 3.5 Multiple oxidation states for polyaniline: a) fully reduced leucoemeraldine; b) half oxidized emeraldine base; c) fully oxidized pernigraniline.

MacDiarmid, Shirakawa, and Heegen were awarded the Nobel Prize in 2000 partly for discovering the conductivity of the green colored acid-doped emeraldine salt of polyaniline in 2000.[15,16] Much research has gone into elucidating the conductive and structural properties of polyaniline.[17-22]

Conductivity of polyaniline is often achieved with hydrochloric acid or camphorsulphonic acid treatment of the blue colored emeraldine base state (Fig. 3.6). As a polymeric semiconductor, PANI is inexpensive and widely available. Patterns of PANI

have been obtained through photolithography,[23] microcontact printing,[24,25] roll to roll nanoimprinting[26] and inkjet printing.[27]

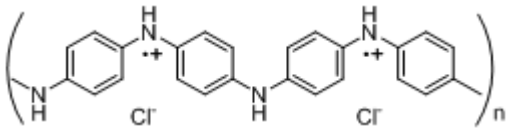

Figure 3.6 Polyaniline emeraldine base, which is blue, is doped with hydrochloric acid to make the conductive green emeraldine salt.

3.3 Experimental Procedure

Instruments

All stamping was conducted with a home-built oven press (constructed by Dr. James Helt). Microscope images were taken through a lens with 40x magnification and then 2x magnification from the CCD camera-microscope adaptor. The CCD camera was a SONY DXC-107A ½ inch CCD-IRIS NTSC color video camera. Atomic force microscope (AFM) measurements were made with an Asylum Research MFP-3D AFM (Santa Barbara, CA). Images were acquired in air using commercial silicon tips (MikroMasch USA, Portland, OR) in AC mode (tapping mode) (NSC15/AlBS) with a typical tip curvature radius of less than 10 nm (NSC15, force constant = 40N/m, resonance frequency = 325 kHz). AFM data was analyzed with the WSxM 4.0 Develop 11.6 Image Browser.[28] Scanning electron microscopy (SEM) images were obtained with a Zeiss EVO 40. A Varian Cary Bio-3 spectrophotometer was used for UV-visible spectroscopy, in double-beam mode.

CD-R Stamp Preparation

A CD-R stamp was prepared, where the aluminum and lacquer layers were removed with scotch tape. The dye was removed with ethanol and water. Finally the CD-R was exposed to concentrated nitric acid for 2-3 minutes, and rinsed with tap water for 5 minutes, followed by rinsing with nanopure water. The stamp was dried under a nitrogen stream and stored in a dessicator overnight.

CD-R Printing on ITO and Silicon Wafer

ITO (25 mm x 25 mm) substrates were ozone cleaned and silicon wafer pieces were soaked in potassium hydroxide for 20 minutes. The CD-R stamp (22 mm x 22 mm) was placed over the substrate and inside the oven press for 5 minutes at 45 °C and 2 PSI. The temperature and pressure were increased according to the experiment. The thinnest lines were produced on silicon wafer at 90 °C and 70 kPa (CD-R stamp was exposed to 2 minutes of nitric acid). The samples were allowed to cool to room temperature, and then gently pulled apart.

Polyaniline Base Films

For polyaniline base films, a 1% by weight solution of PANI emeraldine base (10,000 M.W., Aldrich) in N-methylpyrrolidone (NMP) was used. This was mixed fresh each time, and sonicated for 10 minutes, in air at room temperature. Scotch tape was applied to Lexan® pieces (22 mm x 22 mm), to cover the backside of the slide. A piece was folded over at the top, to function as a handle, when dipping the Lexan into the PANI solution. The dipped Lexan edge was then quickly dabbed on a paper towel, and the scotch tape was quickly removed. The coated pieces were placed in a large glass Petri dish and heated on a hot plate at 95 °C for 1 hour under air. Spin coating would have

greatly enhanced the ability to get an even layer over the Lexan, but as it was, a large area was still available for stamp molding. Sometimes, the area that was dabbed was a slightly thicker. A more even layer, would probably improve printing as well, but for this project, we were still able to fabricate patterns.

Polyaniline Emeraldine Base Film Molding by Passivated Gold CD-R Master

PANI emeraldine base films on Lexan were molded with 1-octanethiol passivated gold CD-Rs (Fig. 3.2). The drier the mold and film, the better the printing. The mold and film were placed on the oven press for 5 minutes at 45 °C and 20 kPa. The temperature was increased to 120 °C and the pressure was increased to 110 kPa, and maintained for 2 minutes. The sample was cooled to room temperature and the pressure was released. The PANI coated Lexan was gently pried from the mold, with a razor blade. Despite the passivation, gold delamination was sometimes a problem, due to residual solvent. Even so, double stick tape applied to the gold, usually lifted the gold from the PANI film with ease, in these cases. Lowering the molding temperature to 110 °C still provided well-made stamps, and gold delamination was less frequent.

Polyaniline Emeraldine Base Stamping onto ITO and Lexan®

Printing at 65 °C and 70 kPa worked best (Fig. 3.8,9). Optical images and SEM images were also obtained for a sample made at 65 °C and 70 kPa (Fig. 3.15) Experimentally, in each case, the PANI base stamp was placed over ITO on the oven press and left for 5 minutes at 45 °C and 20 kPa. The temperature was increased to 65 °C, and the pressure was increased to 70 kPa, and maintained for 2 minutes. The sample was allowed to cool to room temperature, and the pressure was released very slowly. Slow

release of pressure made a significant difference for quantity of pattern observed. A razor blade was used to gently separate the ITO from the stamp.

Patterns were also printed on Lexan (polycarbonate) sheet. Due to residual NMP in the stamp, some molding of the Lexan was observed. Since Lexan, is a thermoplastic, the results were more difficult to analyze. Lowering the temperature was found to significantly diminish molding. A temperature of 55 °C and a pressure of 45 kPa were found to yield the best lines.

3.4 Results and Discussion

CD-R lines on ITO and Silicon Wafer

For a CD-R that was soaked in nitric acid for 3 minutes, rinsed, dried, and printed on ITO at 110 °C and 70 kPa, the printed lines were 400 ± 60 nm in width (Fig. 3.7). Essentially the middles of the lines from the master were missing. Reducing the time in nitric acid slightly reduced the size of the lines (Fig. 3.9), but the greatest reduction in line width was observed for decreasing the stamping temperature to 90 °C, which gave lines with a width of 165 ± 15 nm (Fig 3.9). The peak heights were seen to be anywhere from 6-20 nm in height. In addition, at the lower temperature, frequently only one jagged side of the CD-R line would adhere to the substrate, which provided lines with a pitch of of the CD-R of 1.5 μm.

With analysis of the CD-R master before and after stamping, an explanation can be found in the line edges. With greater time in nitric acid, the line edges also increase in size with oxidative deformation of the polymer (Fig. 3.10-12).

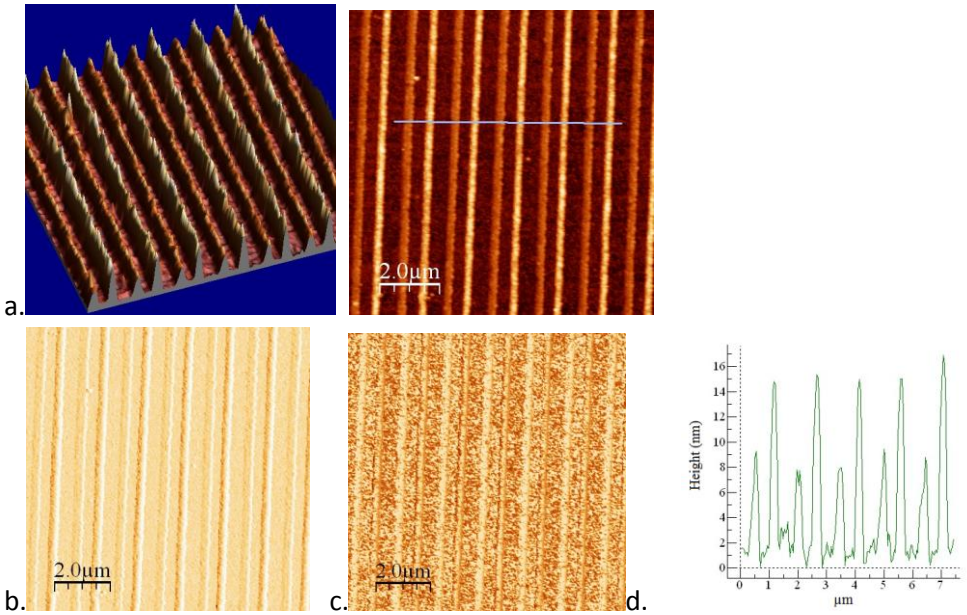

Figure 3.7 a)AFM height images of CD-R lines printed on ITO. For this sample, the aluminum on the CD-R was removed with scotch tape (400 ± 60 nm wide). The bare polycarbonate CD-R was treated with concentrated nitric acid for 3 minutes and rinsed with water. Printing conditions were at 110 °C and 70 kPa, 2 minute dwell time. b) AFM altitude image c) AFM phase image d) AFM height profile.

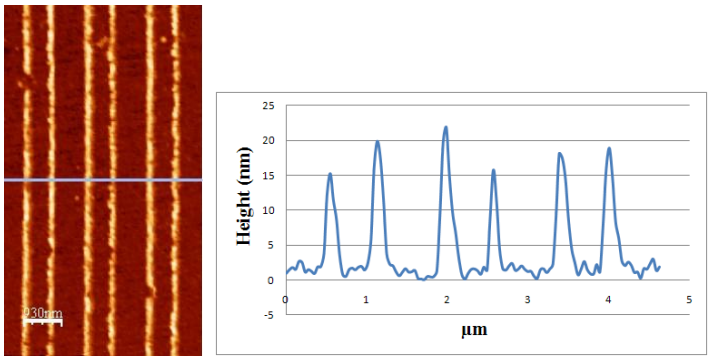

Figure 3.8 AFM images of CD-R lines printed on ITO (250 ± 30 nm wide). For this sample, the aluminum on the CD-R was removed with scotch tape. The bare polycarbonate CD-R was treated with concentrated nitric acid for 30 seconds and rinsed with water. Printing conditions were at 110 °C and 70 kPa, 2 minute dwell time.

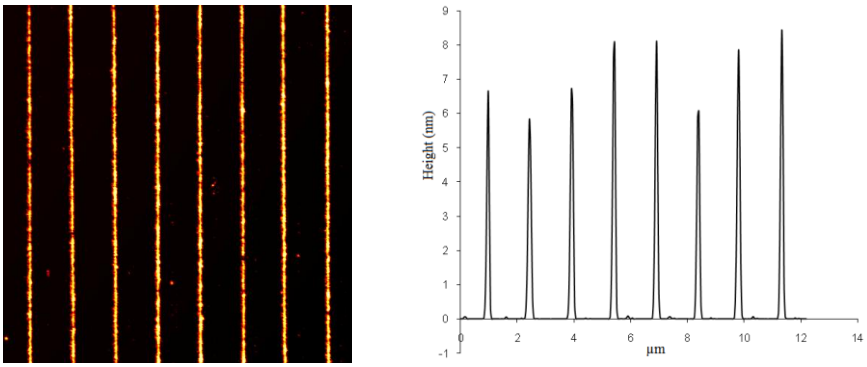

Figure 3.9 AFM images of CD-R lines printed on silicon oxide (165 ± 15 nm). For this sample, the aluminum on the CD-R was removed with scotch tape. The bare polycarbonate CD-R was treated with concentrated nitric acid for 2 minutes and rinsed with water. Printing conditions were at 90 °C and 70 kPa, 2 minute dwell time.

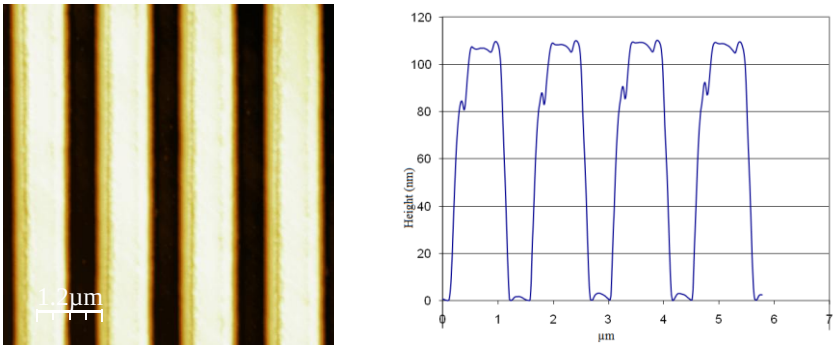

Figure 3.10 AFM images of CD-R master after printing on silicon oxide. The bare polycarbonate CD-R was treated with concentrated nitric acid for 2 minutes and rinsed with water. Printing conditions were at 90 °C and 70 kPa, 2 minute dwell time.

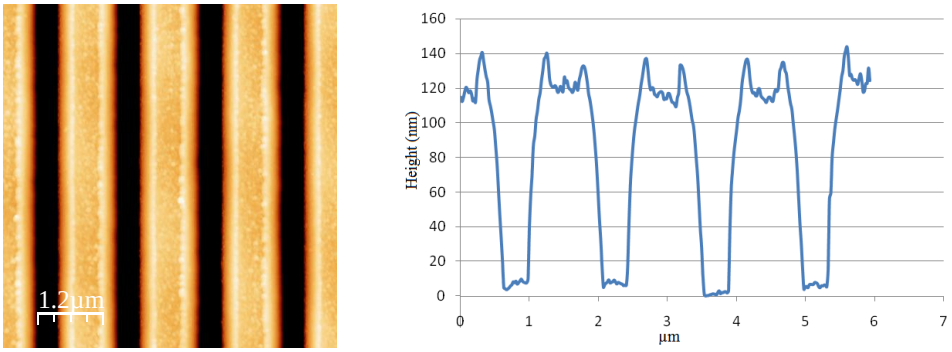

Figure 3.11 AFM images of CD-R master before printing. The bare polycarbonate CD-R was treated with concentrated nitric acid for 2 minutes and rinsed with water.

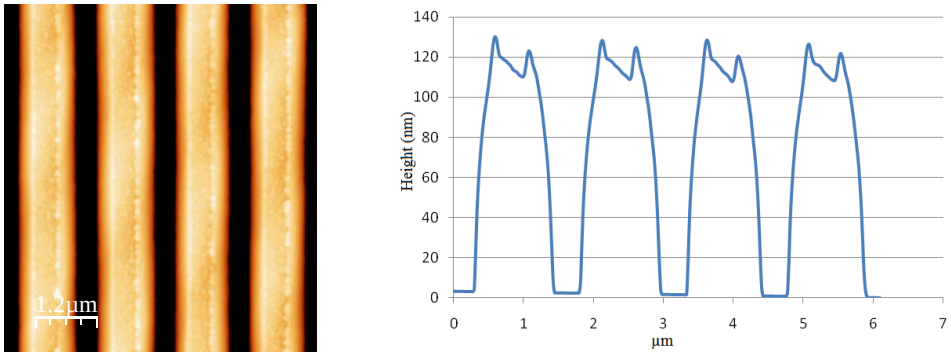

Figure 3.12 AFM image of CD-R stamp before printing, that was exposed to only 1 minute of nitric acid. Polymer stamp is less oxidatively deformed. The peaks are more shallow.

Polaniline Stamps

AFM images of molded PANI emeraldine base films on Lexan showed the expected features of lines with a height of 100-110 nm, and a pitch of 1.5 µm. (Fig. 3.13). Optical images of the stamp showed that the stamp underwent outgassing of NMP over time (see supporting information). The AFM images also show areas of outgassing as well.

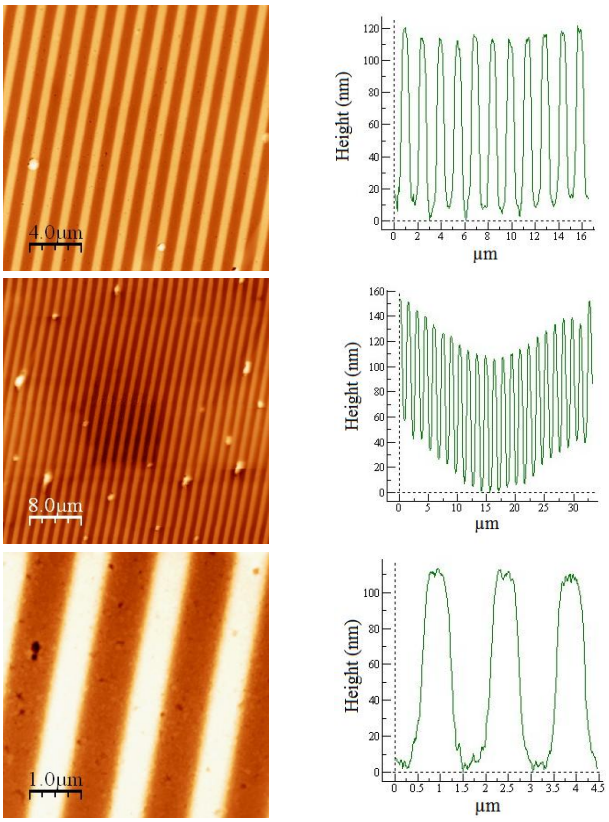

Figure 13. AFM images of molded blue polyaniline films Conditions: 120ºC and 110 kPa for 2 minutes dwell time. AFM images were taken 20 days after making the stamp. Outgassing of NMP is visible in larger images.

Polyaniline Lines on ITO

In general, the patterns of lines printed on ITO were in the area of 2 mm^2 to 5 mm^2 areas, for the best samples, when looking at the rainbow diffraction pattern on the sample. Although the area of lines was not large, the lines are stable for months, by optical imaging. Some obvious ways to optimize the procedure would be to spin coat the Lexan pieces with the PANI base solution, rather than dipping, due to the greater film thickness at one edge. This leads to non-ideal conditions for the best contact with the surface for ITO. Lines varied in thickness from 5 nm to 15 nm. Sometimes, both or one edge was much more pronounced in the pattern, depending on how fast the pressure was released (Fig. 3.14, 15).

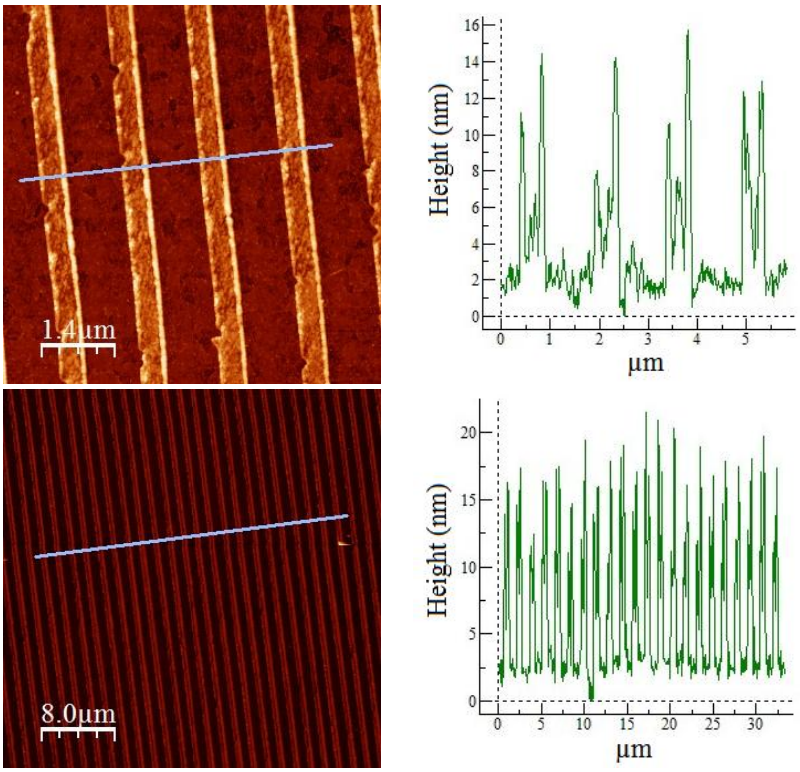

Figure 3.14 AFM images of lines of PANI on ITO. Conditions: 5 min at 20 kPa and 45°C, followed by increased pressure to 70 kPa and temperature to 65 °C, with a 2 minute dwell time. Sample was cooled to room temperature. Pressure was released slowly, and a razor blade was used to separate the sample.

a. 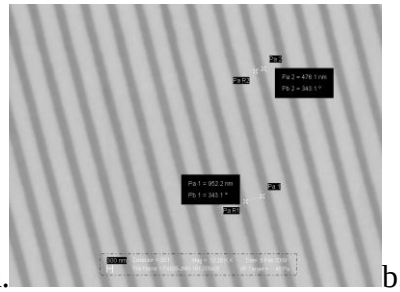 b. 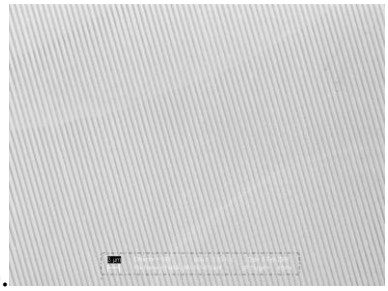

c. 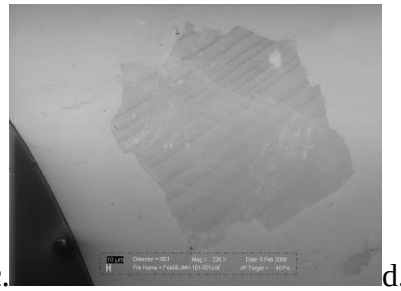 d. 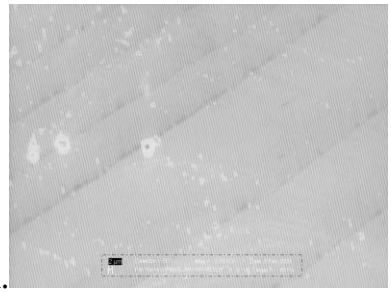

Figure 3.15 a) Scanning electron microscopy images for lines on ITO from a PANI base stamp (same sample as Figure 3.14). Conditions: 5 min at 20 kPa and 45°C, followed by increased pressure to 70 kPa and temperature to 65 °C, with a 2 minute dwell time. b) 104 μm x 80 μm c) 0.42 mm^2 area d) 210 μm x 80 μm

Polyaniline Lines on Lexan

The largest coverage was found in printing on Lexan, where lines were found of areas of greater than 0.5 cm^2. Even so, the variability of the structures was much greater than the structures on ITO. Also, the amount of NMP present in the stamp made a significant difference in printing. Stamp and substrate were always separated with a razor blade. Lines of material were also found to be about 60 nm in height and jagged in appearance (Figure 3.16).

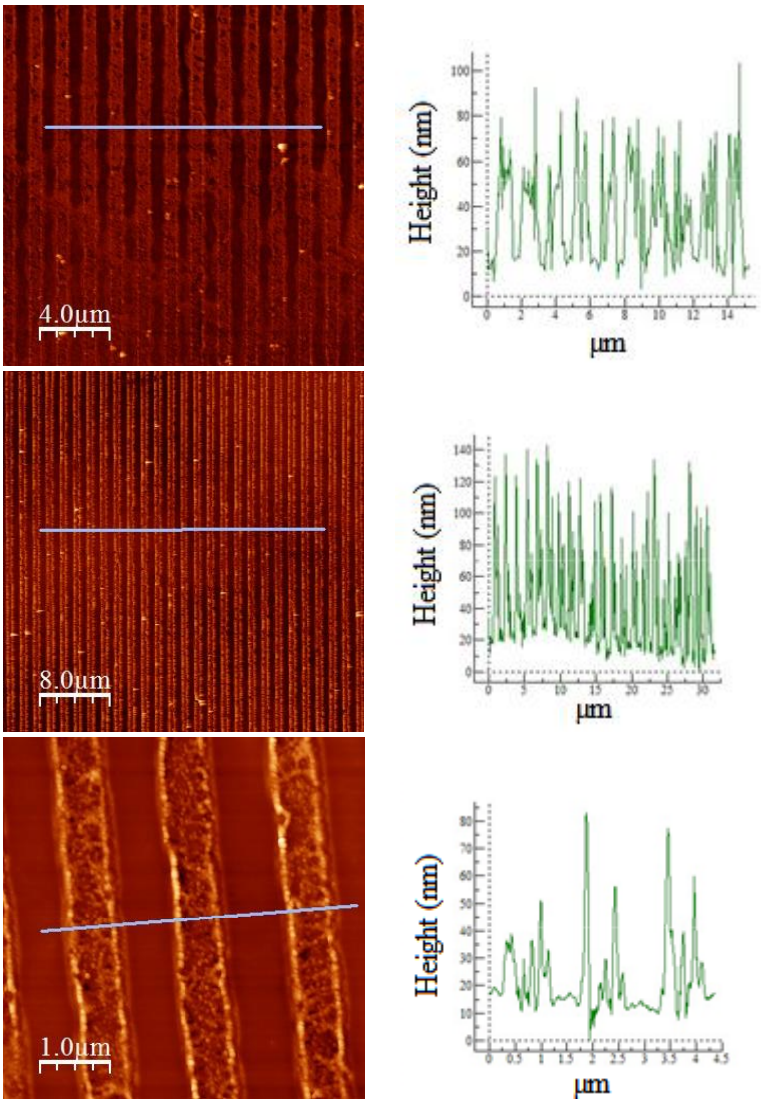

Figure 3.16 AFM images of PANI lines printed on Lexan. Conditions: 5 min at 20 kPa and 45°C, followed by increased pressure to 45 kPa and temperature to 55 °C, with a 2 minute dwell time. Sample was cooled to room temperature. Pressure was released slowly, and a razor blade was used to separate the sample.

UV-Visible Data for Printed Lines on Lexan and ITO

The patterns printed on ITO and Lexan were analyzed for UV-Visible absorbance. As a control, a piece of ozone cleaned ITO was submerged in 1% by weight PANI base solution in NMP. The ITO-PANI film was heated on a hot plate at 95 °C for 1 hour, in the same way as the typical PANI-coated Lexan. The UV-Visible absorbance was taken, the expected 600 nm peak, for the blue emeraldine base was observed.[29] The blue film was then exposed to 30 sec and 1 min of HCl vapor exposure, which was not enough to dope the film. The ITO-PANI film was then submerged in 3 M HCl, and the expected absorbance shift to ~700 nm, for the green emeraldine salt was observed.[29] (See supporting information.)

For these experiments, UV-visible absorbance measurements were taken. Peaks around 645 nm and 730 nm were observed reproducibly. An experiment was then conducted by exposing a sample to concentrated HCl vapor in a closed environment. A UV-Vis absorbance spectra was taken at increasing amounts of time, up to 19 hours. Both characteristic peaks for the patterns diminished in size, and a new peak formed at 790 nm, with increasing HCl exposure. (See supporting information.)

3.5 Summary

Patterns of lines with varied line widths and square centimeter coverage are possible with CD-Rs through simple changes in procedure. By simply delaminating an aluminum coated CD-R, masters capable of printing 900 nm width lines, with a pitch of 1.5 μm are achieved. However, by a simple scotch tape lift off of the aluminum, the CD-R can be treated with nitric acid for access to a master capable of lines less than 500 nm to 175 nm in width depending on the pressure and time in nitric acid. Finally, the

relatively inexpensive semiconductor, polyaniline can also be patterned through passivated gold CD-R moulding to provide lines 900 nm in width, with a pitch of 1.5 μm. Although coverage is still in the square millimeter ranges, several possible steps, such as spin coating the polyaniline instead of dipping, and vacuum oven treatment of the stamps, would lead to more ideal masters for better coverage. Even so, with this method, access to polyaniline base patterns are possible despite the practical solubility issues found with working with this semiconductor. Conversion of the PANI base pattern to the PANI emeraldine salt was also observed with UV-visible spectroscopy.

3.6 Chapter 3 References

(1) Forrest, S. R. *Nature* 2004, *428*, 911-918.

(2) Quist, A. P.; Pavlovic, E.; Oscarsson, S. *Anal. Bioanal. Chem.* 2005, *381*, 591-600.

(3) Balla, T.; Spearing, S. M.; Monk, A. *J. Phys. D: Appl. Phys.* 2008, *41*.

(4) Gates, B. D.; Xu, Q.; Stewart, M.; Ryan, D.; Wilson, C. G.; Whitesides, G. M. *Chem. Rev.* 2005, *105*, 1171-1196.

(5) Leclere, P.; Surin, M.; Brocorens, P.; Cavallini, M.; Biscarini, F.; Lazzaroni, R. *Materials Science and Engineering R* 2006, *55*, 1-56.

(6) Nie, Z.; Kumacheva, E. *Nature Materials* 2008, *7*, 277-290.

(7) Cui, B.; Cortot, Y.; Veres, T. *Microelectronic Engineering* 2006, *83*, 906-909.

(8) Tang, Z.; Kotov, N. A. *Adv. Mater.* 2005, *17*, 951-962.

(9) Helt, J. M.; Drain, C. M.; Batteas, J. D. *J. Am. Chem. Soc.* 2004, *126*, 628-634.

(10) Helt, J. M.; Drain, C. M.; Bazzan, G. *J. Am. Chem. Soc.* 2006, *128*, 9371-9377.

(11) LeGrand, D. G.; Bendler, J. T. *Handbook of Polycarbonate Science and Technology* 2000.

(12) Zarnoch, K. P. *J. Adhesion Sc. Technol.* 1994, *8*, 501-509.

(13) Yu, H.-Z. *Anal. Chem.* 2001, *73*, 4743-4747.

(14) McCall, R. P.; Scherr, E. M.; MacDiarmid, A. G.; Epstein, A. J. *Physical*

Review B 1994, *50*, 5094-5100.

(15) MacDiarmid, A. G. *Synthetic Metals* 2002, *125*, 11-22.

(16) Heeger, A. J. *Angew. Chem. Int. Ed.* 2001, *40*, 2591-2611.

(17) Lee, K.; Cho, S.; Park, S. H.; Heeger, A. J.; Lee, C.-W.; Lee, S.-H. *Nature* 2006, *441*, 65-68.

(18) Shimano, J. Y.; MacDiarmid, A. G. *Synthetic Metals* 2001, *123*, 251-262.

(19) MacDiarmid, A. G. *Synthetic Metals* 1997, *84*, 27-34.

(20) Pouget, J. P.; Josefowicz, M. E.; Epstein, A. J.; Tang, X.; MacDiarmid, A. G. *Macromolecules* 1991, *24*, 779-789.

(21) Pomfret, S. J.; Rebourt, E.; Monkman, A. P. *Synthetic Metals* 1996, *76*, 19-22.

(22) Wang, P.-C.; MacDiarmid, A. G. *Reactive and Functional Polymers* 2008, *68*, 201-207.

(23) Makela, T.; Pienimaa, S.; Jussila, S.; Isotalo, H. *Synthetic Metals* 1999, *101*, 705-706.

(24) Haberko, J.; Raczkowska, J.; Bernasik, A.; Luzny, W. *Macromol. Symp.* 2008, *263*, 47-52.

(25) Haberko, J.; Raczkowska, J.; Bernasik, A.; Rysz, J.; Budkowski, A.; Luzny, W. *Synthetic Metals* 2007, *157*, 935-939.

(26) Makela, T.; Haatainen, T.; Majander, P.; Ahopelto, J. *Microelectronic Engineering* 2007, *84*, 877-879.

(27) Ngamna, O.; Morrin, A.; Killard, A. J.; Moulton, S. E.; Smyth, M. R.; Wallace, G. G. *Langmuir* 2007, *23*, 8569-8574.

(28) Horcas, I. *Rev. Sci. Instrum.* 2007, *78*.

(29) Malinauskas, A. *Polymer* 2001, *42*, 3957-3972.

3.7 Appendix 3.1

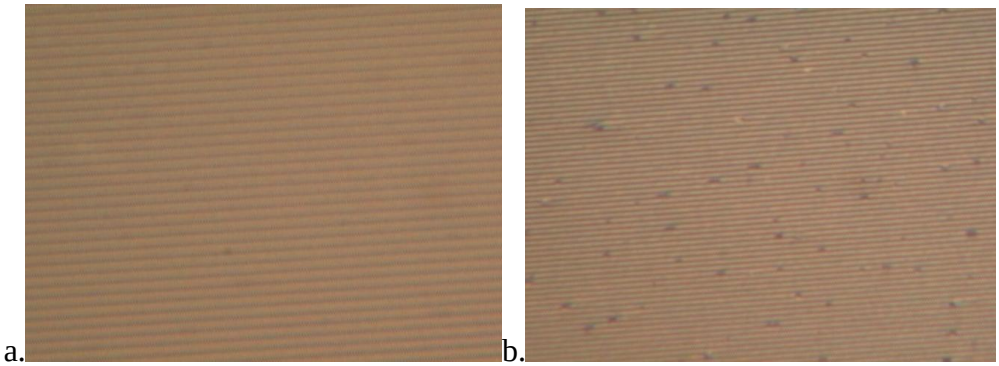

Figure A3.1 Optical images taken of molded PANI emeraldine base film: a) 1 day after molding, and b) 30 days after molding. Outgassing of NMP is visible with time.

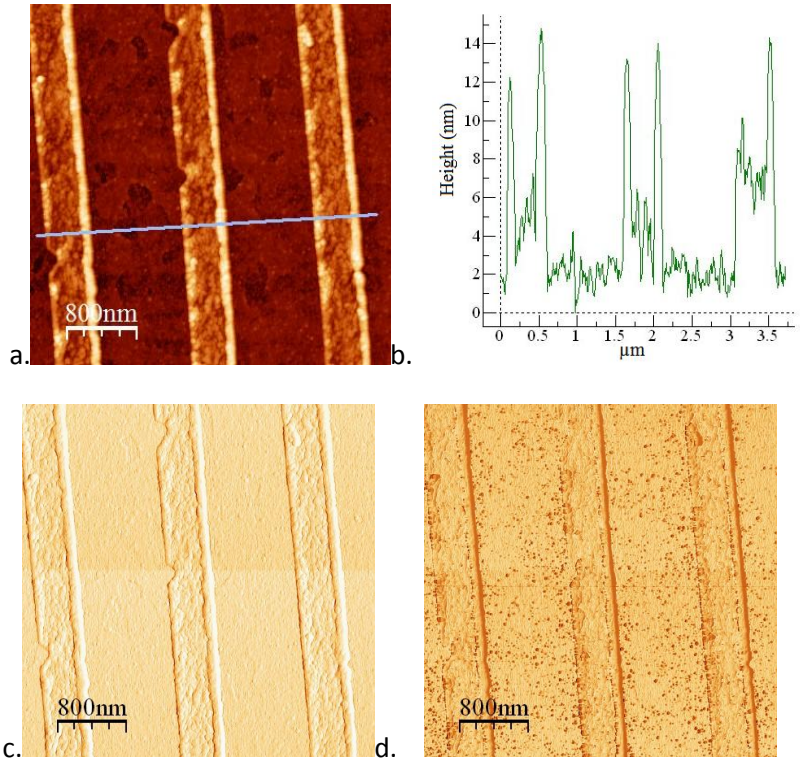

Figure A3.2 AFM images of lines on ITO from a PANI base stamp. Conditions: 5 min at 20 kPa and 45°C, followed by increased pressure to 70 kPa and temperature to 65 °C, with a 2 minute dwell time. Sample was cooled to room temperature. Pressure was released slowly, and a razor blade was used to separate the sample. a) Height image, b) Height profile, c) Altitude image, d) Phase image

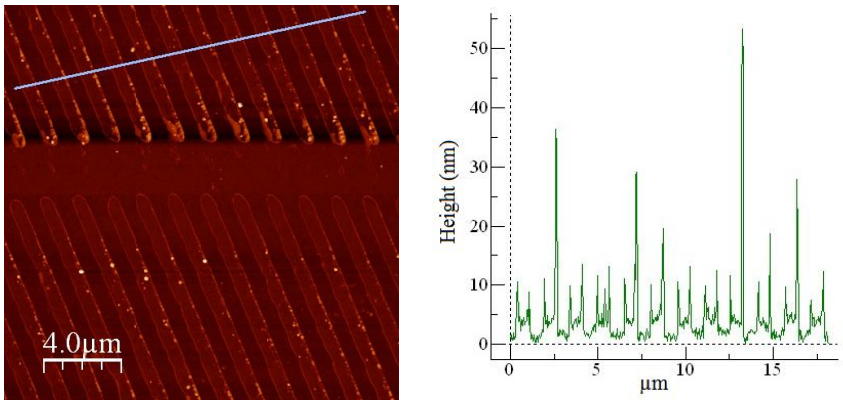

Figure A3.3 AFM images of lines on ITO from a PANI base stamp. Conditions: 5 min at 20 kPa and 45°C, followed by increased pressure to 70 kPa and temperature to 85 °C, with a 2 minute dwell time. Sample was cooled to room temperature. Pressure was released slowly, and a razor blade was used to separate the sample.

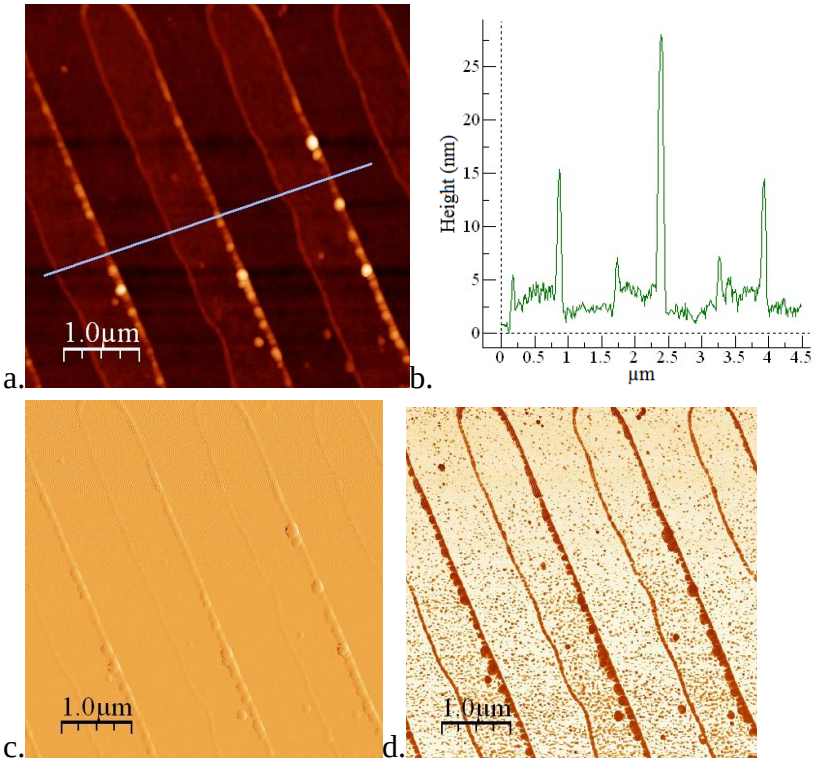

Figure A3.4 AFM images of lines on ITO from a PANI base stamp. Conditions: 5 min at 20 kPa and 45°C, followed by increased pressure to 70 kPa and temperature to 85 °C, with a 2 minute dwell time. Sample was cooled to room temperature. Pressure was released slowly, and a razor blade was used to separate the sample. a) Height image, b) Height profile, c) Altitude image, d) Phase image.

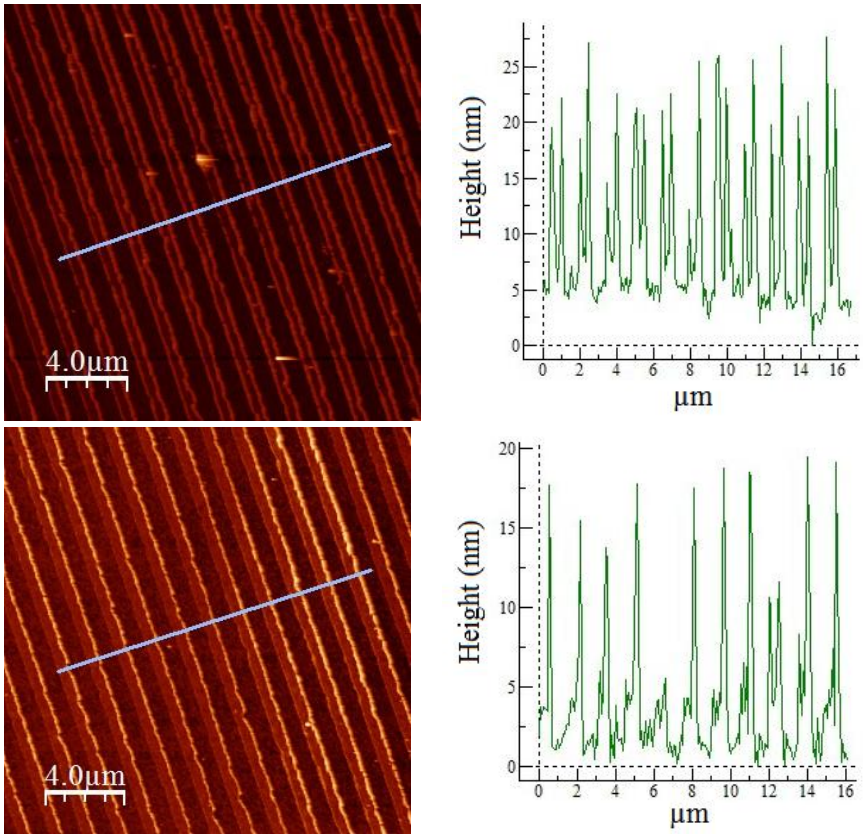

Figure A3.5 AFM images of lines on ITO from a PANI base stamp. Conditions: 5 min at 2 PSI and 45°C, followed by increased pressure to 70 kPa and temperature to 85 °C, with a 2 minute dwell time. Sample was cooled to room temperature. Pressure was released slowly, and a razor blade was used to separate the sample.

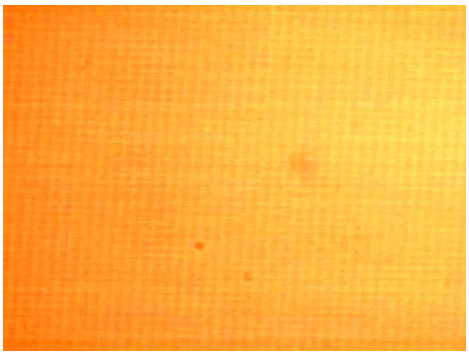

Figure A3.6 Optical image seen through a 40 x objective and magnified 2 x through a CCD camera, for lines on ITO from a PANI base stamp. Conditions: 5 min at 20 kPa and 45°C, followed by increased pressure to 6 PSI and temperature to 65 °C, with a 2 minute dwell time. Sample was cooled to room temperature. Pressure was released slowly, and a razor blade was used to separate the sample.

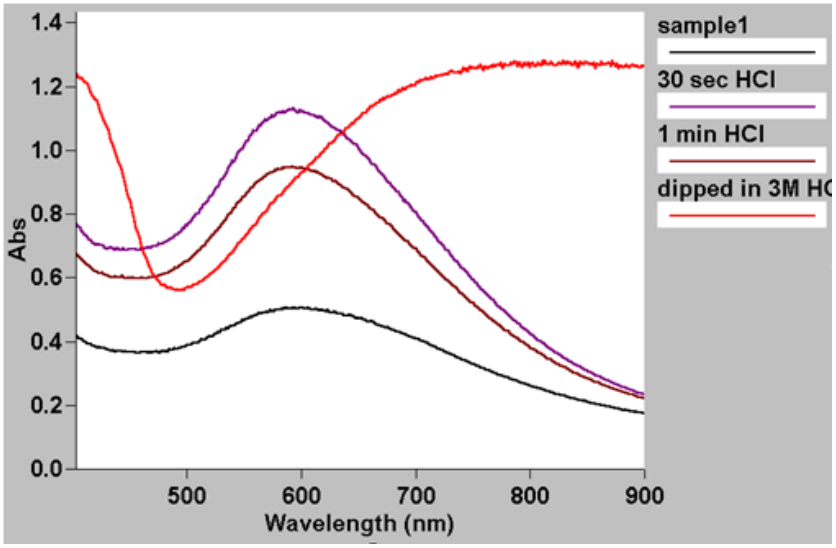

Figure A3.7 UV-Visible trace of blue PANI emeraldine base film on ITO (peak at 600 nm). Traces of 30 seconds of HCl vapor and 1 minute HCl vapor do not show sufficient doping. After dipping the film into 3M HCl, the characteristic broad peak shift (~700 nm) of the green PANI emeraldine salt is observed.

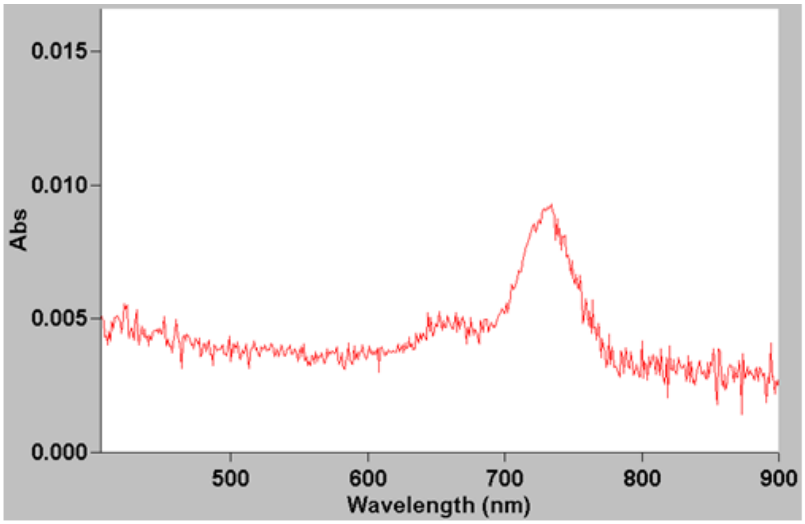

Figure A3.8 UV-Vis for PANI base lines printed on ITO. Peaks observed at 645 nm and 730 nm.

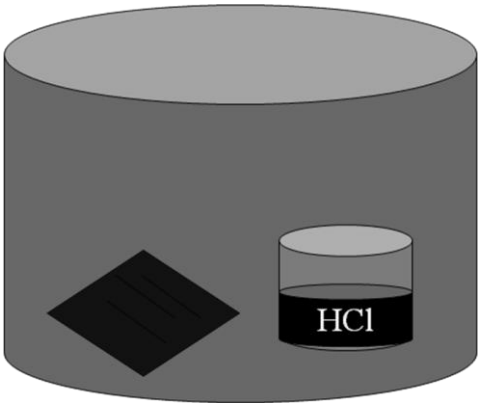

Figure A3.9 PANI lines printed on Lexan were exposed to concentrated HCl vapor underneath a large beaker. UV-Vis spectra were taken at increasing amounts of HCl exposure, up to 19 hours.

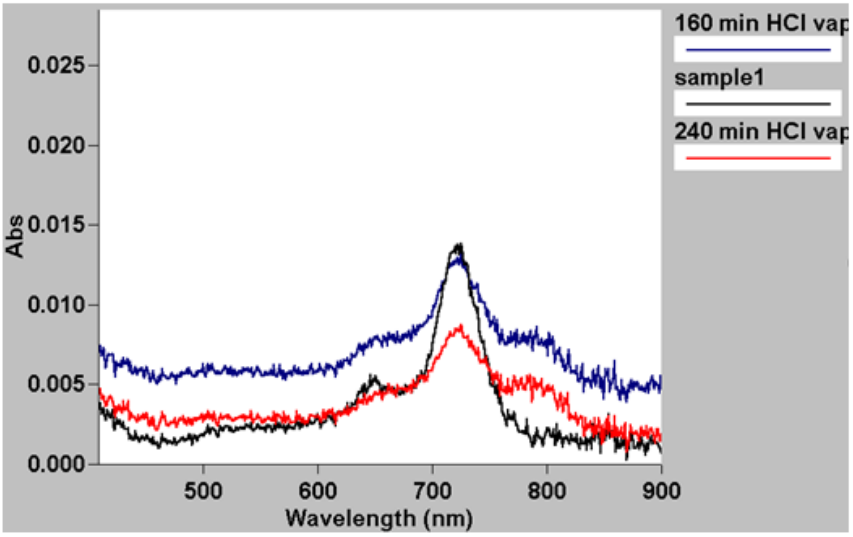

Figure A3.10 UV-Visible spectra for PANI lines on Lexan with increasing time of HCl exposure. In black: initial sample spectra with no acid. In blue: sample after 160 minutes of HCl vapor exposure. In red: sample with 240 minutes of HCl exposure. Decreasing Peaks: 648 nm and 720 nm; New Peak: 790 nm

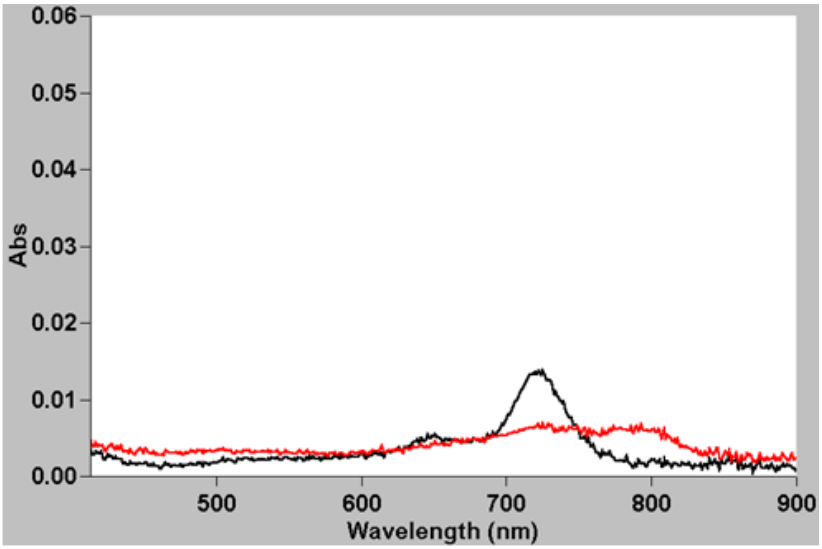

Figure A3.11 19 hours HCl vapor exposure: red line; no HCl vapor: black line.

Chapter 4

Lithography of Polymer Nanostructures on Glass for Teaching Polymer Chemistry and Physics

4.1 Abstract

As nanolithography becomes increasingly important in technology and daily life, a variety of inexpensive and creative methods towards communicating these concepts in the classroom are necessary. Herein is described an experiment that uses simple CD-Rs, C-clamps, an oven, and a freezer that provides concrete examples and insights into the chemistry and principles of nanolithography. The experiment also has flexibility, making is suitable for a range of classroom levels from high school to more advanced labs in college. Since CD-Rs are composed of grooves of polycarbonate, the experiment provides a basis for discussions and exploration into the chemistry and physics of polymers on the nanoscale.

4.2 Lab Summary

Nanomaterials generally have at least one dimension less than about 200 nm, and have many current applications such as light emitting devices and potential applications such as in nanomedicine.[1] New and useful properties emerge in nanostructures because at these dimensions material and electronic properties can be different compared to bulk

materials or molecules. Also, miniaturization of devices requires micro to nanoscale patterns on surfaces, and these are formed by a variety of lithographic processes that in many ways correspond to those used by artists to make etchings, blue prints, stamps, and lithographs.[2-6] In addition to circuitry, nanolithography provides potential access to fabricating sensors, identification tags, optical devices, and molecular electronics. An array of different types of nanoprinting procedures are available that yield patterns of nanostructures on a substrate, such as micro-contact printing, nanoimprint lithography, and laser-assisted direct imprinting. Many of these methods are too expensive as a nanotechnology laboratory experience for undergraduate and high school students because they require specialized equipment. Some micro and nanolithographic methods have been adapted for undergraduate and high school use, including photolithography, selective etching, templating with spheres, and a benchtop method that molds poly(dimethylsiloxane) (PDMS) into CD-rom masters.[7-12] As nanolithography becomes increasingly important and pervasive in industry and society, inexpensive and creative ways of communicating the fundamental science underpinning this technology in the classroom will become more important and desirable.[13]

Thus we developed an exciting college and high school level nanolithography laboratory designed to teach concepts in polymer chemistry and physics, surface chemistry, and nanotechology based on our recently reported method for the transfer of polymer patterns to ceramic surfaces.[2] In this laboratory experience, nanopatterns of carbonate polymers from inexpensive writable compact disks (CD-R) can be printed onto microscope glass slides using a simple C-clamp, a glassware oven, and a freezer. Pieces of the CD-R function as the stamps to print an array of lines that are ca. 900 nm wide,

many mm to cm long, and ca. 15 nm high when pressed against a glass substrate with a simple C-Clamp and heated to well below the glass transition temperature of the polycarbonate. In fact, the procedure was developed, written, and created by an undergraduate student in our lab (AS).

Principles

During the procedure, students will prepare the CD-R stamp, the glass substrate, and characterize the nanoscale patterns that are printed from the stamp onto the glass.

Polymer Stamps. The introduction of polymers, polymer chemistry, and polymer properties serves as the foundation of the lecture. Concepts such as glass transition temperature (Tg), intermolecular interactions, and the interactions of molecules with surfaces in relation to nanolithography will provide the foundation of chemical knowledge that enables students to understand the experiment and the procedures. The ~1.2 mm thick grooved polycarbonate of CD with dimensions described above serves as the stamp.[8] This is exposed upon removing: a thin layer of photosensitive organic dye such as nickel phthalocyanine, a nanometer thick metal layer such as aluminum or gold, and a protective lacquer coating (see Appendix 4.7).

Polycarbonate is used in many applications from eye glass lenses, to bullet proof windows, to compact discs. Any polymer or plastic consists of many repeating molecular units that are connected in long chains. Polycarbonate consists of repeating units of bis-phenol A and a carbonate functional group (Fig. 4.1).[14] In addition, polycarbonate has a glass transition temperature (Tg) of 150 °C. The Tg of a plastic is the temperature, at which the plastic is not fully melted, but the polymer chains are able to begin moving past one another. The physics and physical properties of ultra thin films of polymer

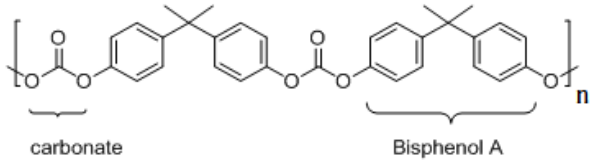

Figure 4.1 Polycarbonate is made of repeating units of Bisphenol A and a carbonate functional group.

plastics is more complicated compared to the bulk plastic.[15] One model for polymer thin film physics is the three layer model, which has been found to be especially useful for describing the patterns of polymer that are observed in this experiment. (Fig. 4.2).[16] Because of strong interactions between the polymer molecules and the surface, the ~15 nm of polymer in contact with a surface is less mobile than the bulk (referred to as a dead layer). Since the dead layer interactions with the surface are often stronger than with the bulk polymer, compression, heating to reach equilibrium, and separating the stamp from the substrate results in cohesive failure at the bulk-dead layer interface and features that are 15 to 20 nm on the substrate. Considering the method, the fidelity is remarkable (see Appendix 4.7).

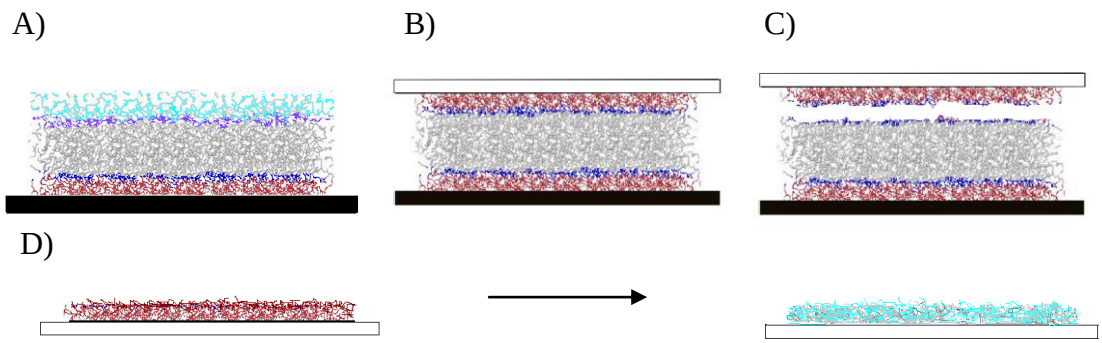

Figure 4.2 Schematic representations of the *three-layer model* used to describe the behavior of thin polymer films at interfaces. A) Substrate supported thin film representing the CD stamp before compression against the glass substrate in the C-clamp. Red: *dead layer* where the polymer chain mobility is strongly diminished by interactions with the substrate. Gray: *bulk-like* layer where the polymer chains have mobilities described by the bulk properties. Light blue: *liquid-like* layer, at the polymer-air interface, has polymer chains with greater mobility. Dark blue: interfaces between these layers where the polymer separates in the stamping process. B) Film confined between the glass substrate and CD during the stamping process. C) Glass substrate is removed from C-clamp, along with the polymer dead layer. D) The printed, dead layer, becomes a liquid layer, upon exposure to air. Illustration adapted from Ph.D. thesis of Dr. Giorgio Bazzan.

4.3 Experimental Procedure

CD-R (Master) Stamp Preparation

A square piece (22mm x 22mm) of CD-R was submersed in concentrated nitric acid for 3 minutes, label side up, and held under with a ceramic spatula, which removed the top layers of dye, aluminum, and lacquer. (*Warning!!! Nitric acid is highly corrosive. This step must be done with protective clothing and in a fume hood.)* The CD-R stamps were rinsed with tap water for 5 minutes, washed with nanopure, and dried under a stream of argon gas.[1] The stamps were dried over night in air. The overnight drying step is important, because solvent embedded in the polymer matrix can be deleterious to obtaining good results when printing on glass. An alternative method to prepare the

[1] Distilled water, nitrogen gas, or purified air can be used. Both the substrate and the CD stamp can be prepared beforehand depending on the level of the students.

stamp using ethanol and water is presented in the supporting information, but the coverage and fidelity of the stamp product is reduced.

Glass Substrate Preparation

A cut microscope slide (25 mm x 25 mm, Fischer plain microscope slide cut in three pieces) was prepared as the substrate. Glass pieces were soaked in concentrated nitric acid for five minutes (see cautions above), followed by rinsing with tap water for five minutes and washed with nanopure water. The glass pieces were dried under a stream of argon gas, and allowed to sit in air overnight to dry. An alternative method soaks the glass in potassium hydroxide, KOH, followed by a tap water rinse (see Appendix 4.7).

Thermal Contact Transfer C-Clamp Stamping

Variables like pressure, temperature, heating time, cooling time, dictate the successful stamping process when using a C-clamp (Fig. 4.3). Students centered the glass substrate on a steel plate (9 cm x 9 cm x 6 mm thick,) and placed the CD-R stamp pattern side down over the glass. A high temperature-stable rubber sheet (2 mm thick x 5 cm diameter), followed by second steel plate (6 mm thick x 5 cm diameter) were carefully placed above the CD-R stamp and glass substrate, and finally pressed together with the C-clamp. Pressure was applied, by tightening the screw as much as possible, and then loosening the clamp half a turn. Using thermal gloves, the students inserted the assembly into the oven at 90-110 °C for 10 minutes. Immediately afterwards, the assembly was placed into a freezer for 15 minutes, and then allowed to warm to room temperature. Very slowly releasing the pressure allows the nanolithographed product on the glass to be removed.

Figure 4.3 C-clamp set up from bottom up: 1) 9x9 cm steel plate, 2) Glass slide, 3) Delaminated CD-R placed face-down over glass, 4) high temperature resistant rubber layer, 5) 6 mm thick x 5 cm diameter steel plate.

4.4 Results and Discussion

When viewing a glass slide printed with a pattern of nanoscale lines underneath an intense desk lamp, a rainbow arising from the diffraction of light from the printed pattern is observed. The causes of the rainbow pattern are discussed elsewhere.[17] These lithographed patterns are also visible with an optical microscope where focusing on the edge of the slide and then moving in from the side provides the best results (Fig. 4.4). One observes these because of the pattern and because of the horizontal dimensions of the lines (mm long by 900 nm wide). Students can observe a diffraction pattern resulting from passing laser pointer light through the repeating nanopattern printed on the substrate, giving an indication of the geometry and spacing.[13]

A) B) C)

Figure 4.4 A) Rainbow diffraction pattern on a stamped glass sample. B) Optical image of CD-R stamp. C) Optical image of lines printed on glass. Both optical images were taken through 40x microscope objective seen through a CCD camera with 2x magnification.

There are several teaching Atomic Force Microscopes (AFMs) available; thus the pattern on the glass substrate can also be probed by AFM to explore both the morphology in terms of images, and to look at defects in the structures (Fig. 4.5).[18] The exact dimensions of the printed lines can be plotted and defects in materials science yield information on the mechanism, in this case of the stamping process.

This experiment was integrated into an instrumental chemistry laboratory and

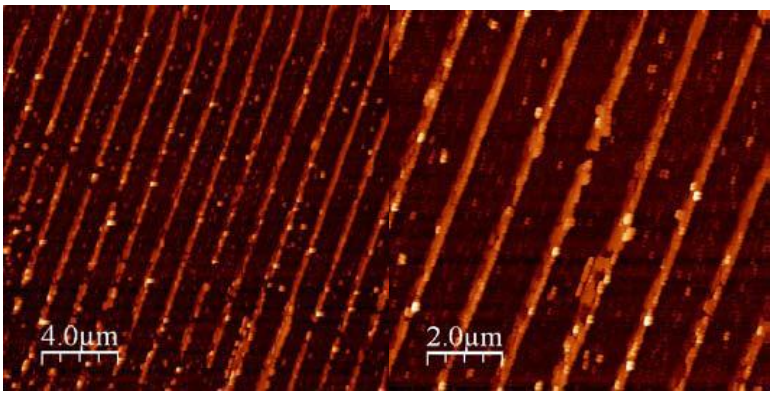

Figure 4.5 AFM characterization of a student's nanolithography product from a CD stamped onto glass; RMS feature height is about 15 nm. This used an Asylum research AFM, but the feature size and periodicity are well within the capabilities of most teaching AFMs.

conducted by 6 third-year chemistry and biochemistry majors. All were able to print and observe the lithographed lines on glass, and rated the experiment highly in terms interest and knowledge gained in surface chemistry and polymer properties. A demonstration and explanation video is available at http://www.youtube.com/watch?v=hO80TzL5-vs&feature=youtube_gdata .

4.5 Summary

As the fabrication of nanostructures becomes increasingly pervasive in everyday technologies and in science, inexpensive and accessible teaching methods for the classroom will be needed. Utilizing common CD-R pieces, microscope slides and C-clamps, together with immediate and clear visible results, provides an accessible laboratory experience that illustrates the roles of surface and polymer chemistry in nanolithography. Steel plates are available for purchase at www.wagnercompanies.com for close to $2 a piece.

Hazards

Concentrated nitric acid is extremely corrosive and should be handled with great caution in a fume hood with appropriate protective gear, and disposed of properly. Addition of water to acid is also highly exothermic and should never be done during the washing procedure.

4.6 Chapter 4 References

1. Ozin, G. A.; Arsenault, A. C.; Cademartiri, L., *Nanochemistry: A Chemical Approach to Nanomaterials* 2nd ed.; Royal Society of Chemistry: London, 2009.
2. Helt, J. M.; Drain, C. M.; Bazzan, G., *J. Am. Chem. Soc.* **2006,** *128*, 9371-9377.
3. Menard, E.; Meitl, M. A.; Sun, Y.; Park, J.-U.; Shir, D. J.-L.; Nam, Y.-S.; Jeon, S.; Rogers, J. A., *Chem. Rev.* **2007,** *107*, 1117-1160.
4. Ahn, S. H.; Guo, L. J., *ACS Nano* **2009,** *3*, 2304-2310.
5. Khang, D.-Y.; Lee, H. H., *Langmuir* **2008,** *24*, 5459-5463.
6. Moran, I. W.; Briseno, A. L.; Loser, S.; Carter, K. R., *Chem. Mater.* **2008,** *20*, 4595-4601.
7. Gerber, R.; Oliver-Hoyo, M., *J. Chem. Educ.* **2008,** *85*, 1108-1111.
8. Meenakshi, V.; Babyan, Y.; Odom, T. W., *J. Chem. Educ.* **2007,** *84*, 1795-1798.
9. Stelick, S. J.; Alger, W. H.; Laufer, J. S.; Waldron, A. M.; Batt, C. A., *J. Chem. Educ.* **2005,** *82*, 1361-1364.
10. Sun, L.; O'Reilly, J.; Tien, C.; Sue, H., *J. Chem. Educ.* **2008,** *85*, 1105-1109.
11. Haynes, C. L.; McFarland, A. D.; Van Duyne, R. P.; Godwin, H. A., *J. Chem. Educ.* **2005,** *82*, 768A-768B.
12. Berkowski, K. L.; Plunkett, K. N.; Yu, Q.; Moore, J. S., *J. Chem. Educ.* **2005,** *82*, 1365-1369.
13. Meenakshi, V.; Babyan, Y.; Odom, T. W., *J. Chem. Educ.* **2007,** *84*, 1795-1798.
14. Abrams, C. F.; Site, L. D.; Kremer, K., *Phys. Rev. E* **2003,** *67*, 021807.
15. Cross, G. L. W.; O'Connell, B. S.; Pethica, J. B.; Rowland, H.; King, W. P., *Rev. Scientific Instr.* **2008,** *79*, 1-13.
16. Fukao, K.; Miyamoto, Y., *Phys. Rev. E.* **2000,** *61*, 1743-1754.

17. G. Planinšič, G.; Corona, A.; Slisko, J., *Phys. Teacher* **2008,** *46*, 329-333.

18. Zhong, C.-J.; Han, L.; Maye, M. M.; Luo, J.; Kariuki, N. N.; Jones, W. E., Jr. , *J. Chem. Educ.* **2003,** *80*, 194-198.

4.7 Appendix 4.1

Lab Documentation: Lithography of Polymer Nanostructures on Glass for Teaching Polymer Chemistry and Physics

Notes to the Instructor:

Be sure to handle all stamps and substrates by the edges with gloves to avoid getting fingerprints and residues from the glove on the surface, which will decrease polymer adhesion to the glass.

Nitric Acid Free Procedure Option*:*

CD-R stamp preparation without the use of nitric acid: To expose the CD-R's lower layer of polycarbonate, we rinse a square piece (22mm x 22mm) of the CDR under tap water. Then, blow a stream of argon gas over the sample in order to dry it, and apply scotch tape. The top layers of aluminum and lacquer are removed as the scotch tape is

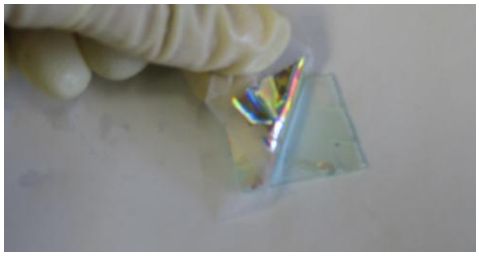

Figure A4.1 Scotch Tape removal of protective lacquer and aluminum metal layer of CD-R.

lifted away from the CD-R. (Fig. A4.1). A slightly greenish transparent polycarbonate stamp, coated with a thin layer of a green phthalocyanine dye is revealed. The phthalocyanine dye may be removed with a brief rinse with ethanol, and rinsing with tap

water. It is important that the stamp be allowed to dry (overnight) before stamping, because embedded solvent in the polymer matrix diminishes the quality when printing on glass. The oven temperature must also be raised to 135-140 ºC for the heating process. This nitric acid free method can be used, but pattern coverage and fidelity is somewhat reduced.

Glass preparation without the use of nitric acid**:** The glass microscope slides can be soaked in 10% by weight potassium hydroxide in water for 10 minutes. The slides are rinsed with tap water for five minutes and washed with nanopurified water, followed by drying under a stream of argon gas, and allowed to sit, under air, overnight to dry.

General CD-R and Glass Preparation: The CD-R pieces can be cut with scissors. Cracking along the edges of the CD-R, during cutting, does not prevent stamping. The microscope glass slides were scored with a scoring tip, flipped over, and

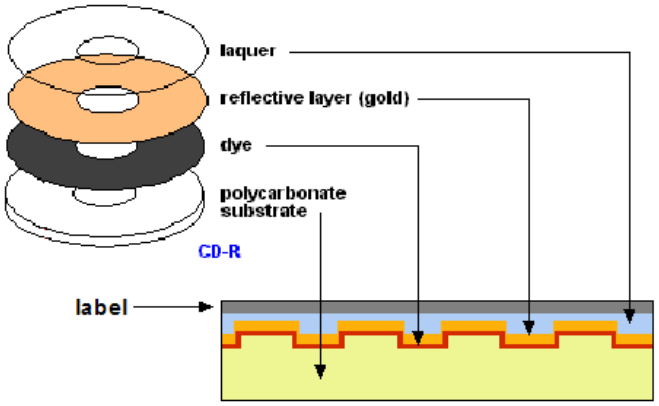

Figure A4.2 CD-R structure. (Reproduced with permission from Computer Desktop Encyclopedia © 1981-2010 The Computer Language Co. Inc., (www.computerlanguage.com)

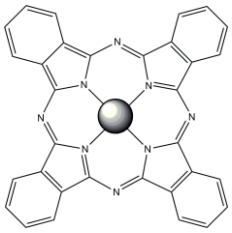

Figure A4.3 Phthalocyanine dyes, usually the Ni(II) complexes, are used in CD-R as part of the active layer.

gentle pressure was applied with a ruler edge. An instructor could prepare the CD-R pieces and glass pieces beforehand. In addition, students are advised to wear rubber gloves.

CAS Registry Numbers*:* Concentrated Nitric Acid, HNO_3 [7697-37-2]; Potassium Hydroxide, KOH [1310-58-3]; Ethanol [64-17-5]

Classroom Survey Results: This experiment was introduced to an undergraduate 3rd level chemistry course at Hunter College. After reviewing the experiment procedure and the basic ideas involved in a laboratory lecture, 6 students conducted the experiment from beginning to end using the CD-R stamp, a simple C-Clamp and an oven. The students had no difficulties in the operations of the experiment. Moreover, all of the students reported immediate visible results (rainbow pattern), and more than 70% of the students were able to locate the nanopatterns they have printed using an optical microscope. The student reports, oral assessments (discussions), and written assessments (exam questions) clearly indicated that the experiment managed to strongly demonstrate and introduce ideas such as diffraction grating, surface chemistry, polymeric materials

characteristics, and the role and importance of nanoprinting processes (see outline of questions below).

More Background Information:

Optical Characterization. In observing nanopatterns, the 400 to 700 nm wavelength of visible light is a limiting factor since only structures larger than ca. half the wavelength of light being used allows us to visualize the pattern. The writable CD stamps possess raised lines that are about 900 nm wide and 150 nm high, and grooves between the lines that are about 600 nm wide. The patterned products on glass reflect the dimensions of the raised features of the stamp, but are about 15 nm high. Consequently, visualization of these features on the CD stamp and the patterned array on glass is possible via the rainbow and with careful focusing of an optical microscope. The rainbow pattern observed for both the CD stamp and the printed pattern is part of the characterization and arises from two interrelated effects,[1, 2] (1) the light reflected from the top of a very thin polymer film that has a different refractive index than the substrate, travels slightly less than light reflected off the bottom, and when the film thickness is close to the wavelength of light, interference occurs (like oil on water); and (2) the pattern serves as a diffraction grating that splits white light into several colored beams traveling in different directions.[2] By passing a laser pointer beam through the sample, one can discern the type of nanolithographed pattern on the surface, in this case parallel lines, by the specific diffraction pattern observed.[3] When using a laser pointer, the diffraction pattern given by the CD-R is easily observed, but the diffraction pattern for the printed

pattern is more difficult to discern sometimes, due to the dependence on the quality and quantity of the lines, as well as the laser intensity.

Atomic Force Microscopy (AFM). The printed lines can also be imaged with AFM. This part of the module can be used to discuss how scanning probe microscopy revolutionized the formation and study of nanomaterials. It is also an excellent introduction to the discussion of intermolecular forces; in this case between the AFM tip and the polymer. Herein we used our research AFM (Asylum) to characterize the patterns formed by several students , but there are good teaching AFMs available.[4]

Further Discussion of the Three Layer Model: For the polycarbonate lines on the CD-R stamp, the hypothesis is that there is a dead layer, a bulk-like layer, and a liquid-like layer within the mm thick film. These three layers have different glass transition temperatures, therefore mobilities.[5] The liquid-like layer at the top surface of the stamp (text Figure 4.2 A) becomes a dead layer because of the strong interactions between these polymer chains and the glass substrate formed during the stamping procedure with applied pressure and heat (text Figure 4.2B). The newly formed dead layer (text Figure 4.2C, 2D) is what remains on the glass because cohesive failure happens at the polymer-polymer interface between the bulk layer and the dead layer (e.g. the glass-dead layer interactions are stronger than the bulk-dead layer interactions). In this experiment, the CD-R stamps prepared by exposure to nitric acid for the delamination step yield better and more consistent patterns on the glass (with more flexible processing T). This is because the nitric acid also somewhat reacts with the exposed polycarbonate to modify the polymer by hydrolyzing the carbonate linkages to yield phenoxy groups.

In the Research Lab: A home-built oven press is used to print CD-R lines on different types of substrates. For the AFM images (Fig. A4.4), glass substrates were cleaned with an ozone cleaner.

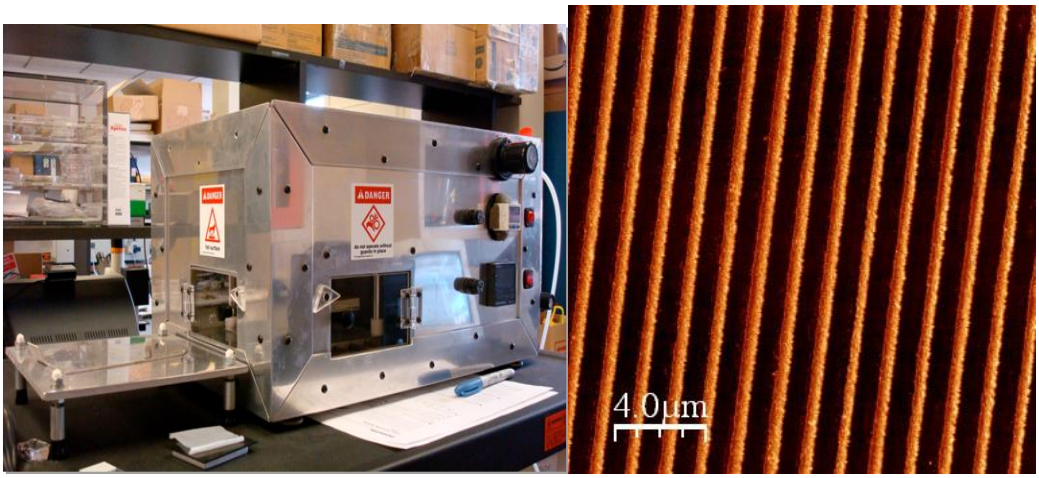

A **B**

Figure A4.4. A) Home-built oven press. B) AFM of CD-R lines printed on glass. RMS height of lines are 20 nm

A4.1 Nanolithography Reviews:

1. Ouseph, P. J., *Phys. Teacher* **2007,** *45*, 11-13.
2. Planinšič, G.; Corona, A.; Slisko, J., *Phys. Teacher* **2008,** *46*, 329-333.
3. Meenakshi, V.; Babyan, Y.; Odom, T. W., *J. Chem. Educ.* **2007,** *84*, 1795-1798.
4. Zhong, C.-J.; Han, L.; Maye, M. M.; Luo, J.; Kariuki, N. N.; Jones, W. E., Jr. , *J. Chem. Educ.* **2003,** *80*, 194-198.
5. Fukao, K.; Miyamoto, Y., *Phys. Rev. E.* **2000,** *61*, 1743-1754.
6. Geissler, M.; Xia, Y., "Patterning: Prinicples and Some New Developments." *Adv. Mater.* **2004,** *16* (15), 1249-1269.
7. Xia, Y.; Rogers, J. A.; Paul, K. E.; Whitesides, G. M., "Unconventional Methods for Fabricating and Patterning Nanostructures." *Chem. Rev.* **1999**, *99*, 1823-1848.
8. Balla, T.; Spearing S. M.; Monk, A., "An Assessment of the Process Capabilities of Nanoimprint Lithography." *J. Phys.: Appl. Phys.* **41** (2008), 174001
9. Gates, B. D.; Xu, Q.; Stewart, M.; Ryan, D.; Wilson, C. G.; Whitesides, G M., "New Approaches to Nanofabrication: Molding, Printing, and Other Techniques." *Chem. Rev.* **105** (2005), 1171-1196.
10. Quist, A. P.; Pavlovic, E.; Oscarsson, S., "Recent Advances in Microcontact Printing." *Anal. Bioanal. Chem.*, **381** (2005), 591-600.
11. Schmidt, R. C.; Healy, K. E., "Controlling Biological Interfaces on the Nanometer Length Scale." *J. Biomed. Mater. Res. Part A* (2009), 1252-1261.

Laboratory Handouts

Lithography of Polymer Nanostructures on Glass for Teaching Polymer Chemistry and Physics

High School Laboratory:

Background:

Nanolithography: a way of printing tiny nanoscale structures (straight lines from a CD-R in this lab) onto another surface (glass).

CD-R: writable compact disc and are covered in nanoscale grooves similar to old music records. CD-Rs are made of polycarbonate plastic. The CD-R will be the stamp in this experiment.

Glass: Microscope slides will be used as surfaces to print the CD-R stamps onto.

Hydrophilic Surface: A surface that is more attracted to water droplets. These surfaces are more polar.

Hydrophobic Surface: A surface that repels water droplets to some extent. These surfaces are less nonpolar.

Surface Energy: Hydrophobic surfaces have a low surface energy and hydrophilic surfaces have a high surface energy. One simple way to compare surface energies is by looking at a water droplet on the surface.

Contact Angle: The more hydrophilic a surface, the smaller the contact angle for a water droplet on that surface. The water droplet looks flatter to the eye. The more hydrophobic a surface, the larger the contact angle for a water droplet. The water droplet looks rounder to the eye.

Polymers: Plastics are a type of polymer. Any polymer or plastic consists of many repeating molecular units that are connected in long chains.

Glass Transition Temperature (T_g): Temperature at which the polymer chains in a plastic are able to move past one another. This temperature is lower than the melting temperature.

Polycarbonate: A plastic that consists of repeating units of bis-phenol A and a carbonate functional group. The CD-R stamps are made of polycarbonate. The printed patterns on glass will be made of polycarbonate.

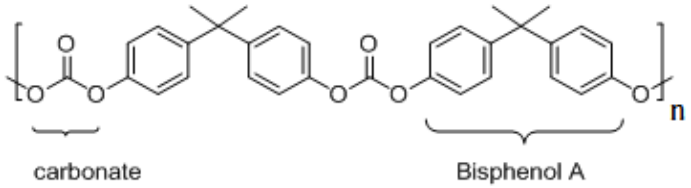

Polycarbonate Plastic Chains

Procedure:

Part 1:

A. CD-R Stamp Preparation:
   CAUTION!!!! Concentrated nitric acid must be used in the FUME HOOD! Do not mix water with nitric acid at any time during the experiment: goggles, gloves, and protective clothing must be worn at all times!!!
   1. Place CD-R (label side up) in a glass Petri dish with concentrated nitric acid for 5 min. Keep the CD-R submersed with a ceramic spatula. The CD-R line pattern is underneath the label. Be sure to keep track of the top side.
   2. Carefully remove with tweezers and hold under running tap water for 5 minutes.
   3. Rinse with nanopurified (or distilled) water.
   4. Dry under a stream of argon or nitrogen gas.
   5. Leave to dry at room temperature overnight
B. Glass Preparation:
   1. Place glass slide in concentrated nitric acid for 5 min.
   2. Carefully remove with tweezers and hold under running tap water for 5 minutes.
   3. Rinse with nanopure (or distilled) water.
   4. Dry under a stream of argon or nitrogen gas.
   5. Leave to dry at room temperature overnight.
C. C-Clamp Nanostamping:
   1. Adjust oven temperature to 90-110 ºC.
   2. Place glass on large 9 cm. x 9 cm steel plate.
   3. Place CD-R stamp facing down on top of the glass.
   4. Place a thermally stable rubber layer on top of the stamp to avoid breaking the slide.
   5. Place the second 5 cm diameter steel disc on top of the rubber layer.
   6. Place layers between C-clamp and tighten as much as possible, and then releas the pressure one half turn.
   7. Place in oven for 10 minutes.
   8. Place in freezer of 15 minutes.
   9. Allow to come to room temperature.
   10. Remove pressure very slowly.

Part 2:

D. Contact Angle Comparisons:

1. Obtain a medicine dropper and water.
2. Place 1 drop of water on a nitric acid treated CD-R
3. Place 1 drop of water on a nitric acid treated glass piece.
4. Place 1 drop of water on a microscope slide with no treatment.
5. Place 1 drop of water on a plastic transparency.
6. Place 1 drop of water on aluminum foil.
7. Obtain a CD-R with the label, and remove the label by applying scotch tape to the label and lifting off. Place 1 drop of water on the non nitric acid treated CD-R.

A video of this nanostamping process is available on You-Tube.

Part 1:

Data Tables and Observations:

Experimental Step:	**Observations / Results:**
CD-R Stamp Preparation	
Glass Preparation	
Nanostamping: Heating the Assembled Stamp in the C-Clamp	
Nanostamping: Cooling / the Stamping Apparatus and Removal of Clamp Pressure	

Characterization	Observations
In a Rainbow Visible from Stamped Pattern on Glass?	Estimation of the % coverage (e.g. use a marker to outline). Does it correspond to what you observed with the CD-R stamp?
Does the Stamped Pattern Diffract Laser Light?	Describe Pattern and experiment.
Microscope observations.	

Part 2.

Data Tables and Observations: Surface Energies by Water Contact Angle

Surface Type Glass or CD-R	Description of Treatment (if any)	Rank Shapes of Water Droplet from 1=most rounded to 6=most flat	Rank Surfaces Energies from 1=most hydrophobic and 6=most hydrophilic

Questions:

1. How did nitric acid treatment of the CD-R change the surface energy? Did it become more or less hydrophilic?
2. How did the nitric acid treatment of the glass change the surface energy? Did it become more or less hydrophilic?
3. Being able to print the CD-R pattern onto glass requires that the CD-R's polycarbonate lines stick to the glass surface and break from the CD-R. Why might forgetting to clean the glass make a large difference for this experiment?
4. What are some changes you could make to the experiment in order to improve the pattern transfer?
5. Conduct an internet search on nanolithography. Name at least one commercial product, where nanolithography was used to produce it.

Questions:

1. How did nitric acid treatment of the CD-R change the surface energy? Did it become more or less hydrophilic?

   The nitric acid treatment increased the surface energy, which was observed by a flatter water droplet, compared to the scotch tape prepared CD-R. The CD-R becomes more hydrophilic with nitric acid treatment.

2. How did the nitric acid treatment of the glass change the surface energy? Did it become more or less hydrophilic?

   The nitric acid removed the oil, which keeps microscope slides from sticking together. The glass slide become more hydrophilic on the surface and the surface energy increased.

3. Being able to print the CD-R pattern onto glass requires that the CD-R's polycarbonate lines stick to the glass surface and break from the CD-R. Why might forgetting to clean the glass make a large difference for this experiment?

   The nitric acid treated CD-R lines are better matched for a hydrophilic glass surface thereby increasing polymer-surface interaction energies. The better the lines stick to the glass the better the stamped pattern and the greater the surface coverage. Because the interactions between the dead layer and the bulk are constant the main variable is the adhesion of the polymer to the glass (modulated by pressure, temperature and surface energetic).

4. What are some changes you could make to the experiment in order to improve the stamping transfer?

   In this experiment, temperature, pressure, cleaning conditions, heating/cooling times and drying times, are all variables which could be changed and explored for better pattern transfer. Even a humid day in the lab can change the results. CD-R brand is another variable as well. The exact composition of the CD-R is different from manufacturer to manufacturer (e.g. fillers, average carbonate polymer molecular weights and dispersity).

5. Do an internet search on nanolithography. Name at least one commercial product, where nanolithography was used to produce it.

   Answers will vary.

Further Discussion Prompts:

Post Lab Questions:

1. What would happen to your nanolithography if you did not clean the oil from the glass slide?
2. Why does nitric acid cleaning improve the ability to stamp these patterns on class?
3. What is the role of temperature in this lithographic process?
4. Why does the rate of cooling make a difference?
5. What is the role of pressure in this experiment? Does PV=nRT apply to polymers?
6. What are the enthalpic and entropic contributions of the rearrangement of the polymer during the stamping process?
7. Based on the above discussions, what would you do to improve the fidelity and quality of the lithographed product?
8. Do you think other patterns and polymers can be used?

Post Lab Questions:

1. What would happen to your nanolithography if you did not clean the oil from the glass slide?

The pattern would not print as well, due to less adhesion between the CD-R polymer stamp and the glass. The polymer lines would not stick as well.

2. Why does nitric acid cleaning improve the ability to stamp these patterns on glass?

   Removing the oil from the glass slide provides a more hydrophilic surface, which is better matched for nitric acid treated CD-Rs lines to adhere. The CD-R surface sticks better to the hydrophilic glass surface.

3. What is the role of temperature in this lithographic process?

   With increasing temperature, the movements (molecular dynamics) of polymer chains increase. Interactions between the polymer in the dead layer and the glass need to be greater than the interactions between the bulk polymeric material and the dead layer. The polymer chains become less entangled and the polymer layers become more defined with temperature (still blow the glass transition, T_g). Thus heating under pressure allows the polymer, especially the new dead layer to come to equilibrium.

4. Why does the rate of cooling make a difference?

   It is likely that the rapid cooling results in a narrower, less molecularly entangled interface between the dead layer and the bulk polymer, i.e. since the boundary between the dead and bulk layers is more defined the cohesive failure between these polymer layers is more uniform and wide spread.

5. What is the role of pressure in this experiment? Does PV=nRT apply to polymers?

   The Ideal Gas Equation (PV=nRT) does not apply to polymers due to significant intermolecular attractions and the molecular volume is too large. Even so, T_g does depend on pressure.

6. What are the enthalpic and entropic contributions of the rearrangement of the polymer during the stamping process?

   The polymer rearrangement and adhesion to the glass involves at least two contributions to the enthalpy (ΔH). First, the water molecules on the surface of the glass must be forced out of the way, which takes energy and is endothermic ($+\Delta H$). Secondly, when a solid undergoes a phase transition to a liquid, this is an endothermic process. In a similar way, the polymer undergoes a transition from the solid phase to the glass transition phase, at glass transition temperature (T_g). At this point the dead and bulk layer become more defined, and polymer chains are becoming less entangled. Entropically, the removal of water is a reduction of entropy on the surface of the glass. In addition, polymer chains are becoming less entangled and disordered, which is a reduction in entropy.

7. Based on the above discussions, what would you do to improve the fidelity and quality of the lithographed product?

   In this experiment, temperature, pressure, cleaning conditions, heating/cooling times and drying times, are all variables, which could be changed and explored for better pattern transfer. Even a humid day in the lab can change the results, so drying the substrate and polymer until just before use may make a difference. Investigations into which CD-R brand yields the best stamped products may lead to investigations into the composition of the polycarbonate stamp.

8. Do you think other patterns and polymers can be used?

   Yes, almost any pattern imaginable can be used, as long as the surface density of the pattern is large (i.e., a few lines per cm^2 likely would not stamp well). The key issue here is how to obtain the master pattern from which stamps can be made, and the fabrication of these masters can be quite expensive. Other polymers can be used, but the T, P, time, substrate, and other processing parameters will need to be evaluated and optimized because the T_g surface energy, and mobility of the liquid/bulk/dead layers are polymer dependent. Secondly, in this case the polymer stamp must be first molded from a master. The CD-R can serve as a master for lower T_g plastics.

Chapter 5

Further Studies Towards Polystyrene, Polycarbonate, and Polyethylene Polymer Nanolithography

5.1 Introduction

Nanoimprint lithography, which involves molding a plastic resist, and etching away the extraneous plastic to provide a patterned surface, utilizes low surface energy plastics such as polycarbonate (PC), poly(methylmethacrylate), polystyrene (PS), and poly(vinyl alcohol).[1-4] With hydrophobic Gold CD-R molds, low density polyethylene and polystyrene stamps were molded and stamped on various surfaces such as conductive indium tin oxide (ITO), glass, Lexan®, and polyethylene terephthalate (PET), and conductive aluminum coated PET. In addition, CD-R derived polycarbonate stamps were printed on these surfaces, as well. For printing results regarding ITO surfaces, chapter 2 and 3 include these results for CD-R derived polycarbonate printing and low density polyethylene. All other printing results are presented here.

5.2 Experimental Procedure

Instruments

All stamping was conducted with a home-built oven press (constructed by Dr. James Helt). Microscope images were taken through a lens with 40x magnification and then 2x magnification from the CCD camera-microscope adaptor. The CCD camera was a SONY DXC-107A ½ inch CCD-IRIS NTSC color video camera. Atomic force microscope (AFM) measurements were made with an Asylum Research MFP-3D AFM

(Santa Barbara, CA). Images were acquired in air using commercial silicon tips (MikroMasch USA, Portland, OR) in AC mode (tapping mode) (NSC15/AlBS) with a typical tip curvature radius of less than 10 nm (NSC15, force constant = 40N/m, resonance frequency = 325 kHz). AFM data was analyzed with the WSxM 4.0 Develop 11.6 Image Browser.[5]

Polystyrene Stamp Fabrication:

Polystyrene sheets, obtained as a sample from Plaskolite, Inc. (1.0 mm) were cut into 22 x 22 mm pieces and easily molded at 110 °C and 110 kPa, with a 12 minute dwell time. The polystyrene sheet and passivated gold CD-R were placed on the oven-press for 5 minutes at 45°C and 20 kPa to equilibrate. The temperature and pressure were then increased for 12 minutes. The sample was cooled to room temp, and gently pulled away from the mold.

Polystyrene Printing:

Conditions for printing polystyrene lines on glass were explored from 60 °C to 90 °C, and from pressures of 20 kPa to 90 kPa. A variety of types of lines were observed and some polymer reorganization into lines of "beads" was seen. Some of the equilibration times were longer than 5 minutes. Longer equilibration times were experimented with and noted with the AFM images. Fidelity and structure of the lines varied greatly.

Low Density Polyethylene Printing:

Stamps of low density polyethylene (LDPE) were molded and this work is described in Chapter 2. LDPE patterns on indium tin oxide (ITO) have been described in Chapter 2. Lexan® sheet (polycarbonate) and glass were also substrates for printing. Lexan® gave the most stable LDPE patterns. The Lexan® or glass substrate was placed

on the oven press with the LDPE stamp above at 20 kPa and 45 °C for 2 minutes. The pressure was then increased to 90 kPa over 40 seconds, and the sample was held at 45 °C for another 3 minutes. The sample was then allowed to cool to 22 °C on the oven press.

Nitric Acid Treated CD-R Polycarbonate Printing:

Besides ITO, nitric acid treated CD-Rs have also been printed on Dura-Lar® polyethylene terephthalate (PET) (0.25 mm), aluminum coated PET, Lexan®, and glass. PET sheets and aluminum coated PET sheets were obtained as a sample from Grafix Plastics. All substrates were prepared as 25 x 25 mm squares. PET and Lexan were rinsed with nanopurified water, dried under an argon stream, and stored in a dessicator. Glass and aluminum coated PET were cleaned with ozone for 20 minutes. Aluminum coated PET was rinsed with water and dried under an argon stream. The cut microscope glass slides were rinsed with absolute ethanol and nanopurified water and dried under an argon stream. Nitric acid CD-R stamps that had been delaminated in concentrated nitric acid for 3-5 minutes, rinsed with tap water for 5 minutes, rinsed with nanopurified water, and dried under an argon stream were placed over the substrate on the oven press. All samples were printed between 105 °C and 110 °C with a 2 minute dwell time. Pressures applied were between 45 kPa and 90 kPa Samples were allowed to cool to room temperature. The stamps were gently pulled away from the substrate.

Scotch Tape (No Nitric Acid) Treated CD-R Polycarbonate Printing:

Scotch tape (no nitric acid) treated CD-R stamps were also printed on Lexan®. Results corresponding to glass and ITO as substrates are found in Chapters 2-4. Printing was conducted at 135 °C for 2 minutes under 110 kPa. Samples were allowed to cool to room temperature. The stamps were gently pulled away from the substrate.

5.3 Results and Discussion:

Polystyrene Stamp Fabrication:

Polystryrene stamp molding resulted in a replica the of the passivated gold CD-R. Polystyrene peak height was 95 nm ± 3, with a pitch of 1.5 µm (Fig. 5.2). Passivated gold CD-Rs were used to mold multiple samples (Fig. 5.1). Even after 6 experiments, CD-R features were still intact by AFM.

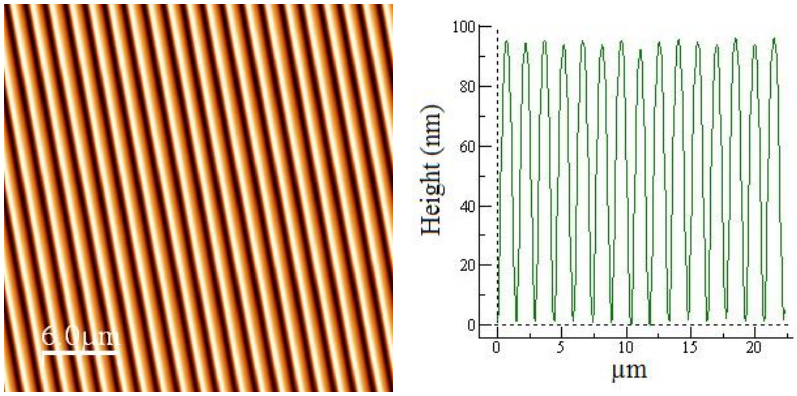

Figure 5.1 Passivated Gold CD-R used to mold plastic sheets of polystyrene and polyethylene.

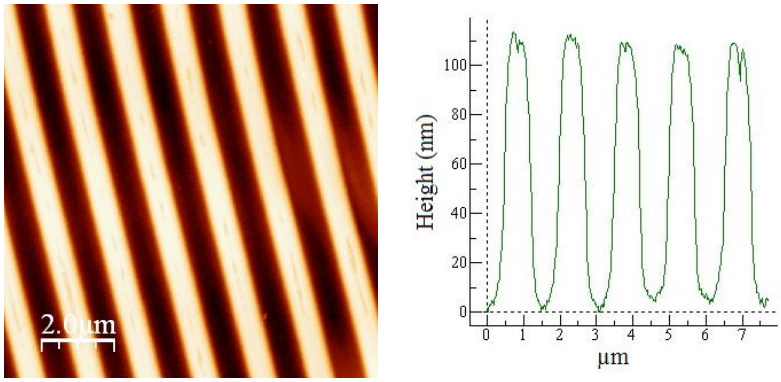

Figure 5.2 AFM image of polystyrene stamp molded with a passivated gold CD-R. Polystryrene and mold were equilibrated for 5 minutes at 45 °C and 20 kPa. Temperature was increased to 110°C and pressure was increased to 110 kPa for 12 minutes.

Polystyrene Printing:

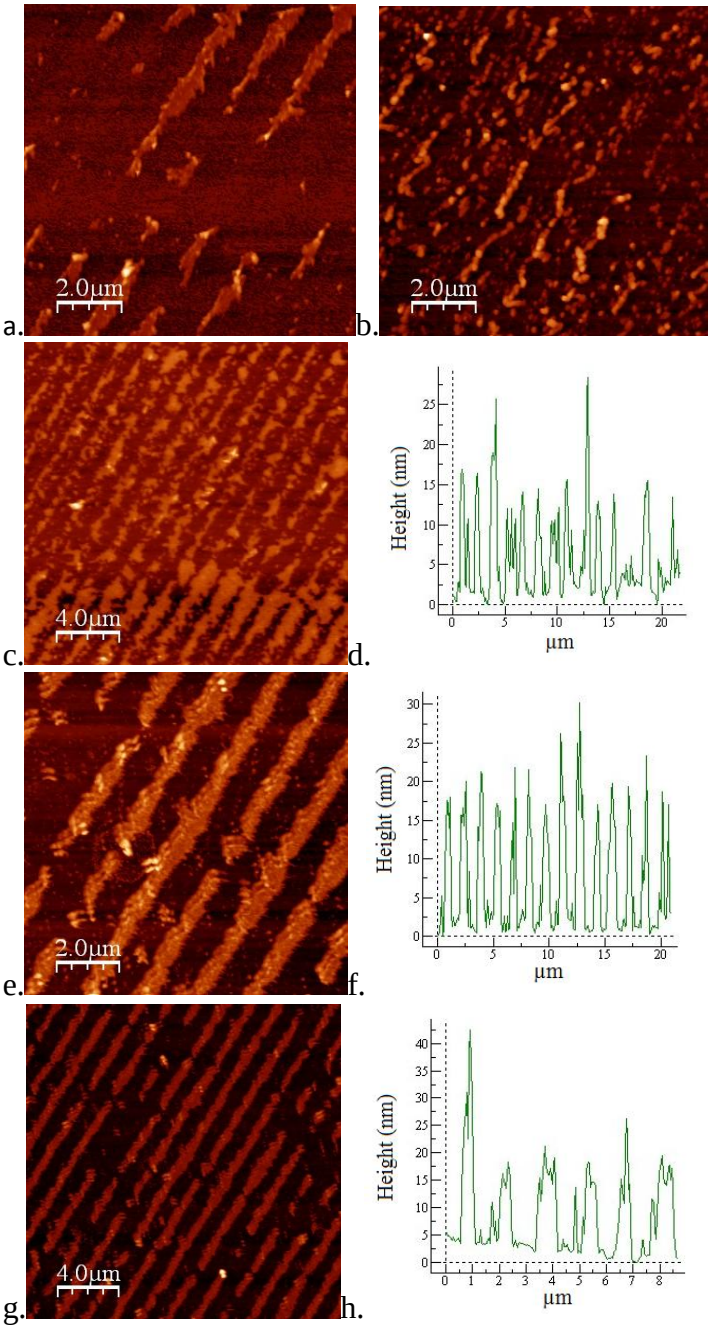

Figure 5.3 AFM images taken from the same sample made from a polystyrene stamp and glass slide. 5 minutes at 45 °C and 20 kPa. Temperature was increased to 90 °C and 45 kPa for 2 minutes. Sample cooled to room temperature.

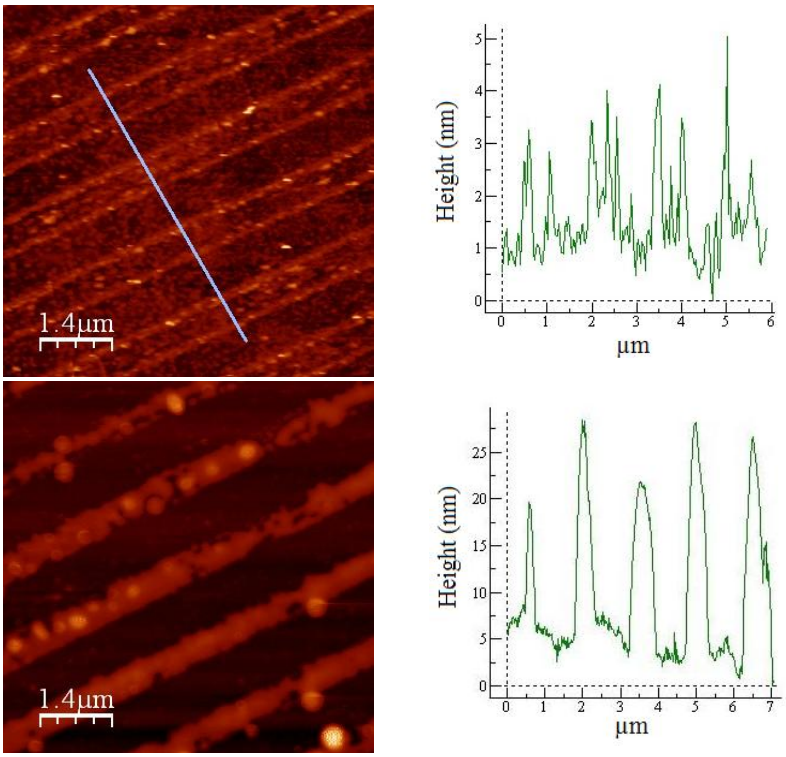

Figure 5.4 AFM images taken from the same sample made from a polystyrene stamp and ITO slide. 15 minutes at 45 °C and 20 kPa. Temperature was increased to 70 °C and 90 kPa for 2 minutes. Sample cooled to room temperature.

Low Density Polyethylene Printing:

Good pattern coverage for Lexan® was observed with 20 to 40% of the sample (Fig. 5.5) Glass had similar coverage, but the lines did not adhere well to the surface (Fig. 5.6, 5.7). Over time (hours to a week) the polymer lines reorganized on the surface of the glass into "beads" (see Appendix 5.7). On some parts of the samples, beads were present immediately after printing, based on optical microscopy. In general, printing LDPE on glass did not produce clean patterns. For Lexan®, AFM images revealed similar line morphologies to LDPE lines printed on ITO, which are described as well formed lines, squished lines, and silhouette (see Appendix 2.6). Although for Lexan®, well formed lines are more common.

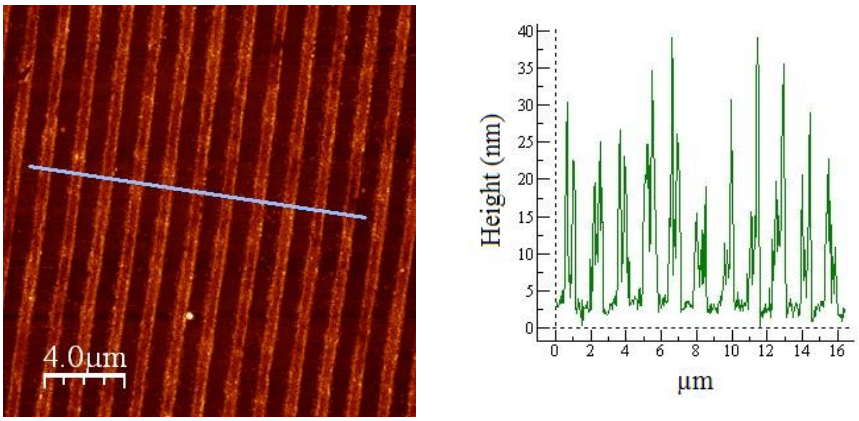

Figure 5.5 AFM image of LDPE lines printed on Lexan sheet (polycarbonate). Lexan and a LDPE stamp were placed on the oven-press for 2 minutes at 45°C and 20 kPa. The pressure was increased to 90 kPa over 40 sec and maintained at 45°C for 220 seconds more. The sample was cooled to room temperature and gently pulled apart.

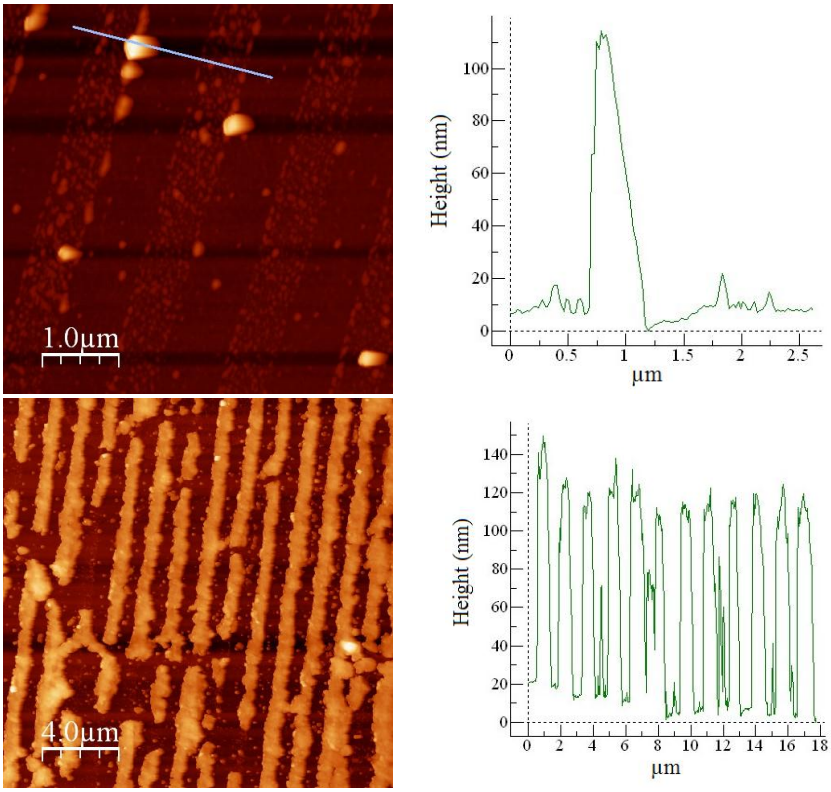

Figure 5.6 AFM images of a glass slide with LDPE lines. Sample was placed on the oven press for 5 minutes at 45°C and 20 kPa. The pressure was increased to 90 kPa over 40 seconds, and the temperature was maintained for another 220 seconds. The sample was cooled to room temperature and gently pulled apart.

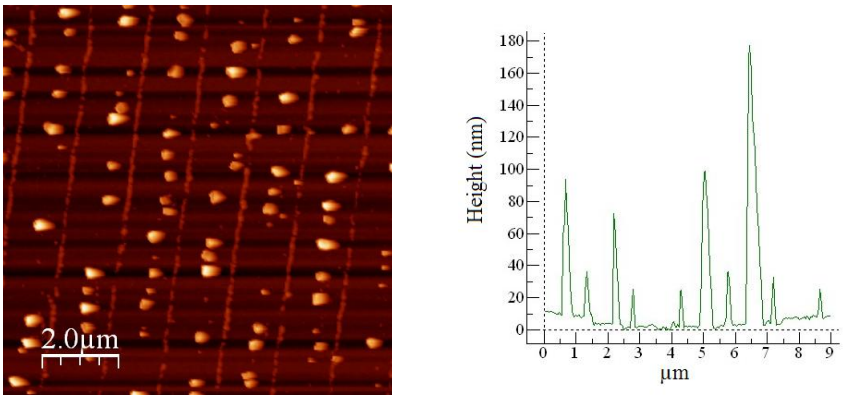

Figure 5.7 AFM image of LDPE lines on glass. Hot glass (120 °C) and a LDPE stamp was placed on the oven press at 21 °C and 90 kPa for 25 minutes. Many broken lines were visible by optical microscopy and AFM.

Nitric Acid Treated CD-R Polycarbonate Printing:

Nitric acid treated CD-R patterns on glass and aluminum coated PET, print well with greater than 1cm^2 coverage (Fig. 5.8, 5.9) The lines on glass are less stable than ITO, but last for more than a year on aluminum-coated PET. Lexan® as a substrate does not exhibit stable patterns (Fig. 5.10). Significant beading or polymer reorganization is observed. Nitric acid treated CD-R patterns printed on polyester (PET) sheet from edge to edge. The lines appeared to slightly reorganize and clump with time, as the AFM displays the resulting pattern after time (Fig. 5.11). Based on previous experiments with attempting to mold PET with diffraction gratings, these PET sheets do not mold particularly well. In addition, the phase image seems to imply two materials. The lines vary in height from 75 nm to 250 nm. The pitch is 1.5 μm.

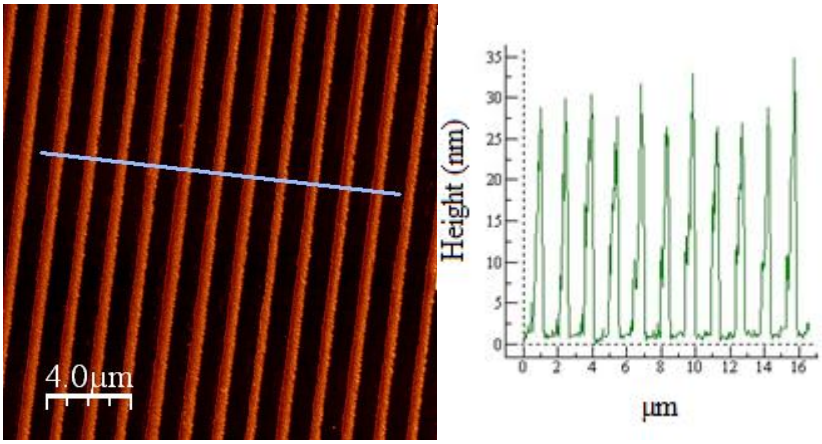

Figure 5.8 AFM image of nitric acid treated CD-R lines printed on glass. Sample was equilibrated at 20 kPa and 45 °C for 5 minutes and printed at 105 °C for two minutes at 45 kPa.

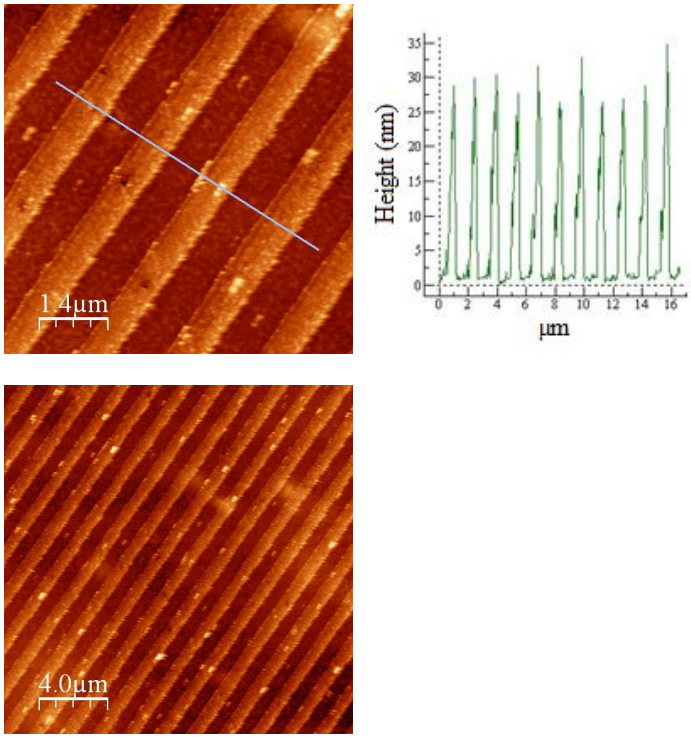

Figure 5.9 AFM image of nitric acid treated CD-R lines printed on aluminum coated PET coated PET. Sample was equilibrated at 20 kPa and 45 °C for 5 minutes and printed at 105 °C for twelve minutes at 90 kPa.

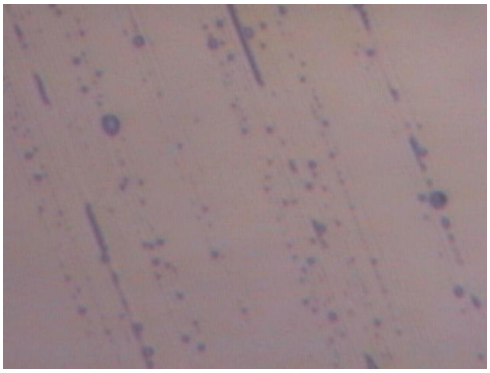

Figure 5.10 Optical image (40 x objective magnified 2x through CCD camera) of Nitric acid treated CD-R lines printed on Lexan®. Sample was equilibrated at 20 kPa and 45 °C for 5 minutes and printed at 110 °C for two minutes at 70 kPa.

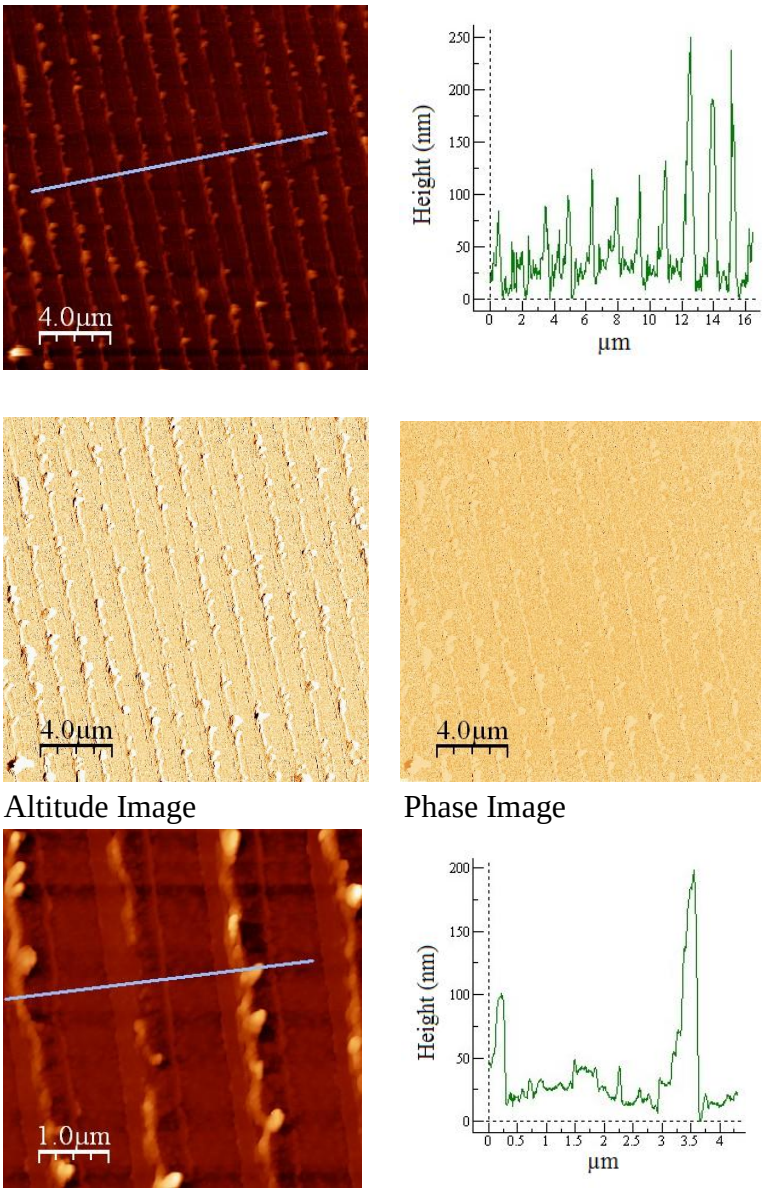

Figure 5.11 Nitric acid treated CD-R printed on polyester (PET). Sample was on oven press for 5 minutes at 45°C and 20 kPa. The pressure was increased to 90 kPa, and the temperature was increased to 105 °C and held for 2 minutes. The sample was cooled to room temperature and gently pulled apart.

Scotch Tape (No Nitric Acid) Treated CD-R Polycarbonate Printing:

CD-R stamps that were not treated with nitric acid printed with more fidelity than the nitric acid treated CD-R stamps, as observed by optical microscopy (Fig 5.12).

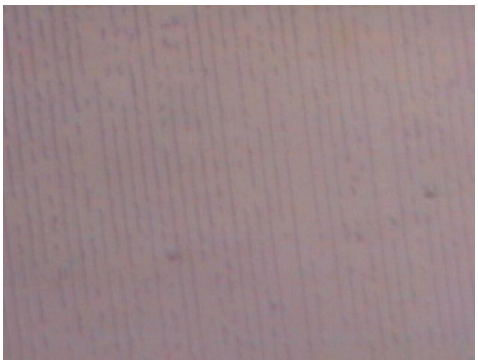

Figure 5.12 Optical image (40 x objective magnified 2x through CCD camera) of scotch tape (no nitric acid) treated CD-R lines printed on Lexan®. Sample was equilibrated at 20 kPa and 45 °C for 5 minutes and printed at 135 °C for two minutes at 110 kPa.

5.4 Conclusions

Printing low surface energy plastics was explored for polystyrene, low density polyethylene, and polycarbonate. The Polystyrene sheets were difficult to print with reproducibility and large coverage. Lines of polystyrene were possible, though. Perhaps, with a higher quality polystyrene sheet, better patterns may be obtainable. Low density lines of polyethylene were printed on glass and Lexan®. LDPE lines are not structurally reliable with regard to glass. Lexan® exhibited good coverage and more stability than ITO samples. Three different line structures were observed, in general. Both the squished and well-formed lines, could possibly function as a useful mask for any kind of gas-phase, kinetic material deposition. Nitric acid treated CD-R derived polycarbonate lines are

stable for more than a year on aluminum coated PET. Good coverage is seen for glass and PET as substrates. On PET in particular, the lines clump over time.

5.5 References for Chapter 5

(1) Leising, G.; Stadlober, B.; Haas, U.; Haase, A.; Palfinger, C.; Gold, H.; Jakopic, G. *Microelectronic Engineering* 2006, *83*, 831-838.

(2) Nie, Z.; Kumacheva, E. *Nature Materials* 2008, *7*, 277-290.

(3) Zhao, Y.; Cui, T. *Journal of Micromechanics and Microengineering* 2003, *13*, 430-435.

(4) Balla, T.; Spearing, S. M.; Monk, A. *J. Phys. D: Appl. Phys.* 2008, *41*.

(5) Horcas, I. *Rev. Sci. Instrum.* 2007, *78*.

5.6 Appendix 5.1

Atomic Force Microscopy of Low Density Polyethylene Patterns

Frequently, when printing polymer patterns, “beading” or “polymer reorganization” occurs. The “beading up” of polymer may occur during the stamping process, months after, or both. In the case of low density polyethylene, this beading process is more rapid on glass. Atomic force microscope (AFM) images were taken of the same sample, 7 days apart. Over time, the polymer on the slide displayed “beads” of polymer, after sitting at room temperature under air (Fig. A5.1, A5.2).

Day 1 After Printing

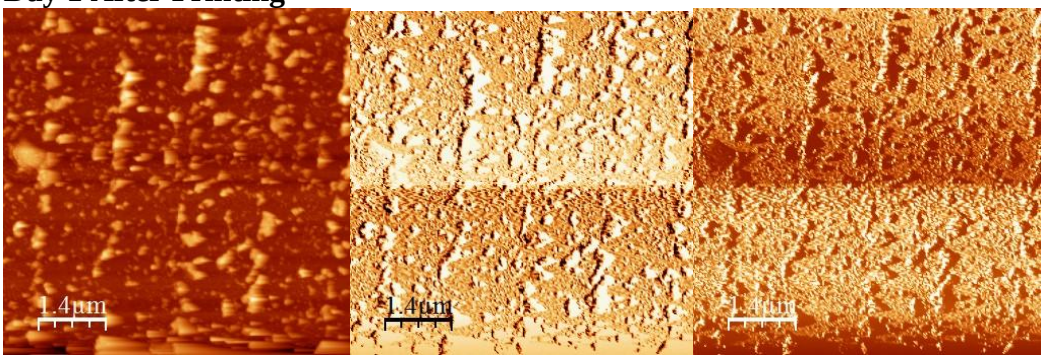

A) B) C)

Figure A5.1 AFM image of first day after printing LDPE onto glass at 45 °C and 90 kPa. A) Height image. B) Altitude image. C) Phase image.

Day 7 After Printing

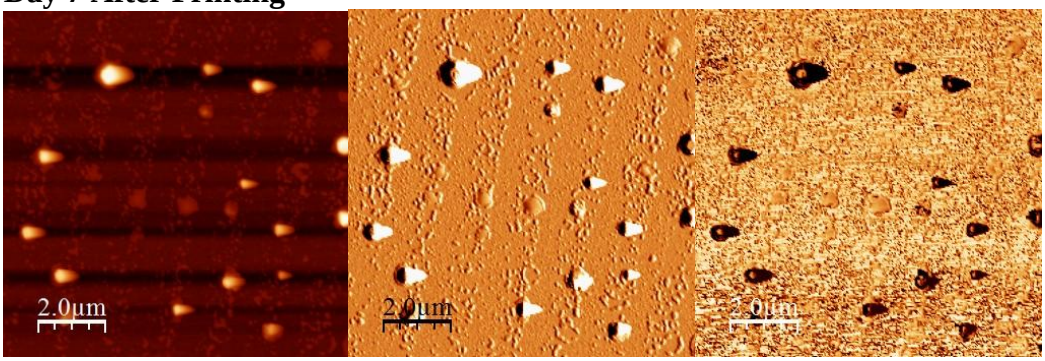

A) B) C)

Figure A5.2 AFM image of day 7 after printing LDPE onto glass at 45 °C and 90 kPa. A) Height image. B) Altitude image. C) Phase image.

In addition, LDPE lines were printed on ITO and analyzed by AFM (Fig. A5.3), and then annealed at 120 °C in an oven overnight. AFM images of the resulting sample also showed "beads" of polymer in place of the well formed lines (Fig. A5.4).

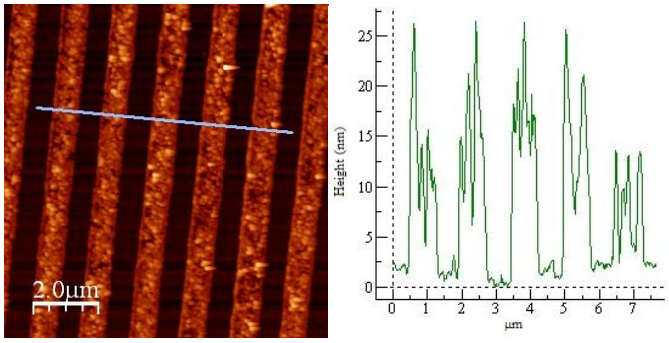

Figure A5.3 AFM height image of LDPE lines printed on ITO at 45 °C and 90 kPa.

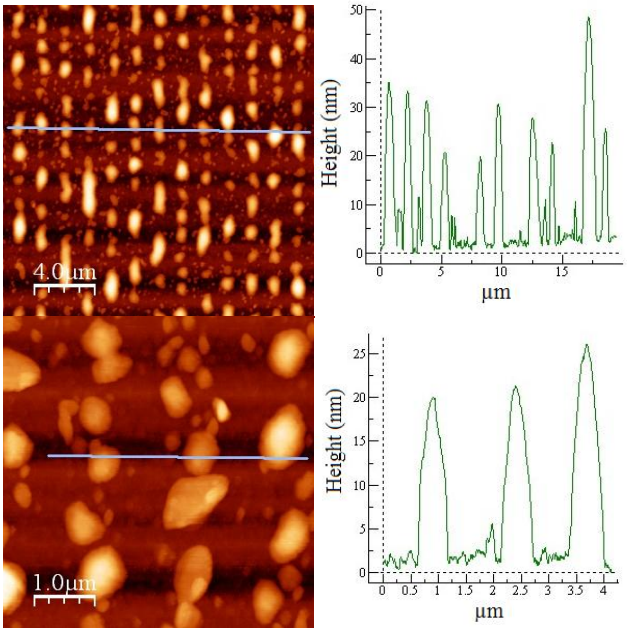

Figure A5.4 Annealing experiment of sample in Figure A5.3. Sample was placed in an oven overnight at 120 °C.

Both at room temperature and with more rapid heating in an oven, polymer reorganization was observed.

Additional AFM images for LDPE Lines Stamped on Glass:

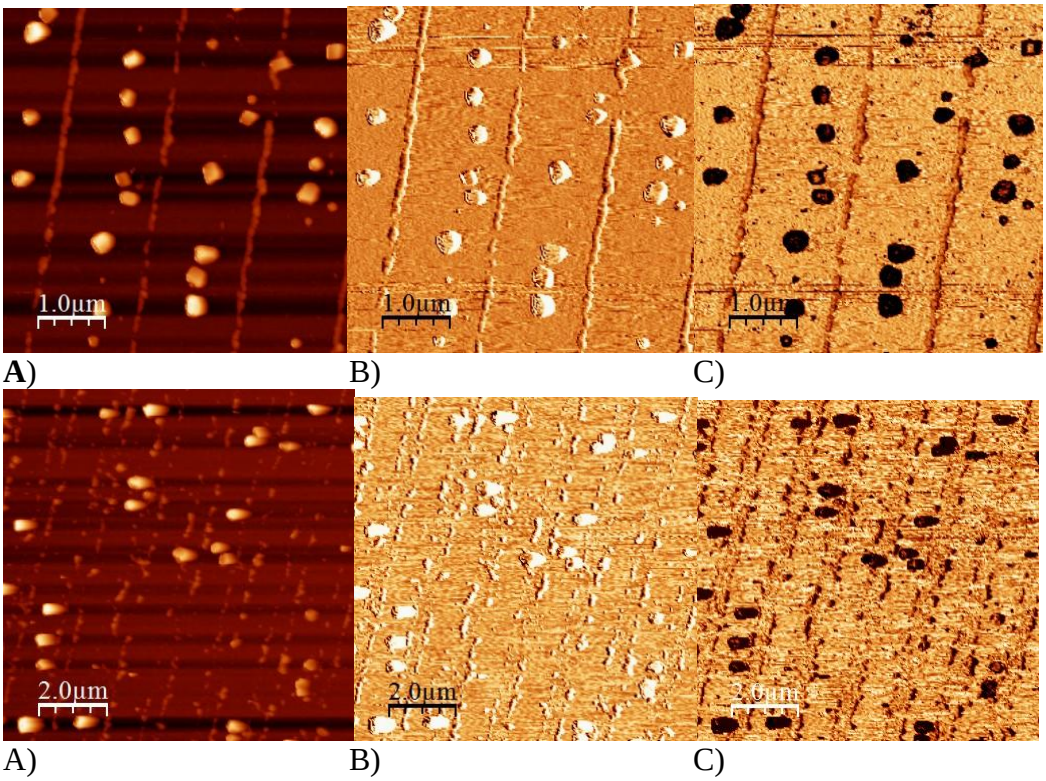

A) B) C)

A) B) C)

Figure A5.5 AFM images taken 2 days after printing LDPE lines onto glass at 21°C and 90 kPa. A) Height image. B) Altitude Image. C) Phase Image.

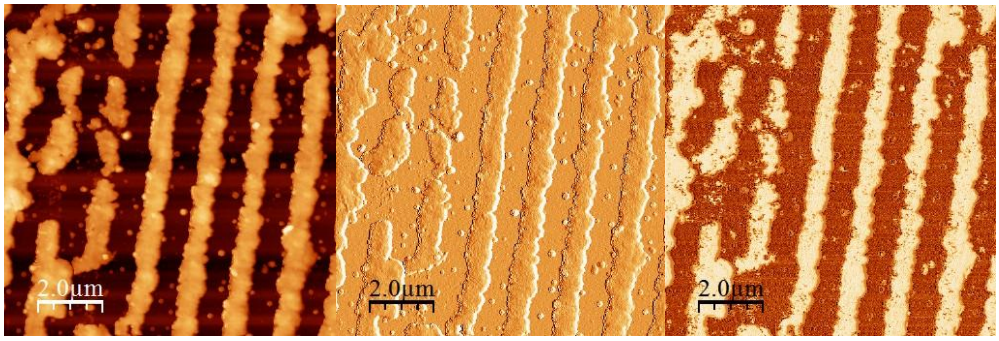

A) B) C)

Figure A5.6 AFM images taken 7 days after printing LDPE lines onto glass at 45 °C and 90 kPa. These lines are 110 nm high and are not reproducible, but this sample provides some information with regard to the phase image of these thicker polymer lines printed on glass. A) Height image. B) Altitude Image. C) Phase Image.

Chapter 6

Polymer Nanolithography and Substrate Matching

6.1 Qualitative Contact Angle Experiment for Nitric Acid Treated CD-R Pieces

Utilizing nitric acid to delaminate the aluminum, lacquer, and phthalocyanine layers from a CD-R, in order to expose the CD-R derived polycarbonate stamp leads to excellent pattern coverage (> 1cm^2) for ITO, polyester, glass, and aluminum-coated polyester substrates. Non-nitric acid delaminated CD-Rs have reduced pattern coverage and only print at higher temperatures and pressures, albeit still at temperatures below the Tg of polycarbonate. A contact angle experiment was conducted by removing the aluminum and lacquer layers with scotch tape. Different CD-R pieces (2.5 x 1.3 cm) were submerged in concentrated nitric acid for the following time intervals: 0 seconds, 5 seconds, 15 seconds, 30 seconds, 1 minute, 2 minutes, 3 minutes, and 6 minutes. The CD-R pieces were rinsed with tap water for 5 minutes, followed by a brief rinse with nanopurified water. Finally, the CD-Rs were dried under a stream of argon gas. The contact angle experiments were completed on the same day of nitric acid treatment.

For the contact angle experiment, 30 µL of water, dispersed by a pipetman, was placed on each CD-R piece and photographed with a digital camera, equipped with a high zoom lens. The angles were measured from the photographs. Although, precise surface energy calculations would have too much error from this experiment, a clear decrease in contact angle (25-30 degrees) was observed for 6 different experiments. With increasing exposure time to nitric acid, the polycarbonate surface becomes more hydrophilic based on these results (Fig. 6.1).

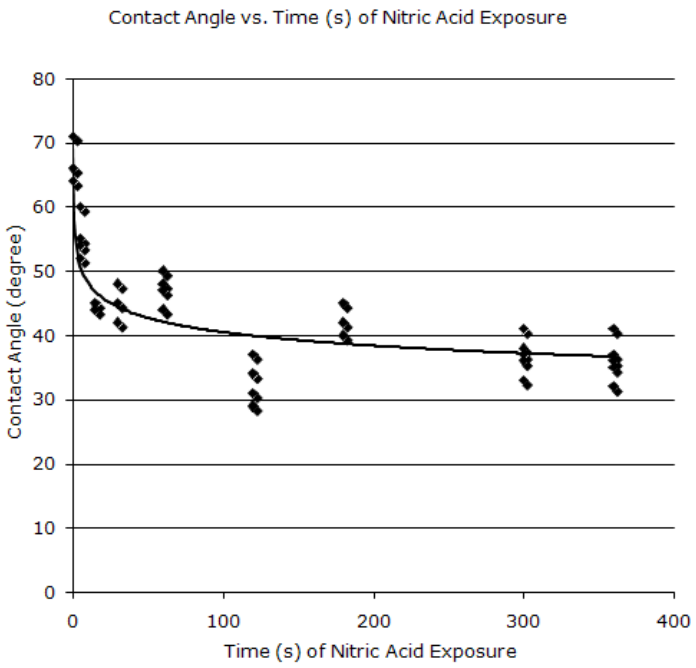

Figure 6.1 CD-Rs were exposed to increasing amounts of time in concentrated nitric acid. All pieces were rinsed with tap water for 5 minutes, followed by a brief rinse with nanopurified water. CD-R pieces were dried with argon. Qualitatively, with increasing time in nitric acid, the polycarbonate becomes more hydrophilic. Data is fit to a power curve.

6.2 Additional Chemical Analysis

The structure of polycarbonate contains alternating units of bisphenol A and a carbonate linker.[1] Based on UV-vis data, only 0.5% of the nitric acid treated CD-R's polymer was nitrated. X-ray photoelectron spectroscopy for nitric acid treated CD-Rs also revealed the presence of nitrogen. Infrared spectroscopy showed the spectra of the nitric acid treated CD-R to be nearly identical to the scotch tape (no nitric acid) treated CD-R. A slight difference in proportion of the carbonyl peak revealed that there was 3% fewer carbonyls, which would indirectly point to a greater concentration of phenoxy groups on the surface of the nitric acid treated polymer (see Appendix 2.7).

6.3 Substrate Surface Energy Matching:

Stamps made from nitric acid treated polycarbonate,scotch tape (no nitric acid) treated polycarbonate, polyethylene, polystyrene, and polyaniline were prepared. ITO, Lexan®, aluminum-coated polyester, polyester, and glass were substrates for printing. The ITO, glass, and aluminum-coated polyester were ozone cleaned for best results.

Material	Surface Energy (N/m)	Surface Roughness (RMS) measured by AFM (nm)	Best Replica Pattern Coverage and Fidelity on Substrate
ITO	56[2]	3	> 1 cm^2 nitric acid treated CD-R
Glass	82.5[2]	2	> 1 cm^2 nitric acid treated CD-R (less stable than ITO)
Aluminum	840[3]	10	> 1 cm^2 nitric acid treated CD-R
Polystyrene (PS)	40.7[4]		
Lexan® Polycarbonate (PC)	42.9[4]	10	> 1 cm^2 LDPE pattern
Polyethylene Terephthalate (PET)	45[5]	17	> 1cm^2 nitric acid treated CD-R, pattern changes
Low Density Polyethylene (LDPE)	31[5]*	35	

*surface energy for polyethylene

Table 6.1 Surface energies and surface roughness (RMS) for different materials. In addition, the best-matched stamp type for a material, when utilized as a substrate.

After many stamping experiments, some trends for increased printing fidelity were observed. These patterns were most obvious with the CD-R stamps, but the patterns were corroborated by other prints. First, nitric acid treatment caused the CD-R derived stamps to print at lower temperatures (110 ºC) on ITO, glass, and hydrophilic silicon wafer with pattern coverage of >1cm^2 (Fig. 6.2, 8). Non-nitric acid treated CD-R stamps printed with reduced coverage on ITO and glass at high temperature (130 ºC), but printed on Lexan® with greater pattern fidelity than the nitric acid treated CD-R (Fig. 6.4). On Lexan®, the nitric acid treated CD-R pattern quickly rearranged (Fig. 6.3). Although the non-nitric acid print on Lexan® did not have the same excellent coverage as the nitric acid treated CD-Rs on ITO, the printing was better on the lower surface energy Lexan® for the non-nitric acid treated CD-R. In addition, polyethylene prints on ITO and glass. On ITO, polyethylene rearranges after a few days to a month. On glass, polyethylene rearranges during printing time to hours after printing. On more hydrophobic Lexan®, polyethylene prints very well (> 1cm^2) (although with some lines less filled in depending on sample) (Fig.6.7). In addition, polyester is a higher surface energy plastic than Lexan®, and nitric acid treated CD-Rs print much better on this surface, than on Lexan®. Even so, the polymer seems to rearrange slightly, but the line patterns stay intact better than Lexan® (Fig. 6.6). Finally, the nitric acid treated CD-Rs also print very well on high surface energy aluminum-coated polyester (> 1cm^2) (Fig. 6.5).

In addition, the surface roughness also plays a role in patterns adhering to the surface of the substrate. ITO, glass, and aluminum-coated polyester are high surface energy substrates (compared to polymer films), but ITO and aluminum-coated polyester produce more stable nitric acid treated CD-R replicas (> 1 year). The surface roughness,

measured by AFM, of glass is 1-2 nm, while ITO is 2-3 nm, and aluminum-coated polyester is 10 nm. The decreased surface area on a glass substrate may override the benefit of the high surface energy.

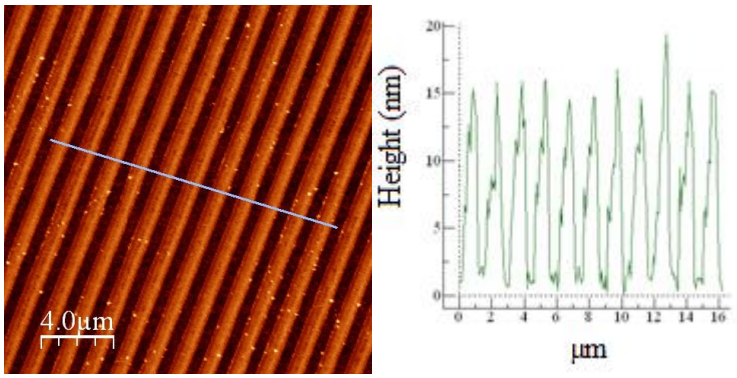

Figure 6.2 AFM height image of nitric acid treated CD-R lines on ITO, printed at 110 °C and 70 kPa with a 2 min dwell time.

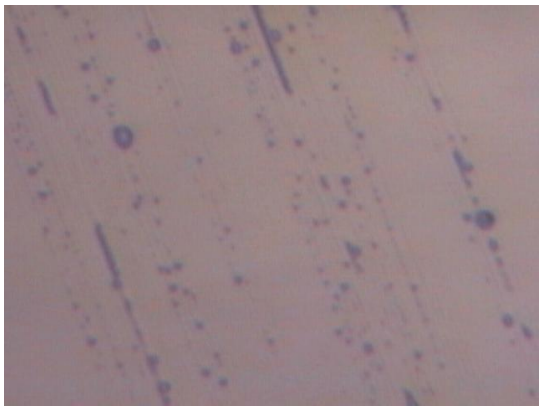

Figure 6.3 Optical image (40x objective magnified 2x through a CCD camera) nitric acid treated CD-R lines on Lexan®, printed at 110 °C and 70 kPa with a 2 min dwell time. Rearranged polymer is seen as lines of "beads."

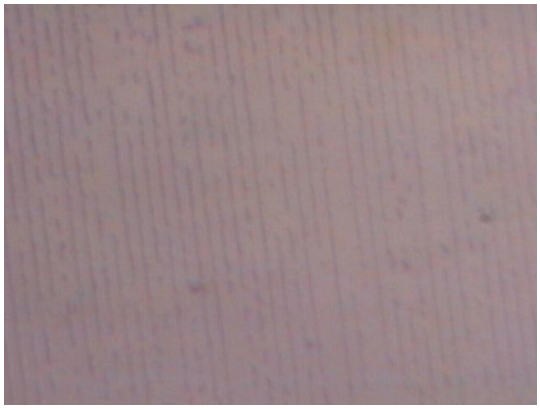

Figure 6.4 Optical image (40x objective magnified 2x through a CCD camera) Scotch tape (no nitric acid) treated CD-R lines on Lexan®, printed at 1305 °C and 110 kPa with a 2 min dwell time.

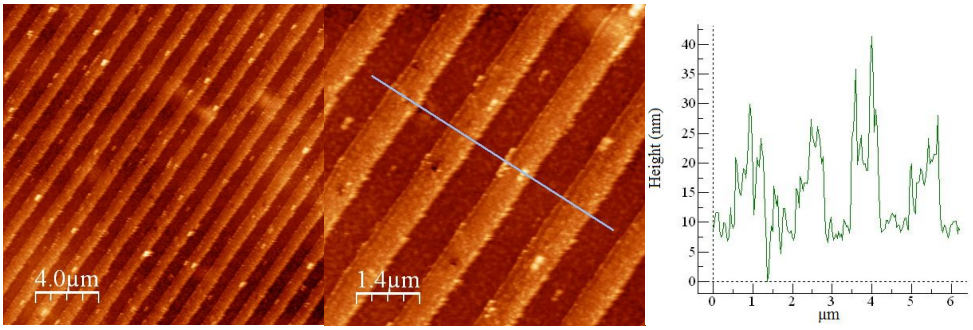

Figure 6.5 AFM height image of nitric acid treated CD-R lines on aluminum coated PET, printed at 105 °C and 90 kPa with a 12 min dwell time.

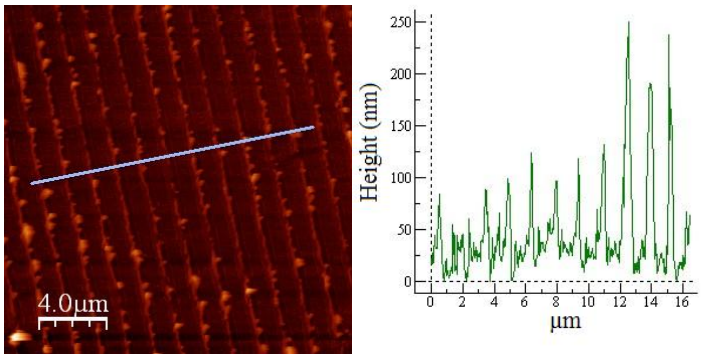

Figure 6.6 AFM height image of nitric acid treated CD-R lines on PET, printed at 105 °C and 90 kPa with a 2 min dwell time.

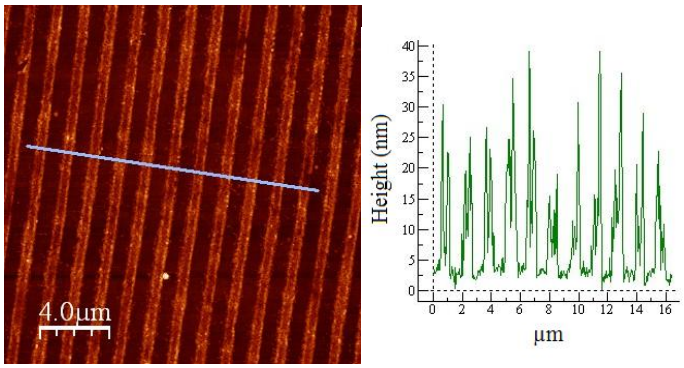

Figure 6.7 AFM image of LDPE lines printed on Lexan sheet (polycarbonate). Lexan and a LDPE stamp were placed on the oven-press for 2 minutes at 45°C and 20 kPa. The pressure was increased to 90 kPa over 40 sec and maintained at 45°C for 220 seconds more. The sample was cooled to room temperature and gently pulled apart.

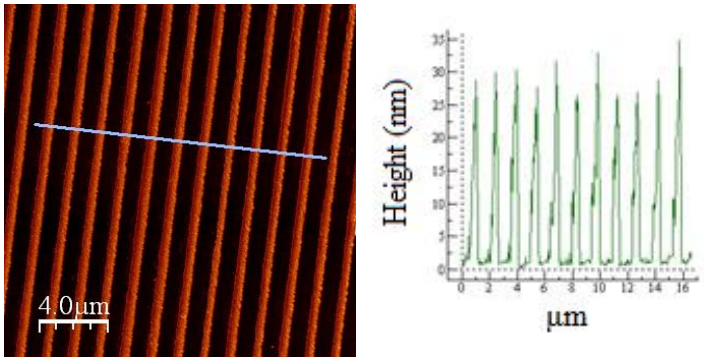

Figure 6.8 AFM height image of nitric acid treated CD-R lines on ITO, printed at 105 °C and 45 kPa with a 2 min dwell time.

6.4 Summary

Fabricating nanostructures with inexpensive CD-Rs as stamps is possible at temperatures below the Tg of polycarbonate and pressures 1000 times less than with nanoimprinting technology.[6] Frequently, with nanofabrication, the source of the pattern is exceptionally expensive and requires specialized equipment and a clean room. In addition, by matching higher surface energy and minimally rough surfaces, nitric acid treated

polycarbonate can be directly adhered to these surfaces with large coverage and fidelity. Conversely, the low surface energy polymer, polyethylene matched with Lexan®, a comparatively low surface energy substrate.

6.5 Chapter 6 References

(1) Abrams, C. F.; Site, L. D.; Kremer, K. *Physical Review E (Statistical, Nonlinear, and Soft Matter Physics)* **2003**, *67*, 021807.

(2) Bazzan, G.; Smith, W.; Francesconi, L. C.; Drain, C. M. *Langmuir* **2008**, *24*, 3244-3249.

(3) Kostyk, B. W. *MachineDesign.com By Engineers for Engineers* **2000**.

(4) Helt, J. M.; Drain, C. M.; Batteas, J. D. *J. Am. Chem. Soc.* **2004**, *126*, 628-634.

(5) Mark, J. E. *Physical Properties of Polymers Handbook*; Springer Science + Business Media: New York, 2007.

(6) Balla, T.; Spearing, S. M.; Monk, A. *J. Phys. D: Appl. Phys.* **2008**, *41*.

6.6 Appendix 6.1

When considering the nano or microscale perspective of CD-R polymer printing, some simple conclusions can be drawn by combining polymer thin film physics and principles in general chemistry. First, a scheme for the molecular composition of CD-R stamps treated with nitric acid is proposed based on chemical data in this thesis. Secondly, polymer stamp-substrate interactions are discussed. Further commentary for CD-R derived nanostructures between 400 nm to 175 nm is provided.

CD-Rs, when stripped of the lacquer, reflective metal, and dye layers, are made of polycarbonate. When nitric acid is used to remove all three layers, the stamp provides printed patterns of lines with a 1.5 μm pitch, 900 nm width, and 15 nm height. These patterns print at 110 ºC, a temperature well below the bulk glass transition temperature of 150 ºC[1] for polycarbonate. Conversely, CD-R stamps prepared without nitric acid, print at 130 ºC, and with less coverage of the substrate. Nitric acid treated CD-R stamps print better than non-nitric acid treated CD-R stamps on higher surface energy substrates.

Polycarbonate consists of molecules of bisphenol A linked by carbonate groups (Fig. A6.1).[2] According to UV-visible data, nitric acid causes less than 0.5% of the polycarbonate stamp to be nitrated.[3,4] Any nitro group that is introduced to the polymer would act as electron withdrawing groups and make the carbonate groups more reactive to nucleophiles.[5] In addition, by infrared spectroscopy, less than 3% of the polycarbonate backbone is hydrolyzed due to nitric acid. Hydrolysis of the carbonate linkers would cause polymer chains to become smaller and molecular weight to decrease. Some parts of the chain might be removed from the stamp, while remaining polymeric material would

exhibit more phenol chain ends. With more hydrogen bonding phenol OH groups, the surface energy of the stamp increases with greater exposure to nitric acid.[5]

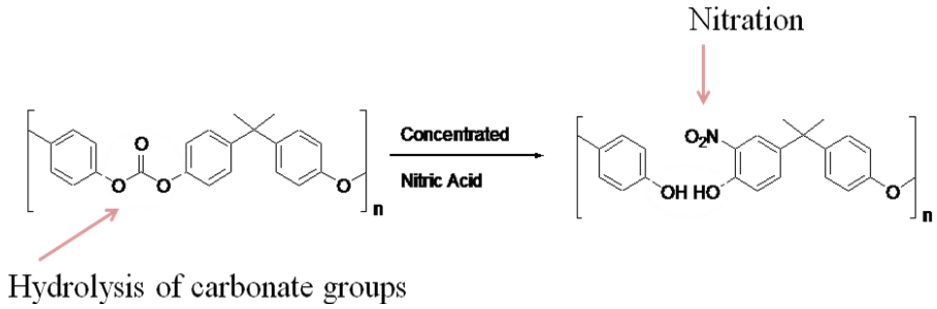

Figure A6.1: Scheme for chemical modification of CD-R polycarbonate with exposure to nitric acid.

When comparing the CD-R stamp treated with nitric acid to the CD-R stamp not treated with nitric acid, the polymer surface that would come into contact with the substrate surface contains more phenol OH group chain ends at the surface, and possibly a few nitrated phenyl groups in the entire stamp (Fig A6.2). The nitric acid treated stamp is more able to form hydrogen bonds with substrates, and is more polar leading to stronger dipole-dipole and dispersion attractive forces with polar substrates. Adhesion of the nitric acid treated CD-R is more favorable with hydrogen bond accepting substrates such as indium tin oxide (ITO), silicon oxide, and aluminum (thin layer of aluminum oxide on surface). There is likely some protonated moieties and possibly even some amount of nitric acid in the polymer stamp, some of the interaction may be electrostatic in nature, due to protonation of oxygen groups.

Conversely, more hydrophobic stamps made from CD-Rs without nitric acid treatment and low density polyethylene adhere better to hydrophobic polymer surfaces,

such as polycarbonate. Substrate-stamp interactions in this case are dominated by dispersion forces.

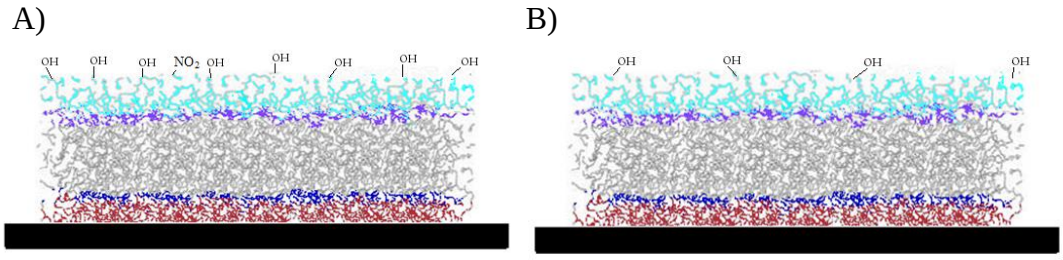

Figure A6.2: A) Nitric acid treated CD-R stamp B) No nitric acid treated CD-R stamp. The polymer surface of a nitric acid treated CD-R stamp has more polar, hydrogen bonding phenol group chain ends than the no nitric acid treated CD-R polymer.

Finally, if scotch tape is used to remove the lacquer and reflective metal layer first, before treating with nitric acid, lines widths from 400 nm to 175 nm are observed based on duration of nitric acid exposure, and stamping temperature. Based on AFM images of stamps treated with nitric acid, the deformation of the polymer increased, and the etched edges of the stamp increased in size. Chemically, the nitric acid hydrolyzes the polycarbonate and creates more hydrogen bonding phenol OH chain ends on the surface. In addition, these etched edges print best at an even lower temperature of 90 ºC. In regard to the lower temperature, this may be due to a greater surface area for free phenol groups exposed in the liquid layer. As the radius of gyration becomes closer to the thickness of the film, the T_g decreases.[6,7] These etched edges are only about 10-20 nm deep, and are exposed to nitric acid on both sides. With greater surface area, the exposed edges, hydrolyze at a greater rate than other parts of the stamp (Fig A6.3).

A)

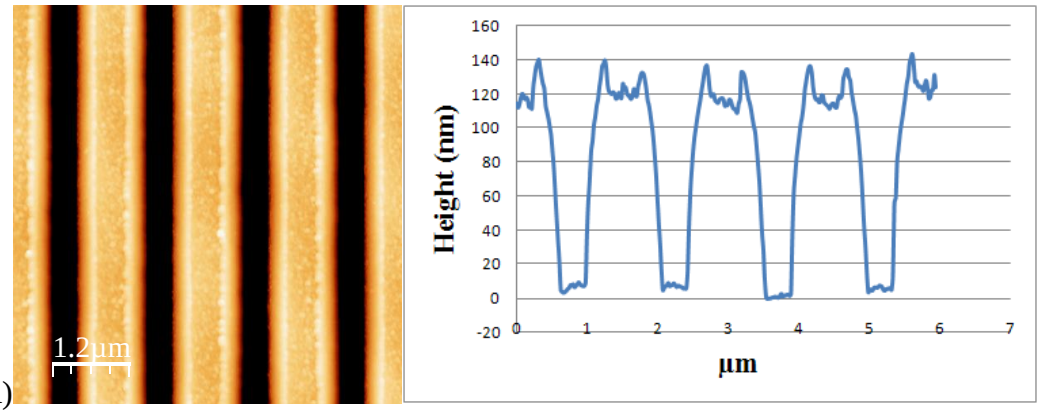

B)

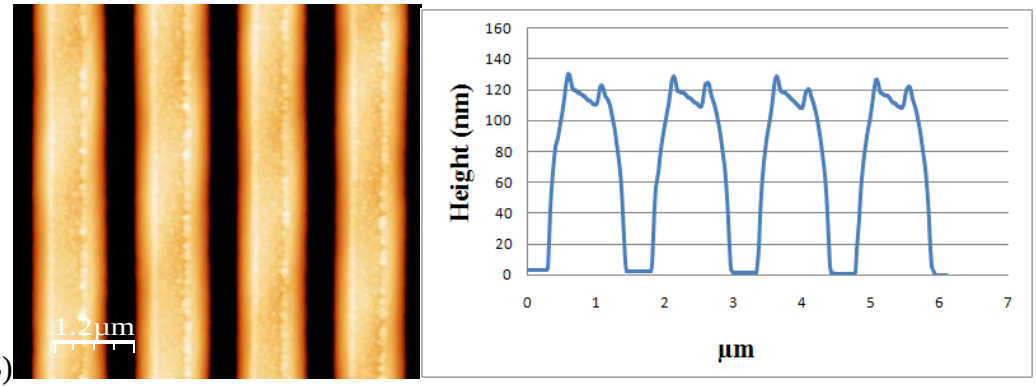

Figure A6.3: A) AFM image and profile of a CD-R stamp treated with nitric acid for 2 minutes after scotch tape removal of the lacquer and metal layers. B) AFM image and profile of a CD-R stamp treated with nitric acid for 1 minute after scotch tape removal of the lacquer and metal layers. Less deformation and smaller edges are observed for the second stamp.

Summary

Polycarbonate stamps are chemically modified with nitric acid, which leads to increased potential for hydrogen bonding with polar, hydrogen bond accepting substrates, such as ITO, silicon oxide, and aluminum oxide. Polycarbonate undergoes hydrolysis at carbonate linkers to form phenol OH end groups at the surface. In the case of non-nitric acid treated CD-R stamps and low density polyethylene stamps, a greater dependence on dispersion forces for adhesion occurs. Consequently, low surface energy substrates are suitable in these cases.

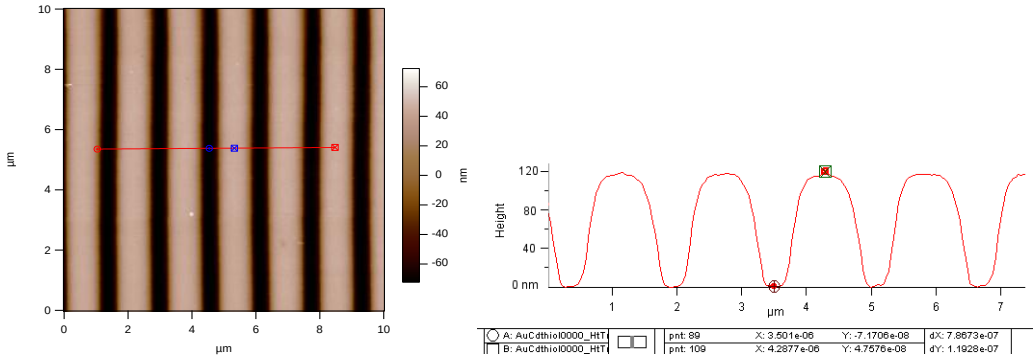

Figure A6.4 AFM image of the flatter lines of a CD-R stamp, which still had the protective aluminum layer, when treated with concentrated nitric acid (Bazzan thesis).

There are two surface morphologies of the nitric acid treated stamps. One is where the aluminum layer protects the top of the raised features and the nitric acid removes the polymer and aluminum from the sides towards the surface to give a flat feature with rounded corners (Fig. A6.4). The second, where nitric acid is used to treat the bare carbonate, results in the etching away of more of the center of the raised feature, and this is controlled by the kinetics of the reaction, thus the time of the treatment, to yield the raised edges seen in Figure A6.3. We observe that the longer the treatment with nitric acid, the narrower the spikes on each side of the raised feature.

A6.1 Appendix 6.6 References

(1) LeGrand, D. G.; Bendler, J. T. *Handbook of Polycarbonate Science and Technology*, 2000.

(2) Abrams, C. F.; Site, L. D.; Kremer, K. *Physical Review E (Statistical, Nonlinear, and Soft Matter Physics)* **2003**, *67*, 021807.

(3) Sulzberg, T.; Cotter, R. J. *Polymer Letters* **1969**, *7*, 185-191.

(4) Sivalingham, G.; Madras, G. *Applied Catalysis A : General* **2004**, *269*, 81-90.

(5) Zarnoch, K. P. *J. Adhesion Sc. Technol.* **1994**, *8*, 501-509.

(6) Forrest, J. A.; Dalnoki-Veressb, K. *Advances in Colloid and Interface Science* **2001**, *94*, 167-196.

(7) Fukao, K.; Miyamoto, Y. *Physical Review E* **2000**, *61*, 1743-1754.

Bibliography

Chapter 1

(1) Xia, Y.; Rogers, J. A.; Paul, K. E.; Whitesides, G. M. *Chem. Rev.* 1999, *99*, 1823-1848.

(2) Nie, Z.; Kumacheva, E. *Nature Materials* 2008, *7*, 277-290.

(3) Schmidt, R. C.; Healy, K. E. *Journal of Biomedical Materials Research Part A* 2009, 1252-1261.

(4) Geissler, M.; Xia, Y. *Advanced Materials* 2004, *16*, 1249-1269.

(5) Balla, T.; Spearing, S. M.; Monk, A. *J. Phys. D: Appl. Phys.* 2008, *41*.

(6) Singh, T. B.; Sariciftci, N. S. *Annu. Rev. Mater. Res.* 2006, *36*, 199-230.

(7) Yablonovitch, E.; Gmitter, T. J.; Meade, R. D.; Rappe, A. M.; Brommer, K. D.; Joannopoulos, J. D. *Physicall Review Letters* 1991, *67*, 3380-3383.

(8) Siegel, A. C.; Tang, S. Y.; Nijhuis, C. A.; Hashimoto, M.; Phillips, S. T.; Dickey, M. D.; Whitesides, G. M. *Accounts of Chemical Research* 2010.

(9) Gates, B. D.; Xu, Q.; Stewart, M.; Ryan, D.; Wilson, C. G.; Whitesides, G. M. *Chem. Rev.* 2005, *105*, 1171-1196.

(10) Xia, Y.; Whitesides, G. M. *Annu. Rev. Mater. Sci.* 1998, *28*, 153-183.

(11) Cui, B.; Cortot, Y.; Veres, T. *Microelectronic Engineering* 2006, *83*, 906-909.

(12) Quist, A. P.; Pavlovic, E.; Oscarsson, S. *Anal. Bioanal. Chem.* 2005, *381*, 591-600.

(13) Huo, F.; Zheng, Z.; Zheng, G.; Giam, L. R.; Zhang, H.; Mirkin, C. A. *Science* 2008, *321*, 1658-1660.

(14) Reis, N.; Ainsley, C.; Derby, B. *Journal of Applied Physics* 2005, *97*, 1-6.

(15) Fukao, K.; Miyamoto, Y. *Physical Review E.* 2000, *61*, 1743-1754.

(16) Forrest, J. A.; Dalnoki-Veressb, K. *Advances in Colloid and Interface Science* 2001, *94*, 167-196.

Chapter 2

(1) Special; Report *Technol. Rev.* **2003**, *106*, 36.

(2) Chou, S. Y.; Krauss, P. R.; Renstrom, P. J. *Science* **1996**, *272*, 85-87.

(3) Stephen Y. Chou, P. R. K. P. J. R. *Applied Physics Letters* **1995**, *67*, 3114-3116.

(4) Michael, D. A.; Haixiong, G.; Wei, W.; Mingtao, L.; Zhaoning, Y.; Wasserman, D.; Lyon, S. A.; Stephen, Y. C. *Applied Physics Letters* **2004**, *84*, 5299-5301.

(5) Dahl-Young, K.; Hong, H. L. *Applied Physics Letters* **1999**, *75*, 2599-2601.

(6) Heyderman, L. J.; Schift, H.; David, C.; Gobrecht, J.; Schweizer, T. *Microelectronic Engineering* **2000**, *54*, 229-245.

(7) Zankovych, S.; Hoffmann, T.; Seekamp, J.; Bruch, J. U.; Torres, C. M. S. *Nanotechnology* **2001**, *12*, 91-95.

(8) Jung, G. Y.; Li, Z.; Wu, W.; Chen, Y.; Olynick, D. L.; Wang, S. Y.; Tong, W. M.; Williams, R. S. *Langmuir* **2005**, *21*, 1158-1161.

(9) Khang, D. Y.; Kang, H.; Kim, T. I.; Lee, H. H. *Nano Lett.* **2004**, *4*, 633-637.

(10) Huang, X. D.; Bao, L. R.; Cheng, X.; Guo, L. J.; Pang, S. W.; Yee, A. F. *J. Vac. Sci. Technol. B* **2002**, *20*, 2872-2876.

(11) Dahl-Young, K.; Hong, H. L. *Applied Physics Letters* **2000**, *76*, 870-872.

(12) Baily, T.; Choi, B. J.; Colburn, M.; Meissl, M.; Shaya, S.; Ekerdt, J. G.; Sreenavasan, S. V. *J. Vac. Sci. Technol. B* **2000**, *18*, 3572-3577.

(13) Menard, E.; Meitl, M. A.; Sun, Y.; Park, J. U.; Shir, D. J. L.; Nam, Y. S.; Jeon, S.; Rogers, J. A. *Chem. Rev.* **2007**, *107*, 1117-1160.

(14) Guo, L. J.; Cheng, X.; Chao, C. Y. *Journal of Modern Optics* **2002**, *49*, 663-673.

(15) Cheng, X.; Hong, Y. T.; Kanicki, J.; Guo, L. J. *J. Vac. Sci. Technol. B* **2002** *20*, 2877-2880.

(16) Austin, M. D.; Chou, S. Y. *Applied Physics Letters* **2002**, *81*, 4431-4433.

(17) Helt, J. M.; Drain, C. M.; Bazzan, G. *J. Am. Chem. Soc.* **2006**, *128*, 9371-9377.

(18) Helt, J. M.; Drain, C. M.; Batteas, J. D. *J. Am. Chem. Soc.* **2004**, *126*, 628-634.

(19) Forrest, J. A.; Dalnoki-Veress, K.; Dutcher, J. R. *Physical Review E* **1997**, *56*, 5705.

(20) Keddie, J. L.; Jones, R. A. L.; Cory, R. A. *Faraday Discussions* **1994**, 219-230.

(21) Horcas, I. *Rev. Sci. Instrum.* **2007**, *78*.

(22) Rice, R. W.; Sarode, D. V. *Ind. Eng. Chem. Res.* **2001**, *40*, 1872-1878.

(23) Zarnoch, K. P. *J. Adhesion Sc. Technol.* **1994**, *8*, 501-509.

(24) Yu, H. Z. *Anal. Chem.* **2001**, *73*, 4743-4747.

(25) *Eur. Phys. J. E* **2002**, *8*, 101-261.

(26) Fryer, D. S.; Nealey, P. F.; de Pablo, J. J. *Macromolecules* **2000**, *33*, 6439-6447.

(27) Ranjeet, S. T.; David, S. F.; Silvia, P.; Martha, F. M.; Juan, J. d. P.; Paul, F. N. *Journal of Chemical Physics* **2001**, *115*, 9982-9990.

(28) Yamamoto, S.; Tsujii, Y.; Fukuda, T. *Macromolecules* **2002**, *35*, 6077-6079.

(29) Fryer, D. S.; Peters, R. D.; Kim, E. J.; Tomaszewski, J. E.; de Pablo, J. J.; Nealey, P. F.; White, C. C.; Wu, W. l. *Macromolecules* **2001**, *34*, 5627-5634.

(30) *Springer Handbook of Nanotechnology*; 1 ed.; Bhushan, B., Ed.; Springer: Berlin, 2004.

(31) Durig, U.; Cross, G.; Despont, M.; Drechsler, U.; Haberle, W.; Lutwyche, M. I.; Rothuizen, H.; Stutz, R.; Widmer, R.; Vettiger, P.; Binnig, G. K.; King, W. P.; Goodson, K. E. *Tribology Letters* **2000**, *9*, 25-32.

(32) DeMaggio, G. B.; Frieze, W. E.; Gidley, D. W.; Zhu, M.; Hristov, H. A.; Yee, A. F. *Physical Review Letters* **1997**, *78*, 1524-1527.

(33) Fukao, K.; Miyamoto, Y. *Physical Review E* **2000**, *61*, 1743-1754.

(34) Abrams, C. F.; Site, L. D.; Kremer, K. *Physical Review E (Statistical, Nonlinear, and Soft Matter Physics)* **2003**, *67*, 021807.

(35) Soles, C. L.; Douglas, J. F.; Wu, W. l.; Peng, H.; Gidley, D. W. *Macromolecules* **2004**, *37*, 2890-2900.

(36) LeGrand, D. G.; Bendler, J. T. *Handbook of Polycarbonate Science and Technology*, 2000.

(37) Araki, K.; Wagner, M. J.; Wrighton, M. S. *Langmuir* **1996**, *12*, 5393-5398.

(38) Beinhoff, M.; Appapillai, A. T.; Underwood, L. D.; Frommer, J. E.; Carter, K. R. *Langmuir* **2006**, *22*, 2411-2414.

Appendix 2.7

(1) Bornmann, J. A.; Wolf, C. J. *Journal of Polymer Science: Polymer Chemistry Edition* **1984**, *22*, 851-856.

(2) Zarnoch, K. P. *J. Adhesion Sc. Technol.* **1994**, *8*, 501-509.

(3) Sulzberg, T.; Cotter, R. J. *Polymer Letters* **1969**, *7*, 185-191.

(4) Sivalingham, G.; Madras, G. *Applied Catalysis A : General* **2004**, *269*, 81-90.

(5) Wikipedia *Wikipedia The Free Encyclopedia* **2010**.

Chapter 3

(1) Forrest, S. R. *Nature* 2004, *428*, 911-918.

(2) Quist, A. P.; Pavlovic, E.; Oscarsson, S. *Anal. Bioanal. Chem.* 2005, *381*, 591-600.

(3) Balla, T.; Spearing, S. M.; Monk, A. *J. Phys. D: Appl. Phys.* 2008, *41*.

(4) Gates, B. D.; Xu, Q.; Stewart, M.; Ryan, D.; Wilson, C. G.; Whitesides, G. M. *Chem. Rev.* 2005, *105*, 1171-1196.

(5) Leclere, P.; Surin, M.; Brocorens, P.; Cavallini, M.; Biscarini, F.; Lazzaroni, R. *Materials Science and Engineering R* 2006, *55*, 1-56.

(6) Nie, Z.; Kumacheva, E. *Nature Materials* 2008, *7*, 277-290.

(7) Cui, B.; Cortot, Y.; Veres, T. *Microelectronic Engineering* 2006, *83*, 906-909.

(8) Tang, Z.; Kotov, N. A. *Adv. Mater.* 2005, *17*, 951-962.

(9) Helt, J. M.; Drain, C. M.; Batteas, J. D. *J. Am. Chem. Soc.* 2004, *126*, 628-634.

(10) Helt, J. M.; Drain, C. M.; Bazzan, G. *J. Am. Chem. Soc.* 2006, *128*, 9371-9377.

(11) LeGrand, D. G.; Bendler, J. T. *Handbook of Polycarbonate Science and Technology* 2000.

(12) Zarnoch, K. P. *J. Adhesion Sc. Technol.* 1994, *8*, 501-509.

(13) Yu, H.-Z. *Anal. Chem.* 2001, *73*, 4743-4747.

(14) McCall, R. P.; Scherr, E. M.; MacDiarmid, A. G.; Epstein, A. J. *Physical Review B* 1994, *50*, 5094-5100.

(15) MacDiarmid, A. G. *Synthetic Metals* 2002, *125*, 11-22.

(16) Heeger, A. J. *Angew. Chem. Int. Ed.* 2001, *40*, 2591-2611.

(17) Lee, K.; Cho, S.; Park, S. H.; Heeger, A. J.; Lee, C.-W.; Lee, S.-H. *Nature* 2006, *441*, 65-68.

(18) Shimano, J. Y.; MacDiarmid, A. G. *Synthetic Metals* 2001, *123*, 251-262.

(19) MacDiarmid, A. G. *Synthetic Metals* 1997, *84*, 27-34.

(20) Pouget, J. P.; Josefowicz, M. E.; Epstein, A. J.; Tang, X.; MacDiarmid, A.

G. *Macromolecules* 1991, *24*, 779-789.

(21) Pomfret, S. J.; Rebourt, E.; Monkman, A. P. *Synthetic Metals* 1996, *76*, 19-22.

(22) Wang, P.-C.; MacDiarmid, A. G. *Reactive and Functional Polymers* 2008, *68*, 201-207.

(23) Makela, T.; Pienimaa, S.; Jussila, S.; Isotalo, H. *Synthetic Metals* 1999, *101*, 705-706.

(24) Haberko, J.; Raczkowska, J.; Bernasik, A.; Luzny, W. *Macromol. Symp.* 2008, *263*, 47-52.

(25) Haberko, J.; Raczkowska, J.; Bernasik, A.; Rysz, J.; Budkowski, A.; Luzny, W. *Synthetic Metals* 2007, *157*, 935-939.

(26) Makela, T.; Haatainen, T.; Majander, P.; Ahopelto, J. *Microelectronic Engineering* 2007, *84*, 877-879.

(27) Ngamna, O.; Morrin, A.; Killard, A. J.; Moulton, S. E.; Smyth, M. R.; Wallace, G. G. *Langmuir* 2007, *23*, 8569-8574.

(28) Horcas, I. *Rev. Sci. Instrum.* 2007, *78*.

(29) Malinauskas, A. *Polymer* 2001, *42*, 3957-3972.

Chapter 4

(1) Ozin, G. A.; Arsenault, A. C.; Cademartiri, L., *Nanochemistry: A Chemical Approach to Nanomaterials* 2nd ed.; Royal Society of Chemistry: London, 2009.

(2) Helt, J. M.; Drain, C. M.; Bazzan, G., *J. Am. Chem. Soc.* **2006,** *128*, 9371-9377.

(3) Menard, E.; Meitl, M. A.; Sun, Y.; Park, J.-U.; Shir, D. J.-L.; Nam, Y.-S.; Jeon, S.; Rogers, J. A., *Chem. Rev.* **2007,** *107*, 1117-1160.

(4) Ahn, S. H.; Guo, L. J., *ACS Nano* **2009,** *3*, 2304-2310.

(5) Khang, D.-Y.; Lee, H. H., *Langmuir* **2008,** *24*, 5459-5463.

(6) Moran, I. W.; Briseno, A. L.; Loser, S.; Carter, K. R., *Chem. Mater.* **2008,** *20*, 4595-4601.

(7) Gerber, R.; Oliver-Hoyo, M., *J. Chem. Educ.* **2008,** *85*, 1108-1111.

(8) Meenakshi, V.; Babyan, Y.; Odom, T. W., *J. Chem. Educ.* **2007,** *84*, 1795-1798.

(9) Stelick, S. J.; Alger, W. H.; Laufer, J. S.; Waldron, A. M.; Batt, C. A., *J. Chem. Educ.* **2005,** *82*, 1361-1364.

(10) Sun, L.; O'Reilly, J.; Tien, C.; Sue, H., *J. Chem. Educ.* **2008,** *85*, 1105-1109.

(11) Haynes, C. L.; McFarland, A. D.; Van Duyne, R. P.; Godwin, H. A., *J. Chem. Educ.* **2005,** *82*, 768A-768B.

(12) Berkowski, K. L.; Plunkett, K. N.; Yu, Q.; Moore, J. S., *J. Chem. Educ.* **2005,** *82*, 1365-1369.

(13) Meenakshi, V.; Babyan, Y.; Odom, T. W., *J. Chem. Educ.* **2007,** *84*, 1795-1798.

(14) Abrams, C. F.; Site, L. D.; Kremer, K., *Phys. Rev. E* **2003,** *67*, 021807.

(15) Cross, G. L. W.; O'Connell, B. S.; Pethica, J. B.; Rowland, H.; King, W. P., *Rev. Scientific Instr.* **2008,** *79*, 1-13.

(16) Fukao, K.; Miyamoto, Y., *Phys. Rev. E.* **2000,** *61*, 1743-1754.

(17) G. Planinšič, G.; Corona, A.; Slisko, J., *Phys. Teacher* **2008,** *46*, 329-333.

(18) Zhong, C.-J.; Han, L.; Maye, M. M.; Luo, J.; Kariuki, N. N.; Jones, W. E., Jr. , *J. Chem. Educ.* **2003,** *80*, 194-198.

Appendix 4.7

(1) Ouseph, P. J., *Phys. Teacher* **2007,** *45*, 11-13.

(2) Planinšič, G.; Corona, A.; Slisko, J., *Phys. Teacher* **2008,** *46*, 329-333.

(3) Meenakshi, V.; Babyan, Y.; Odom, T. W., *J. Chem. Educ.* **2007,** *84*, 1795-1798.

(4) Zhong, C.-J.; Han, L.; Maye, M. M.; Luo, J.; Kariuki, N. N.; Jones, W. E., Jr. , *J. Chem. Educ.* **2003,** *80*, 194-198.

(5) Fukao, K.; Miyamoto, Y., *Phys. Rev. E.* **2000,** *61*, 1743-1754.

(6) Geissler, M.; Xia, Y., "Patterning: Prinicples and Some New Developments." *Adv. Mater.* **2004,** *16* (15), 1249-1269.

(7) Xia, Y.; Rogers, J. A.; Paul, K. E.; Whitesides, G. M., "Unconventional Methods for Fabricating and Patterning Nanostructures." *Chem. Rev.* **1999**, *99*, 1823-1848.

(8) Balla, T.; Spearing S. M.; Monk, A., "An Assessment of the Process Capabilities of Nanoimprint Lithography." *J. Phys.: Appl. Phys.* **41** (2008), 174001

(9) Gates, B. D.; Xu, Q.; Stewart, M.; Ryan, D.; Wilson, C. G.; Whitesides, G M., "New Approaches to Nanofabrication: Molding, Printing, and Other Techniques." *Chem. Rev.* **105** (2005), 1171-1196.

(10) Quist, A. P.; Pavlovic, E.; Oscarsson, S., "Recent Advances in Microcontact Printing." *Anal. Bioanal. Chem.*, **381** (2005), 591-600.

(11) Schmidt, R. C.; Healy, K. E., "Controlling Biological Interfaces on the Nanometer Length Scale." *J. Biomed. Mater. Res. Part A* (2009), 1252-1261.

Chapter 5

(1) Leising, G.; Stadlober, B.; Haas, U.; Haase, A.; Palfinger, C.; Gold, H.; Jakopic, G. *Microelectronic Engineering* 2006, *83*, 831-838.

(2) Nie, Z.; Kumacheva, E. *Nature Materials* 2008, *7*, 277-290.

(3) Zhao, Y.; Cui, T. *Journal of Micromechanics and Microengineering* 2003, *13*, 430-435.

(4) Balla, T.; Spearing, S. M.; Monk, A. *J. Phys. D: Appl. Phys.* 2008, *41*.

(5) Horcas, I. *Rev. Sci. Instrum.* 2007, *78*.

Chapter 6

(1) Abrams, C. F.; Site, L. D.; Kremer, K. *Physical Review E (Statistical, Nonlinear, and Soft Matter Physics)* **2003**, *67*, 021807.

(2) Bazzan, G.; Smith, W.; Francesconi, L. C.; Drain, C. M. *Langmuir* **2008**, *24*, 3244-3249.

(3) Kostyk, B. W. *MachineDesign.com By Engineers for Engineers* **2000**.

(4) Helt, J. M.; Drain, C. M.; Batteas, J. D. *J. Am. Chem. Soc.* **2004**, *126*, 628-634.

(5) Mark, J. E. *Physical Properties of Polymers Handbook*; Springer Science + Business Media: New York, 2007.

(6) Balla, T.; Spearing, S. M.; Monk, A. *J. Phys. D: Appl. Phys.* **2008**, *41*.

Appendix 6.6

(1) LeGrand, D. G.; Bendler, J. T. *Handbook of Polycarbonate Science and Technology*, 2000.

(2) Abrams, C. F.; Site, L. D.; Kremer, K. *Physical Review E (Statistical, Nonlinear, and Soft Matter Physics)* **2003**, *67*, 021807.

(3) Sulzberg, T.; Cotter, R. J. *Polymer Letters* **1969**, *7*, 185-191.

(4) Sivalingham, G.; Madras, G. *Applied Catalysis A : General* **2004**, *269*, 81-90.

(5) Zarnoch, K. P. *J. Adhesion Sc. Technol.* **1994**, *8*, 501-509.

(6) Forrest, J. A.; Dalnoki-Veressb, K. *Advances in Colloid and Interface Science* **2001**, *94*, 167-196.

(7) Fukao, K.; Miyamoto, Y. *Physical Review E* **2000**, *61*, 1743-1754.